Departamento de Genética

Instituto de Biomedicina de Sevilla

Programa de doctorado en Biología molecular, biomedicina e investigación clínica

Molecular bases of proliferative heterogeneity in *Saccharomyces cerevisiae*

Irene Delgado Román

Directores:

María de la Cruz Muñoz Centeno Sebastián Chávez de Diego

Content

1. Introduction

1.1 Proliferative heterogeneity: definition and key concepts.

Heterogeneity can be defined as "the quality or state of being diverse in character or content" (Oxford language dictionary), in other words, the presence of different features within a population of any kind. Cell populations are also characterized by the presence of heterogeneity among its members (Ackermann, 2015; Ryall et al., 2012a; Sánchez-Romero & Casadesús, 2014a). It has been widely studied that isogenic cells show phenotypical heterogeneity that does not depend on mutations or environmental changes, and this is common on all organisms. Not only do they differentiate from other cell types, in an organ or tissue, for example, but also in monoclonal populations. In the latter case, this heterogeneity is known as cell to cell variability and can be present on any aspect of their phenotype or genotype: shape, growth rate, differential expression of genes, size, mutations, etc. [4–7].

There is a particular type of heterogeneity that affects the velocity or the capacity of certain cells to divide. This is referred as proliferative heterogeneity[8–10] and it is commonly studied from unicellular microorganisms to human cells, due to its major role in population fitness and survival and to its relationship with resistance mechanisms in pathogenic infections and in cancer cells (figure 1 and 2)[11–14]. For this reason, the understanding of the mechanisms underlying this proliferative heterogeneity and its consequences is of great importance and could be easily translated to humans from microorganisms' studies. In this thesis, we will focus on proliferative heterogeneity.

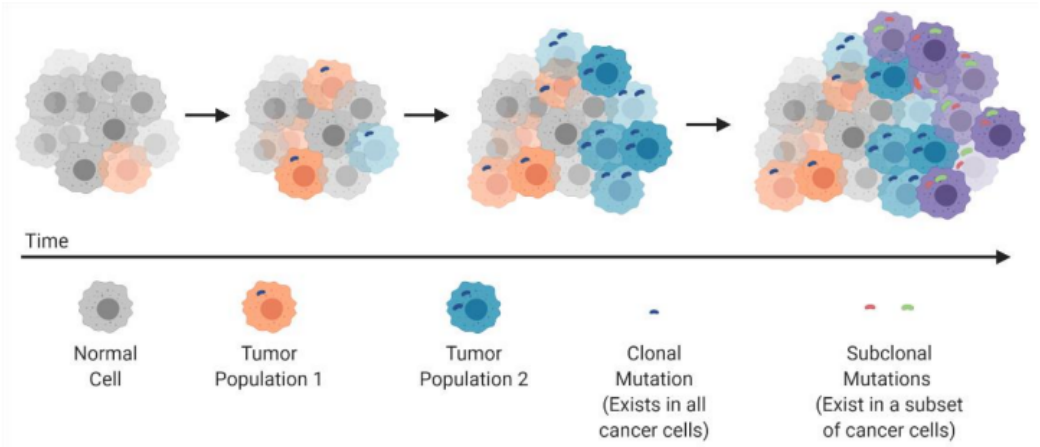

Figure 1 Effects of clonal heterogeneity in the progression of a tumour caused by mutations. Due to the enhanced proliferation and uncontrolled division of tumorigenic cells, the probability of mutations is increased. As a result, in one tumour that comes from the division of clonal cells, there are different subset of cancer cells in this population with different proliferation rates and characteristics [14].

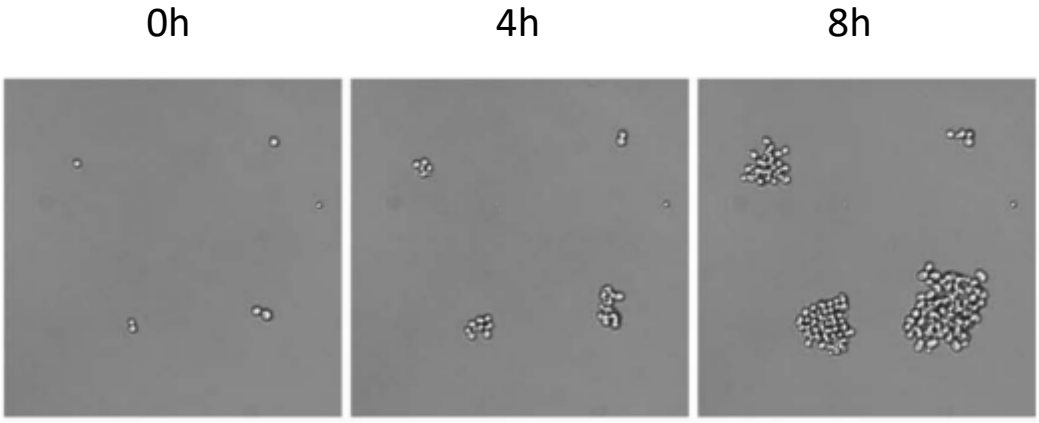

Figure 2. Proliferative heterogeneity in a clonal culture of S.cerevisiae. We observe a real time imaging of the proliferation of 3 different cells from a clonal yeast culture. Even though these cells share the same genetic information, their proliferation is very different[6].

1.2 Heterogeneity: genetic and non-genetic

The differences among cells within the same culture, arisen by mutations or any other kind of changes in cells genome that alters their DNA sequence, are known as genetic heterogeneity [15–20]. Alterations in the DNA sequence can lead to phenotypical changes creating a source of heterogeneity within, originally, clonal cultures. A typical example of heterogeneity caused by genetic alterations are tumoral cells. Their genomic instability leads to the accumulation of certain mutations that, eventually, leads to uncontrolled proliferation and resistance to death signals.
However, and interestingly, there are differences among genetically identical cells, designed as "non-genetic heterogeneity" or phenotypical heterogeneity, and they can be displayed at different levels: morphology, resistance to drugs, tolerance to different types of stress or heterogeneity in proliferation capacity, among others [6,21–24].

Within the non-genetic heterogeneity category, one of the more studied sources of heterogeneity on isogenic population are epigenetic differences among clonal cells. Despite the lack of consensus on the definition of epigenetics, most of the scientific community considers epigenetic changes those that meet the following two criteria: they alter chromatin configuration, and they are hereditable [25]. Epigenetic phenomena are broadly studied and a lot of advances have been made on this field, identifying a wide range of chromatin modifications and thousands of different patterns related to one or another state of the chromatin. Bacteria and yeast have been a great tool for these studies, since their epigenetic footprints are simpler than higher eukaryotes but still hold a lot of similarities [26,27]. In case of *Saccharomyces cerevisiae* and *Schizosaccharomyces pombe*, histone acetylation is the main chromatin mark linked to epigenetic phenomena [25].

Another source of non-genetic proliferative heterogeneity are differences in expression patterns of several genes [8,21,28,29] among clonal cells exposed to the same environment, caused by small fluctuations in certain protein concentrations, mRNA levels, or small differences in cell cycle progression that leads to this proliferative heterogeneity. These changes are referred as "noise" and they may be caused by stochastic differences in gene expression, mRNA degradation or different mRNA isoforms expression, or it can be caused by other phenomena such as asymmetric division in *S. cerevisiae*. In this thesis work, we will focus on the heterogeneity that arises from non-genetic sources.

It has been proposed that the evolutional significance of said heterogeneity is the perseverance of part of the population even if the environment changes drastically, and therefore, it would mean a favorable trait for its own survival as a culture [30]. In budding yeast, proliferative heterogeneity is also well described as a fitness and survival mechanism but, in addition to this, heterogeneity also plays a role in fitness through the replicative life of the culture.

1.2.1 Importance of proliferative non-genetic heterogeneity

Commonly in all microorganisms, variability in phenotypic attributes increase the population fitness when exposed to fluctuating conditions or environments.

In bacteria and yeast cultures, bistable systems conform a bet-hedging strategy to survive challenging conditions. This bistability consists of a two steady phenotypical state in a clonal population, which gives it a selective advantage within variable environments. Thanks to this mechanism part of the population will survive to a specific change in culture conditions and, this way, ensure the production of more offspring. Something interesting about bet-hedging is that the differential gene expression that will eventually lead to survival of part of the population is prior to any change[30–33]

Bacteria populations guarantee their survival as a group betting on two or several phenotypic states that will favor part of the culture in one condition but may be deleterious in others. As an example, heterogeneity in expression patterns in critical functions within resistance mechanisms contributes to resistance to antibiotics in *Salmonella enterica*.[34] studies reveal that there is heterogeneous expression of OmpC, an outer-membrane porin, and this heterogeneity is also responsible for the heterogeneity found in *S. enterica* against Kanamycin. Cells expressing lower levels of this porin, showed an increased resistance to the antibiotic. As ompC expression is downregulated by Kanamycin presence, and this increases resistance, it is possible that a feedback loop is also participating in

this resistance mechanism. This implies that ompC expression is noisy enough to produce two subpopulations: one has reached the lower expression threshold necessary for resistance in the event of Kanamycin appearance in their environment; the other one have enough porin to have great fitness at the expense of susceptibility to Kanamycin. This is an example of how populations "bet" on a particular expression profile, which is usually decided stochastically, either betting on their fitness in normal conditions, or in their survival given any deleterious change in the environment.
Another strategy example are persistent cells: these bacteria have a slow growth phenotype, sometimes entering a spore state, allowing them to better face adverse conditions. In this case, this part of the bacterial population is somehow "waiting" for environment changes rather than betting on an expression pattern that will favor them in case of a specific condition change. In the first case, slow growth phenotype favors resistance to stress or enables a better adaptive response [35].

In yeast, cell to cell variation and bet hedging strategies are also present. Proliferative heterogeneity is tightly related to growth rate heterogeneity, and this is commonly observed in *Saccharomyces cerevisiae* cultures, growing in identical environments[36,37]. As a proof of that, Murat A, et al. (Acar et al., 2008b) designed a quite simple experiment in which it is demonstrated that yeast populations improve its fitness thanks to the natural fluctuations in gene expression that would make part of the population better fit to a changing environment. Under normal conditions, fast growers out-compete slow growers, however, when environment conditions change, slow growers take over the culture. This suggest a survival mechanism in which yeast cultures ensures the survival of, at least, part of the population under changing conditions.

Levy et al. [36], studied bet hedging in yeast and found that clonal yeast populations display a wide range of growth rates and that this growth rate is inversely proportional to several stresses resistance. They found that older cells (generally, those cells that have undergone more than 17-20 divisions) , which usually grow slower than younger cells, had more Tsl1 (trehalose synthase) expression abundance, a protein involved in stress response, making them more resistant to acute stress conditions. However, not only older cells had more Tsl1, they found that a heterogeneous expression of Tsl1 exists among clonal cells and this correlated with the growth rate. Moreover, following studies [38] showed that the responsible element for this heterogeneity in the expression of Tsl1 is a heterogeneous expression of cAMP. cAMP is implied in nutrient sensing and other stress-related responses through the Ras/cAMP/PKA pathway. In glucose deficit conditions, cAMP levels decrease, which decrease PKA levels (cAMP inhibits bcy1 in normal conditions, a PKA inhibitor). This dephosphorylates Msn2 and Msn4, allowing it to go to the nucleus. As a consequence, there is a decrease in growth rate and an activation of stress-response genes transcription.

Their findings suggest that cAMP and PKA levels are implicated in the correlation between slow growth and stress tolerance. In fact, increasing cAMP levels in cells, reduces the number of slow growers in the culture and a decrease in the heterogeneity of Tsl1 expression. Complementary to this, cells expressing more Tsl1 were slow growing subpopulation and had less natural cAMP expression. Interestingly, Msn2 nucleus localization is also heterogeneous among clonal cells and correlates with growth rate. Msn2 and Msn4 are both responsible for the correlation between slow growth phenotype and Tsl1 abundance. This means that fluctuations in cAMP levels ends in differential Msn2 and Msn4 expression, having as consequence heterogeneity in growth rates and in stress tolerance.

On another hand, *S. cerevisiae* replicative aged cells lose progressively proliferative capacity until they reach senescence[39]. This means that aged cells grow slower than young cells and may overcome challenging environments better than the latter. Though the relationship between replicative aging and proliferative heterogeneity will be more deeply addressed later, it is important to notice that age is a source of proliferative heterogeneity and it is also crucial for fitness and survival[40,41]. In fact, when yeast cells are exposed to a limited resource environment such as low-metal media, the proliferation of the culture is restricted to mother cells, that retain the limiting resource in their vacuoles, and daughter cells arrest in G1[42]. This has been proven to be a stress-response strategy that enhances the survival and fitness of the culture.

Bringing everything together, it is clear that the fluctuating nature of gene expression in microorganisms is a source of survival advantage in population sharing the same environments, ensuring the proliferation of, at least, part of the population and the progression of the progeny and perpetuation of the culture, and that it is tightly related to growth rate [40,41,43–45]. It seems that microorganisms ensure their survival as a population thanks to fluctuations in critical set of genes expression, which leads to proliferative and stress tolerance heterogeneity. in this way, slow growing cells would be at disadvantage (in terms of proliferation) in normal conditions, but if the environment turns hostile, their slow growth give them a critical advantage in the opportunity of adaptation and survival to several external stresses[34,46–48].

Slow growing subpopulation of cells is not only characterized by higher resistance and tolerance to challenging environments, it is also characterized for having a quite interesting expression profile. [49]shows that this subpopulation expresses more diversity of genes than fast growing cells, which have higher expression of a smaller subset of genes. This way, slow growing cells diversify their expression profile at the expense of their proliferation rate, but in beneficial of their survival if the environment changes. That is, because among those genes that are more expressed in slow growers that are not or little expressed in the faster subpopulation, there is higher probability that there are some useful gene for

stress tolerance. Moreover, slow growing cells displays less RNA polymerase fidelity. Having more prone to errors RNA polymerase will increase mutations which could be deleterious for protein function, but in some cases, it can also diversify protein functions, and diversity is a well-known ally for survival and resistance when the environment changes.

1.3 Experimental methods to address proliferation heterogeneity.

Recently, it has become patent for the scientific community that the study of whole populations has been of great importance to have a rough idea of how living organisms function, however, these studies overlook the differences that can be observed when we look at a single cell level. For this reason, in the last few years, the necessity to develop different techniques that would allow the study of populations at a single-cell level increased and, consequently, nowadays there have been developed plenty of different methods to isolate single cells from the rest of the culture.

1.3.1 Single cell microencapsulation

Microencapsulation has been used for years in different fields such as biochemistry, pharmacology and biomedicine[50,51]. In the field of biomedicine, it has been of great importance on the development of specific drug release in certain parts of the body, or the protection of biological active substances from any damage (as for example, protection from the immune system). In this thesis, microencapsulation technique is employed for the isolation of S.*cerevisiae* cells within an alginate particle that allows the flow of media in and out from the microcapsule. These isolated cells can be cultured and later analyzed using microscopy and flow cytometry. This technique has the important advantage of not only separating one cell from the others, but also the progeny of that single cell. This way, for every capsule, it can be analyzed how one single cell has progressed and divided, as well as its progeny for a given time of culture[52] .

As an example, to microencapsulate cells from a wildtype *S.cerevisiae* culture, we use a mixture of cells and a solution of sodium alginate. The concentration of cells used was previously optimized to keep the degree of capsule occupation low. This will dramatically increase the number of empty microcapsules, but will ensure that the vast majority of microcolonies analyzed are produced by a single cell. After the solution preparation, this is injected on a Cellena encapsulator (Ingeniatrics) that will use a nebulizer with constant air flux to form droplets of this solution. The droplets jellify when they fall into a calcium chloride solution forming regular 100µm alginate particles with, in some cases, a single cell trapped

inside. These microcapsules are collected and incubated on rich media and the analyzed by optical microscopy. Interestingly, the microcolonies produced from a clonal culture of *S. cerevisiae* cells, display a wide range of microcolonies sizes as a consequence of different proliferation capacities[52 37].
In light of these facts, the microencapsulation technique not only enables the identification of these proliferation differences, but also allows the study of the possible causes beneath this heterogeneity.

1.3.2 Real-time imaging

Other methods more recently developed consist of microfluidic devices that allows real time imaging of living cells[53–58] . These techniques enable the study of very interesting aspects of living cells, such as growth rate, replicative life span, protein localization changes upon environment fluctuations, etc.

Within this category of methods, we can find different devices: Lee et al. [59] developed a microfluidic device that trapped cells in a uniform focal plane (**Figure 3**). This attached to a fluorescence microscope and adapted into a 96 well plate enables the recording of living cells. Moreover, this device allows the change of media flux (for example, to change the concentration of glucose or any other element of the media) without misplacing the cells, which is of great importance for the following tracking of the cells during the recording. This is not exactly a single cell trapping device, but allows the imaging of several cells trapped in the chamber through the recording time.

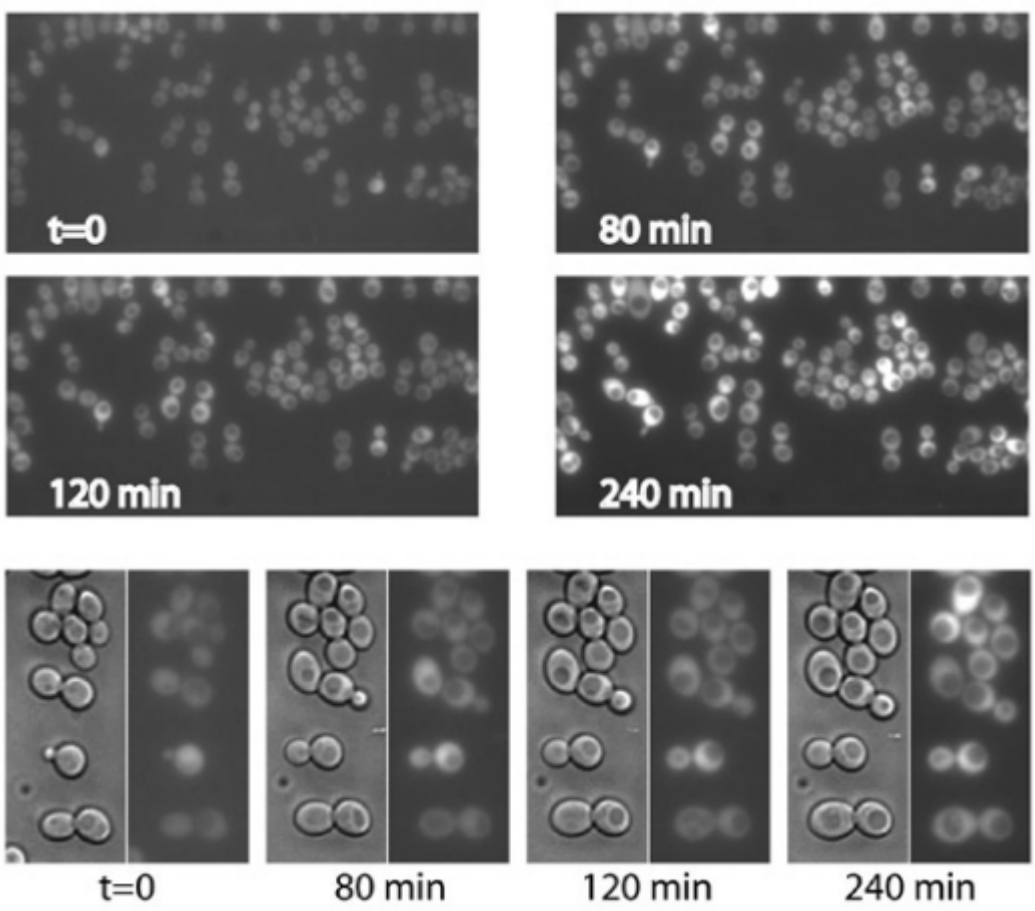

Figure 3. Live imaging of yeast cells. This microfluidic device is attached to a fluorescent microscope coupled with a camera, that allows the recording of living cells within a focal plane. This device enables the live-imaging of several cells under controlled environment that can be changed according to the experiment requirements (adapted from [59].

Similar devices were developed in Welkenhuysen et al. [60] In this model, cells are trapped into wells, also forming a monolayer, allowing the recording of cells and their daughters across time. In this case, single cells can be trapped into the wells if necessary, by adjusting cell concentration. However, several cells fit on every well. This device is also attached to a fluorescence microscope and enables the imaging of fluorescent tagged elements in the living cell.

Other microfluidic methods consist of the trapping of mother cells, which are commonly developed to study replicative life span (**Figure 4).** These devices[58,61,62] trap single cells in a chamber that allows the rotation of this cell, which is important for the release of the new born cell after the budding through the flux network. This is quite useful for studying how replicative age affects mother cells on a variety of aspects, however, it loses all the information from new born cells, which are washed away by the media flow.

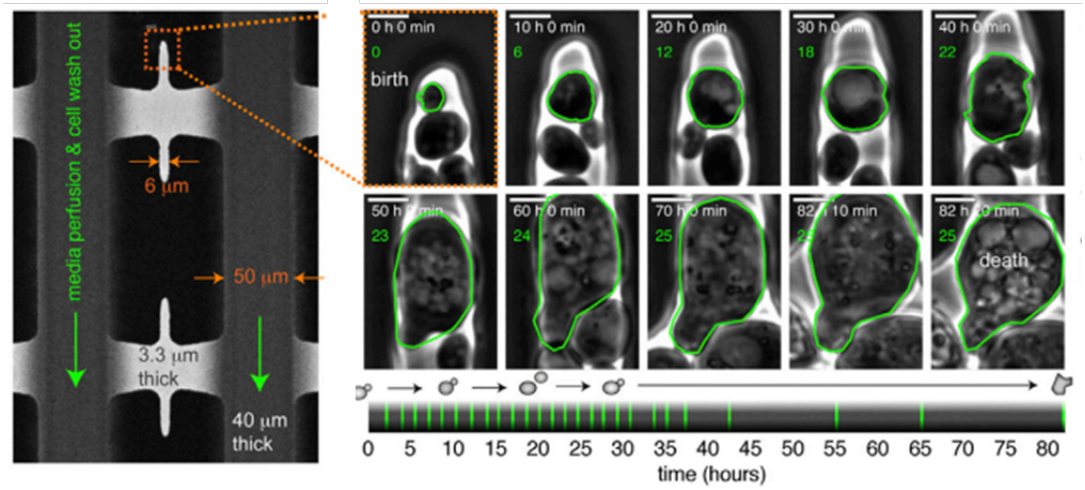

Figure 4. Live- imaging of replicating mother yeast cells. With this device, mother cells can be recorded through their entire lifespan, providing us with a huge amount of information on how mother cells bud, as well as their changes in shape, cell cycle progression, expression of certain genes or size through their replicative lifespans. Daughter cells, however, are removed by the flow [62].

All methods described above, are great powerful tools for heterogeneity studies. Their common limitation is the reduced number of cells that can be analyzed per time unit. However, they enable the study of the high heterogeneity found in every characteristic analyzed on single cells that, if they were to be studied on bulk populations, may be overlooked.

1.3.3 Flow cytometry

Even though this technique does not analyze cells at a single-cell level, it is a powerful tool for heterogeneity analysis of cell populations. Thus, flow cytometry measures a specific trait of cells within a population by making them flow individually in front of its detectors[63]. Depending on the cytometer, these detectors can measure size, complexity and several fluorescent markers by exposing cells to a source of light or exciting laser (in case of fluorescence detection). Fluorescence plays an important role in flow cytometry, and is commonly used to tag different proteins or some other cell elements [64,65]. By measuring the intensity of fluorescent markers, flow cytometers can distinguish small differences of expression among different cells, providing a lot of information about the expression of that particular molecule within a population. The scattered light registered gives information about cell size and complexity of every cell that goes through the detectors, which means, that flow cytometry can provide information about several characteristics. Another advantage of this technique is the high number of cells that it can analyze per time unit. However, the main limitation is the lack of information at a single cell level, which may overlook heterogeneous traits among cells not detectable by cytometry.

In conclusion, all devices to study heterogeneity among isogenic cells have advantages and disadvantages, the choice of one or another depends on which aspect of heterogeneity needs to be studied.

1.4 Aging as a source of proliferative heterogeneity in clonal cultures

1.4.1 Aging model in *S. cerevisiae*

In *S.cerevisiae,* aging can be considered from two points of view. The first one, considers the number of divisions that cells can make before entering senescence and it is known as replicative life span (RLS). In this thesis work, we center our attention in the RLS of mother cells. The second one, is calculated by the maximum time of survival of non-dividing cells and it is denominated chronological life span (CLS) [39,66,67].

Laboratory yeast strains have a mean RLS of approximately 20 divisions (depending on the background this number can vary by some divisions)(MORTIMER RK & JOHNSTON JR., 1959). This aging process is characterized by accumulation of oxidative reactive species (ROS), increased cell volume, increased generation times and in the latest states of aging, increased DNA damage, loss of DNA repair capacity and failure to activate cell cycle checkpoints[62,69–72]. All this combined, leads to cell senescence and death of mother cells after a high number of divisions [73,74].

Interestingly, in *S.cerevisiae*, the replicative aging process is tightly linked to asymmetric division. Due to this phenomenon, mother cells retain aging factors, which are deleterious for cell survival and division, allowing the new-born daughter cell to gain full proliferative capacity [74]. In this way, mother cells keep accumulating aging factors on every division until they reach senescence [75–77]. The canonical model of replicative aging in yeast can be explain using a spiral [67] in which every loop represents a cell division (**Figure 5**)**.** The mother cell gives birth to a new-born cell with full proliferative capacity for most of its replicative lifespan, retains aging factors and grows in size. However, the retention of aging factors, maybe due to the excessive cell volume[78] and the severe accumulation of them, is defective at late stages or the mother cell lifespan, and it starts giving birth to new-born cells with less proliferative capacity and lower replicative lifespan.

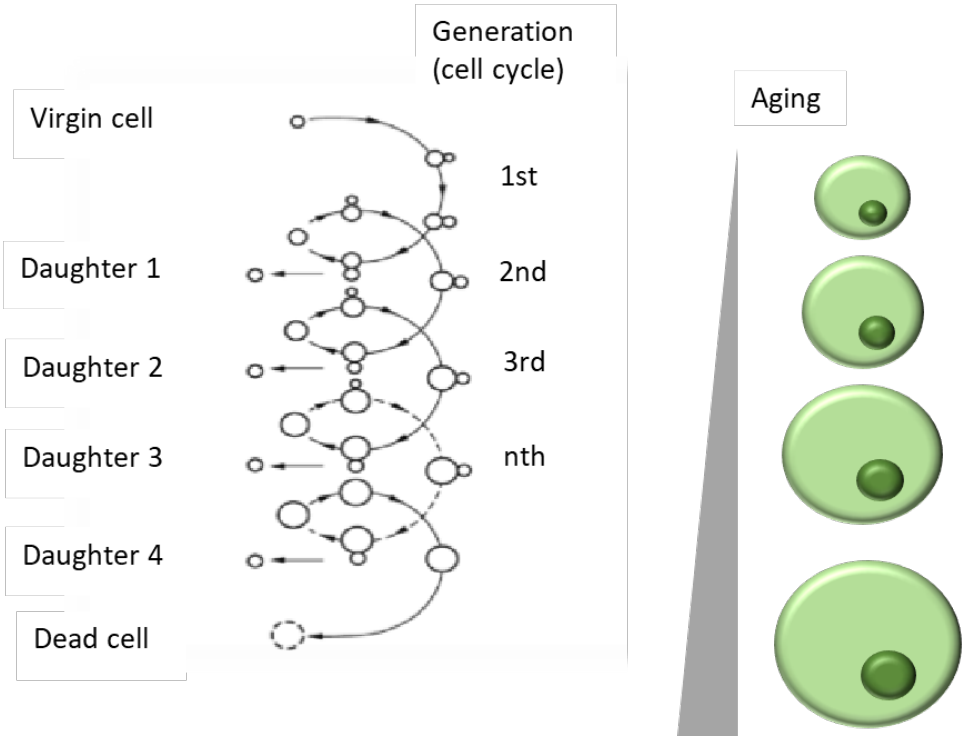

Figure 5. Spiral model of replicative aging in S.cerevisiae. This model exemplifies the replicative lifespan of any given cell. This cell starts dividing and, with every division, the mother cell gives a new-born cell with full proliferative potential but, in turn, the mother cell retains damage and aging factors, as well as growing bigger in size. Finally, due to the accumulation of these aging factors, the mother cell dies (Adapted form (Michael Breitenbach et al., 2012)).

In *S. cerevisiae*, this aging process can be monitored thanks to the formation of bud scars on every division, a chitin accumulation on the cell wall of the mother cell. This allows the quantification of how many divisions a mother cell has produced by simply staining the cell wall with calcofluor and the subsequent counting of the bud scars number (**Figure 6**).

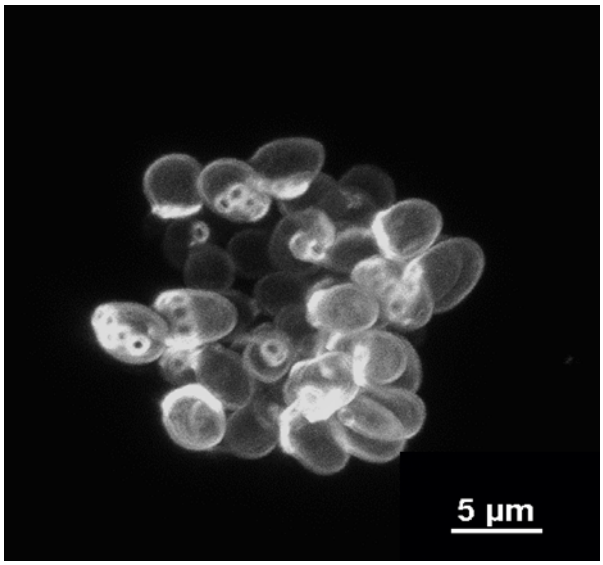

Figure 6. Calcofluor staining of a *S.cerevisiae* microcolony. The calcofluor stain has high affinity for the chitin accumulation that forms the bud scars. This impressions on the cell wall are left every time the mother cell divides.

1.4.2 Replicative aging and heterogeneity in *S. cerevisiae*

There are several aspects of replicative aging that impacts on the proliferative heterogeneity found in clonal cultures [79–83]. The first one and more evident is the effect of asymmetric cell division. Moher and daughter cells make a symmetric repartition of the majority of the cytoplasmic proteins, however, certain proteins and other elements such as ERCs (extrachromosomal rDNA circles) are retained in mother cells[77,84–86].

Asymmetric division constitutes an important source of heterogeneity among clonal cells in *S. cerevisiae*. Apart from differential inheritance of deleterious aging factors such as misfolded protein aggregates and ERCs between mother and daughter cells, the newly replicated Spindle Pole Body (SPB) is also asymmetrically inherited by the mother cell. This has been proven to be necessary for rejuvenation of the daughter cell, and crucial for its replicative lifespan [75]. There are a lot of mechanisms implied in maintaining the correct asymmetric segregation of aging factor to the mother cell, that includes the old SPB systematic inheritance by the daughter cell, in order to preserve the fitness of the culture. It basically consists of continuously creating an immortal lineage with full replicative capacity, and this confers proliferative heterogeneity to the culture, which is also a strategy for fitness and survival itself. In normal conditions, cells with higher proliferative capacity outcompete those with lower proliferation rates, but are also known for having more susceptibility to toxic agents and stresses. Cells with lower proliferation rates, however, conforms the subpopulation more resistant to challenging changes in the environment [30].

The accumulation of aging factors in older cells in a progressively and continuous way constitutes a source of heterogeneity among clonal cells proportional to the different replicative ages found in the culture. As a consequence, intracellular heterogeneity increases with replicative age due to asymmetric cell division. As older cells generally have slower proliferation rates, which provides them with better adaptation to environment and a more heterogeneous expression profile [42], they conform a subpopulation of slow grower cells very heterogeneous among themselves.

A specific example of this is the accumulation of ERCs and other circular DNAs during aging. They are asymmetrically retained into the mother cell during cell division, which leads to exponentially higher concentrations of this ERCs with replicative age, until a certain threshold of repeats that is too high for the cell to maintain cell homeostasis and leads senescence entry and cell death. An increased rDNA regions activity produces more ERCs. These are formed by double strand breaks and recombination events of the rDNA cluster, caused by the action of Fob1, a nucleolar protein that binds rDNA repeats and blocks the transcription

fork in order to avoid the collision between DNA replication and rDNA transcription machinery [84]

As ERCs, other circular DNAs are also asymmetrically segregated to the mother cell and may as well have their own replication fork, which allows its replication during S phase. However, some circular DNAs do not have a replication fork or, despite having it, the do not replicate efficiently during S phase, so their concentration decreases with age. Interestingly, this accumulation of circular DNAs is not random. For example, Hull et al. [86] shows that formation of circular DNA containing a stress protectant against cooper (CUP1) is proportionally dependent on transcription of CUP1 chromosomal locus, and this is regulated by cooper presence. This means that mother cells that have been previously exposed to cooper, having accumulated circular DNAs containing CUP1 will have advantage compared to young cells when a future exposure to cooper occurs. If we could extrapolate this to other stress protectant genes, we could explain why older cells are more prone to resist environmental changes than young cells, having a proliferative advantage in these situations at the expense of having less proliferation capacity in not deleterious conditions.

Finally, the more studied gene in aging, *SIR2,* can also explain some of the heterogeneity caused by replicative aging. Sir2 is a NAD+ dependent histone deacetylase involved in silencing of heterochromatin regions, especially in the regulation of rDNA region stability, and it has been long described as a longevity gene. Loss of Sir2 produces instability of rDNA region which leads to a decreased replicative lifespan. However, it has little effect on chronological aging, or even *sir2Δ* mutants display a shortened CLS [87]. This means that Sir2 activity prolongs the number of times a cell can divide before entering senescence (RLS), but is has the opposite effect on the time the cell lives before entering senescence (CLS).

Some studies [87–89] reveals stochasticity in Sir2 expression, which may lead, once surpassed the threshold, to significant differences among cells in terms of their replicative life destiny: Higher Sir2 activity increases deacetylation of heterochromatin and rDNA regions, silencing them and decreasing genomic instability, and this favors an increased proliferation capacity. ERCs accumulates almost completely in mother cells, and are thought to interfere with nucleolar machinery, leading to senescence and death. This means that cells with higher silencing in these regions produce less ERCs and they will have longer proliferative lifespan. Interestingly, this differences in epigenetic patterns, that produces proliferation heterogeneity among clonal cells, are also caused by stochastic variations in Sir2 levels, which suggest that heterogeneity is an undeniably complex phenomenon. In terms of replicative capacity, cells with higher Sir2 expression will have more advantage. It has been described that cells with an increased size have less Sir2 expression and, therefore, a reduced replicative lifespan [87]

In summary, replicative aging together with asymmetric cell division are responsible for great part of the proliferative heterogeneity found in clonal yeast cells. Therefore, we considered it an important element worthy of study in our proliferative heterogeneity field together with cell cycle, as a key connector element between asymmetric cell division and cell replicative aging.

1.5 Cell cycle as a source of proliferative heterogeneity

1.5.1 Cell cycle in S. cerevisiae

Cell cycle in yeast have great similarities with mammalian cells. In both, cell cycle starts with the commitment of the cell to divide. This decision depends on the integration of internal and external signals and, once they have committed, there is no way back to the previous cell cycle phase[90,91].
In yeast, as in all eukaryotes and, therefore, similarly to mammals, cells undergo through G1 phase to S phase to enter after that G2 and mitosis in which cells segregates the chromatids between mother and daughter and finally, the cytokinesis separates both cytoplasm.

The restriction point in mammals, or START in yeast, is the point beyond which cells commit to cell cycle [90]. In yeast cells, START point mainly controls, between others, that cells have the correct size to divide. The mechanisms by which cell "sense" that they have reached the correct size remains unclear and is a subject in discussion. Nevertheless, there seems to be a consensus in that cyclin Cln3 responds to the "correct-size-signal" forming a complex with Cdc28, the only cyclin dependent kinase in yeast. This complex Cln3/Cdc28 inhibits the repressors Whi5 and Stb1. They stop repressing the transcription factors SBF and MBF, which are responsible for the transcription of more than 200 genes implied in the cell cycle progression[92]. This generates a pulse of transcription that will activate the transcription of activators of the cell cycle, but also inhibitors of cell cycle repressors (Whi5, among them) [93,94]. An example of this are the G1 cyclins Cln1 and Cln2 that are activators of the G1/S transition but also repressors of Whi5. This creates a positive feedback loop that guarantees the no-return of cells to the previous cell cycle phase. This transcription pulse, moreover, also enhances the transcription of several cyclin repressors that, eventually leads to the degradation of the G1 cyclins and the activation of the correct subset of genes for the next cell cycle phase (**Figure 7**)[90,95–97].

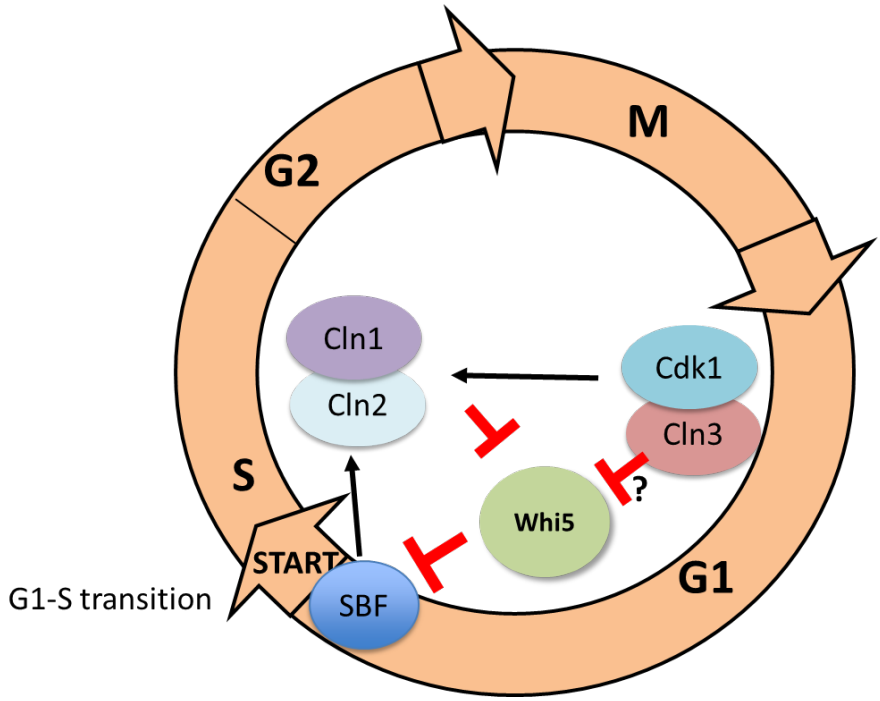

Figure 7. G1/S transition through START. The Cln3-Cdk1 (Cdc28) complex enhances the activity of transcription factors SBF and MBF, although it is still not clear whether it does through Whi5 direct inhibition or not. This produces the transcription of G1 cyclins Cln1 and Cln2, among other necessary genes for cell cycle progression. These G1 cyclins further inhibit Whi5 creating a positive feedback loop that ensures the cell commitment to progress through the cell cycle.

As expected for a critical mechanism for cell survival, cell cycle is tightly regulated. There are several checkpoints during cell cycle that control the accuracy and correct replication and segregation of the chromosomes, as well as other aspects as correct cell size and right spindle body localization. START is the first and essential control point during cell cycle and mainly controls, among others signals, cell size and nutrients availability. Whi5, as mentioned above, is a G1/S transition inhibitor necessary for accurate input into S phase*, thus* Whi5 mutants enter cell cycle with smaller size as the wildtype [98–101]. Cln3 also controls cell size upon cell cycle progression, however, the lack of this cyclin is neither essential for cell cycle progression but, *cln3Δ* mutants are larger than wildtype cells because the longer time spent in G1[102,103]

This suggest that cell size is important for division commitment, maybe even for culture fitness, but it is not essential. Finally, at START are also controlled other aspects of great importance for cell survival as nutrient deprivation or other kind of stress. In case of low nutrient availability, cells arrest in G1 trough Sic1, a cyclin dependent kinase inhibitor or CDKI. Sic1 is stabilized by the inhibition of TORC1 pathway upon nutrient restriction and arrest cells in G1, preventing them of entering a new cell cycle and enlarging the population in case of nutrient deprivation[104].

In other stresses such as osmotic stress, cells are also arrested in G1 by downregulation of G1 cyclins thanks to the activity of Hog1. Hog1 is a stress-activated protein kinase responsible for adaptive responses upon stress, and

targets cell cycle regulator such as Whi5 and Msa1[105] (a cell cycle activator) to coordinately repress G1 cyclins expression [106].
Another important checkpoint is the DNA damage control in G2/M phase. The activation of this checkpoint prevents cells from going through metaphase/anaphase transition to avoid chromatids segregation in case of DNA damage or incomplete DNA replication of the sister chromatids, and it depends on the activation of several proteins implied in the DNA Damage Response or DDR. Among these proteins, there are Rad9 and Mec1, necessary for the phosphorylation of Rad53, which is essential for DNA damage reparation, G2/M arrest and stabilization of replication forks[107–109].

The correct progression of the cell cycle and the survival of the progeny depends on the correct functioning of these regulatory pathways, that guarantee the correct propagation of the genetic material to the next generation.

1.5.2 Whi5 and asymmetric cell division

In light of the information displayed, cell cycle is an utterly essential process for cell survival and culture fitness. In *S.cerevisiae*, the cell cycle is an asymmetric division between mother and daughter cell. In this type of division, mother cells retain the aging factors, achieving a full replicative potential and rejuvenation for their daughters. This has been proven to be of great importance for culture fitness [75–77].
Asymmetric cell division has another characteristic, and it is the size difference between mother and daughter cells. In addition to the aging factors, mother cells also retain a great part of the cytoplasm, making daughter cells smaller in size. This explains why daughter cells spend more time in their first G1 until they reach the correct size to divide, although the mechanisms implied in this regulation is still poorly understood.

1.5.3 Whi5 role in cell size regulation

What seems clear is that Whi5 plays an important role on this size regulation prior to cell cycle entry in daughter cells. It has been shown that daughter cells spend more time in G1 thanks to the retention of Whi5 in their nucleus by preventing its exportation through the nuclear pore complexes (NPC) [110]. These NPC are deacetylated by Hos3, a lysine deacetylase that is specifically located to NPCs in daughter cells, retaining Whi5 in daughter nuclei but not in their mothers. However, how cells decide to enter cell cycle once they have reached the correct cell size is still on debate. The fact that cells divide in a very narrow range of size, reveals a thigh control of cell size prior to cell division, which why a great number of researchers have tried to unravel the mechanisms behind its regulation.

Until very recently, some studies [96,101,111–113] shed some light to the mechanisms underlying size control and cell division: Whi5 concentration dilution. In this study, they postulate that Cln3 and Whi5 synthesis rates escalate differentially with cell size. Whi5 is synthesized during late G2/M phase and, in this model, does not scale with cell size, which leads to a dilution of the repressor with cell growth. In contrast, Cln3 does not increase its activity prior to G1/S transition, but its synthesis rate does scale with cell size. This means, that Cln3, the activator, has constant concentration and activity while cell grows, however, Whi5 is diluted due to the increase in cell size during G1 phase. Reaching the correct threshold of Cln3 activity and Whi5 dilution would lead to a rapid Whi5 inhibition and the outbreak of cell cycle transition.

Nonetheless, some other recent studies [114–117] suggest that Whi5 dilution is not the key to understand how cells achieve to divide in such a small range of size. Although they have found evidences that are consistent with Whi5 dilution taking place, some other experiments show that the dilution model is not sufficient to explain how cells control the size at which they divide. Firstly, when Whi5 is expressed from a galactose-dependent GAL1 promoter, its synthesis rate does scale with cell size and, therefore, it is not diluting with cell growth. However, these cells show very similar sizes as cells that express Whi5 from their endogenous promoters. Secondly, cln3 [114,115] studies reveal that Cln3 concentration does peak prior to G1/S transition and that this increased activity determines cell cycle entry. Moreover, there are studies that suggest that Whi5 is not a good phosphorylation target of Cln3. Rather than that, what drives G1/S transition is an increased Cln3 activity, that leads to RNA polymerase II activation in SBF and MBF promoters, which eventually transcribe G1 cyclins Cln1 and Cln2 that finally phosphorylate and inhibit Whi5. This transcription pulse is enough to activate cell cycle progression.

Furthermore, other studies suggest that Whi5 concentration does not even vary through G1 and that the previous observations are biased by the techniques employed [115].

To summarize, cell cycle and size are tight connected and regulated by still poorly understood mechanisms. However, Whi5 plays an important role in both, especially in daughter cells, that is yet to determine.

1.5.4 Whi5 in replicative aging and senescence

Recent studies have provided a new insight of replicative aging and senescence, portraying aging as a continuous process since early divisions. On this aspect, Whi5 has been identify as a key element in cell cycle deregulation and mortality in old yeast cells [118].

Since the first divisions, mother cells start accumulating aging factor, as proteins aggregates among others. In fact, protein aggregates form in yeast cells an age-dependent protein deposit (APOD) since early in their replicative lifespan.

Proteostasis deregulation is a well-studied hallmark of aging and is mainly due to the lack of chaperone availability. This leads to arrest in G1 and death in half of yeast old cells. [119]proposes that chaperone availability is key in replicative lifespan of cells, and compromised chaperone availability leads, possibly through a decay in Cln3 activity (which responds to chaperone status) leading to a G1 arrest that ends in cell death. During the last few divisions, they also find Whi5 accumulation in old yeast cells, previous to their G1 arrest and cell death.
In Amon et al, the same accumulation of Whi5 in old yeast cells is described. In this study, there seem to be Whi5 dependent and independent mechanisms that lead to G1 and S cyclins expression defects. This causes a delay in G1/S transition that is responsible for DNA replicative stress and replication errors, driving old yeast cells to G1 arrest and cell death.

In conclusion, cell replicative aging starts since the first divisions, accumulating aging factors and, possibly, other proteins as Whi5. Although not all cells arrest in G1 before entering senescence (the other possibility is progressively longer G2/M phases and arrest in this phase), it has been described that, for some cells, the accumulation of aging factors as well as Whi5, eventually leads to G1/S transition delay and replication defects that arrest old cells in G1 and finally, causes cell death. We might consider, then, that this arrest in G1 may not be an abrupt event at late stages or replicative lifespan, but also a continuous process since the first divisions and that, inherent heterogeneity also plays a role in the effects that this accumulation and cell cycle deregulation produce in yeast cells [118,119].

2. Objectives

1. To stablish a reliable method to study the influence of replicative age on proliferation heterogeneity.

2. Determining the role of Whi5 in proliferative heterogeneity.

3. Decipher the role of cell cycle regulation in coupling replicative age and proliferative heterogeneity

3. Results

3.1 Chapter 1: Development of a new methodology for replicative age determination in slow proliferative populations: a single cell and microcolony analysis

3.1.1 Replicative age determination of single small microcolonies founder cell by confocal microscopy

The first aim of this part of the project was to determine the possible causes for slow proliferation rates in small microcolonies after encapsulation to get insights into proliferative heterogeneity bases. It is well known that there is a positive correlation between replicative age and slow proliferation rates [79,119,120]so we decided to establish a method for founders replicative age determination in small microcolonies.

In order to identify the founder cell and check its replicative age, the first step was to microencapsulate a wildtype culture as described in Materials and Methods. The microcolonies obtained after the incubation were stained with calcofluor, whose affinity for the chitin polysaccharides in the fungi cell wall allows the visualization of bud scars under the fluorescent microscope. Bud scars are left on the cell wall every time a mother cell divides and is an indicative of how many times that cell has given birth to a new-born cell. We took advantage of this property of fungi to quantify the number of bud scars on every cell of the small microcolony analysed and, by doing this, study the genealogy of the small microcolony.

After this, microcapsules were disposed into a slide and then analysed under the confocal microscope. We considered that small microcolonies were those that do not exceed half the radio of the capsule (that is, if the capsules measures around 100µm, a small microcolony does not exceed 25µm) and the microcolonies that met this criterion were analysed by capturing one image every 0,5µm in the Z stack of the microcolony in brightfield and with DAPI filter. The last one allows the visualization of the calcofluor staining of bud scars in every cell into the microcolony. An example of this single cell analysis is shown in **Figure 8** where we can observe in the upper part of the panel a small microcolony as seen under the confocal microscope when it combines the light perceived in every Z plane under the DAPI filter. Noticeably, cells and bud scars are hardly quantifiable. However, if we decompose this image into several Z stacks, we can more easily count the number of cells and bud scars going through every plane of the small microcolony (**Figure 8 Z-01 to Z-09**).

The first thing we noticed is that small microcolonies have between 4 and 64 cells, and that this small number allowed us to clearly quantify the number of cells in every small microcolony and, most important, the quantification of the bud scars present in every cell that conformed that small microcolony on the

majority of the small microcolonies analysed (96 small microcolonies out of 155 analysed).

Among other advantages, confocal microscopy enables the analysis of 3D structures as are the small microcolonies. By capturing imaging on Z plane of the microcolonies, we could quantify cell number as well as bud scars for every cell, even if this cell was in the centre of the sphere that the small microcolony forms within the alginate microcapsule.

For every small microcolony analysed, cells and bud scars were counted taking onto account every Z plane image of the microcolony, and then these data were used to estimate the replicative age of the founder cell. We reasoned that a good approach to understand the proliferative heterogeneity bases, is, first, try to understand how low proliferating small microcolonies are generated. In order to do so, the identification of the founder cell was essential, and we determined that by finding and counting the bud scars of the cell with more bud scars on its cell wall. After this, we counted the total number of cells and the number of bud scars in every cell in order to reconstruct the genealogy of the small microcolony.

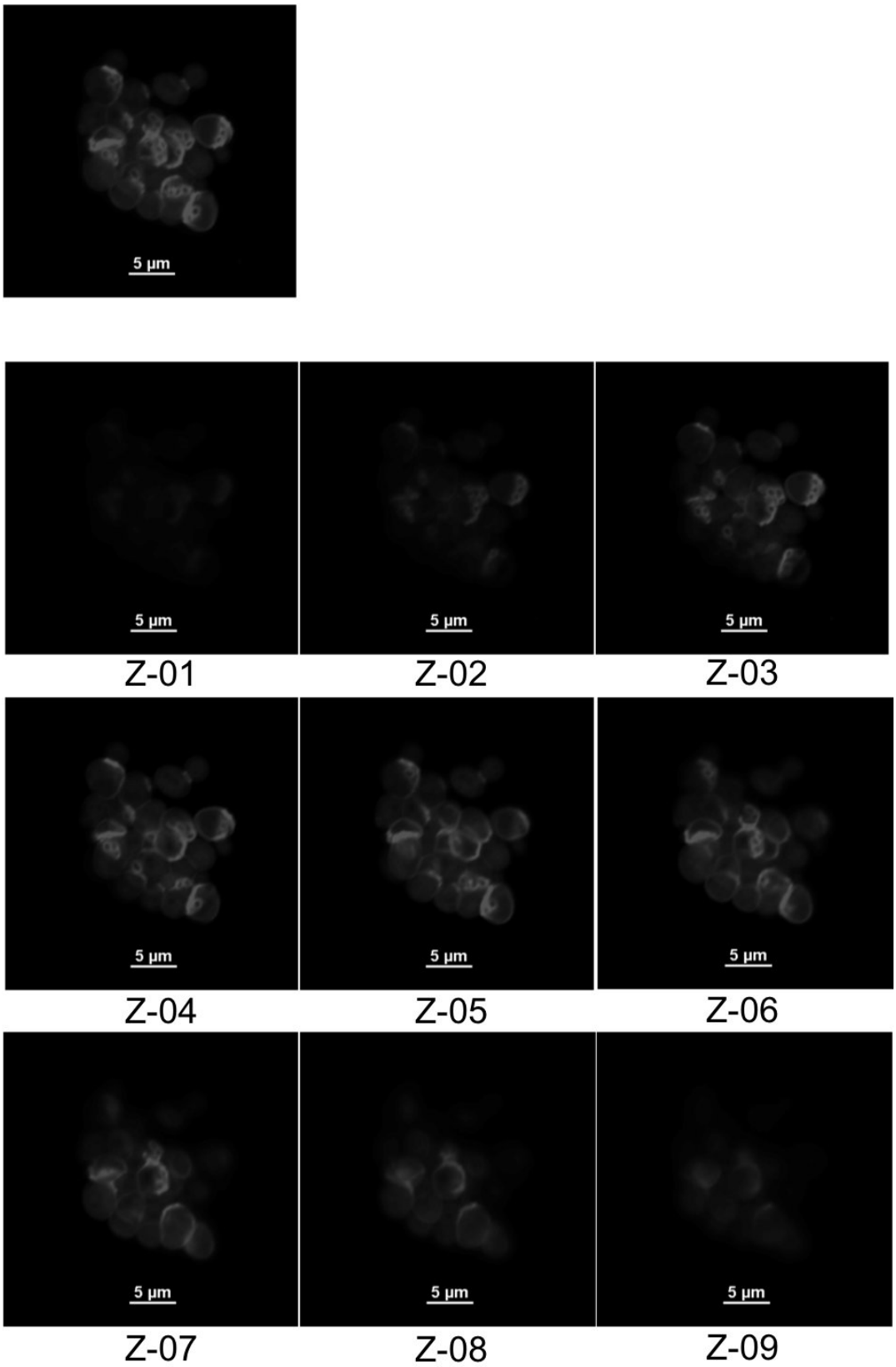

Figure 8. Confocal images of 9 different Z stacks from a small microcolony stained with calcofluor. In the upper part of the panel, the Z projection of this small microcolony, which is the sum of the highest signal of every pixel for every Z stack. Although in the latter it seems impossible to identify the founder cell or even quantify the number of cells and bud scars, the confocal microscope allows the segregation of a 3D small microcolony into several 2D images in the third plane. This enables the quantification of cells and bud scars for the majority of small microcolonies.

3.1.2 Genealogy studies reveals two different proliferative growth patterns for small microcolonies

Once the method to study the genealogy of small microcolonies was stablished, we obtained the data of 96 small microcolonies (these are the ones of which we could correctly estimate the total number of cells and the total number of bud scars), and the first thing that we realised was that small microcolonies present two different proliferation phenotypes: the first one, and more common (84 out of 96 small microcolonies analysed), is characterised by the equal division of every cell that forms the small microcolony. In this case, every cell within the microcolony contributes proportionally to its formation because every cell divides more or less at the same rate. We have called this pattern "isotropic proliferation" and we can see an example of this in the **Figure 9.A**. This pattern could be easily seen because bud scars are present in almost every cell (with the exception of new-born cells that did not divide before the fixation of the microcolonies) and, curiously, there was decreasing gradient of bud scars number present on cells from the centre of the small microcolony towards the edge. In the **Figure 9.B** we can observe a scheme of how this small microcolony might have been formed. In light orange we can see the founder cell of the small microcolony. In order to reproduce what we can see in the confocal images of this small microcolony, which can be seen in **Figure 9.A** and represented as the 7^{th} generation in the scheme of **Figure 9.B**, we can infer how these cells might have divided from the first generation to the last one to explain the results observed under the microscope. Thus, what we see from our small microcolony is the last stage of its formation, and it can be observed 1 cell with 5 bud scars, 3 cells with 2 bud scars and 4 cells with 0 bud scars. The simplest explanation to this is represented in the scheme of **Figure 9.B**: the founder cell had 4 bud scars prior to forming the small microcolony, and its daughter (daughter cells are represented in green when they are newly born and in red when they undergo their first division) divides twice. One of the daughters of the first-born cell divides twice as well and then, one of the daughters of these cells (from the first or the second born cell, this is not known) divides another 2 times. This way we can approximately reconstruct the genealogy of the small microcolony and determine that its proliferation was isotropic. We can also observe for this specific example that the founder cell was not a new born cell. However, this is not the case for all small microcolonies with an isotropic proliferation pattern as we will show later in **Table 1**.

The second proliferation phenotype that we detected was characterised by the almost exclusive presence of bud scars in the founder cell (**Figure 9.C**). We have called these patterns "anisotropic proliferation". This probably meant that the founder cell was almost the single contributor to the small microcolony formation and this is represented in the scheme of **Figure 9.D**. For a reason that we are yet

to clarify, cells born from this mother cells are not able to produce any division and the mother is the only one with proliferative capacity. In this example, we can observe that the founder cell had 0 bud scars when it founded the small microcolony.

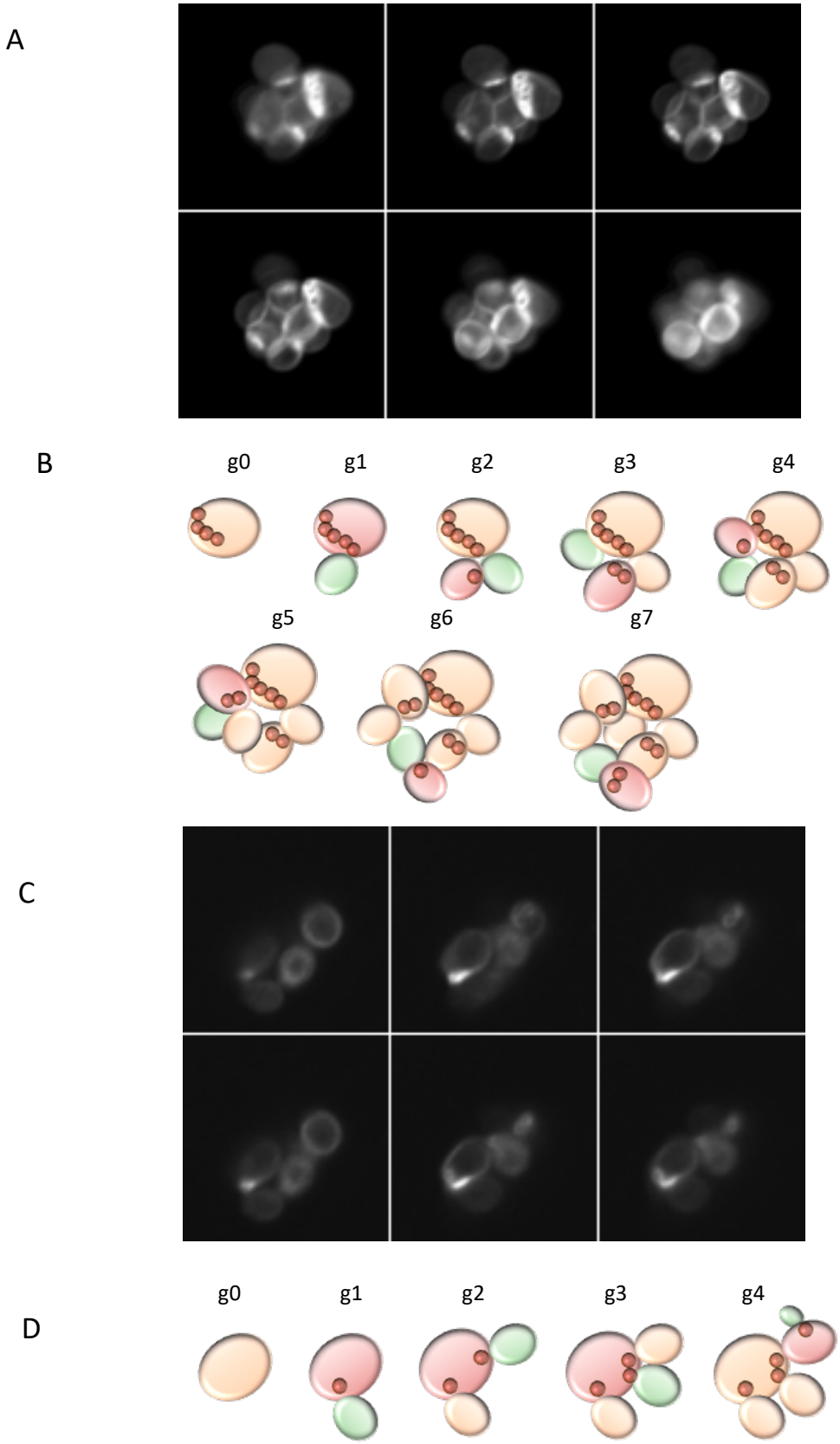

Figure 9. Examples of the two categories of small microcolonies found, differentiated by the division pattern of the cells within the microcolony. (A) Different Z-stacks taken by confocal microscopy of the same small microcolony after 13 hours of growth. This small microcolony founder cell was not virgin when it founded the microcolony at g0. In this category are included those whose founder cell or first-born cell are the only one dividing. (B) Graphical representation of an isotropic small microcolony genealogy. In this category are included those whose cells divide equally. The header letters g0-g7 indicates the hypothetical time at which a new division occurs. For every division,

the mother cell is coloured in red and the daughter new-born cell in green. (C) Confocal image of said small microcolony at 13 hours of growth. This small microcolony was founded by a virgin cell. (D) Genealogy of an anisotropic small microcolony.

The last case explains the formation of, at least, a small portion of small microcolonies. In this situation, the proliferation rate is not low, it is simply the inability of daughter cells to divide and produce more new-born cells.
A summary of all these data is detailed on **Table 1**. We noted that the vast majority of small microcolonies, 84 out of 96 analysed, presented isotropic growth, in which every cell within the small microcolony contributes to its formation. 12 of them presented an anisotropic growth, or a proliferation phenotype in which only one of the cells, typically the founder or one of its daughters, is the only contributor to the small microcolony formation. If we estimate the replicative age of each small microcolony founder cell, we can see that new born and non-new born founder cells contributed equally to the formation of small microcolonies with both isotropic or anisotropic growth. However, in the case of the anisotropic small microcolonies, the number is not representative enough to reach any conclusion, although it seems that there are more aged founders in these cases. In any case, to continue with this work, we will focus on small microcolonies showing an isotropic growth which represent the vast majority of small microcolonies.

Small microcolony type	Number of small microcolonies	Founder cell type	Number of small microcolonies
Isotropic growth	84	Newborn	40
		Non-newborn	44
Anisotropic growth	12	Newborn	3
		Non-newborn	9

Table 1. Table showing the number of small microcolonies that presents an anisotropic growth, or an isotropic growth type. Small microcolonies are classified as "isotropic" when all cells within that microcolony divide equally. They are classified as "anisotropic" when one cell (that can be the founder, or first-born cell) produces almost all the divisions within the small microcolony. Either new-borns founder cells or more replicative aged founders, are represented equally in both kinds of growth small microcolonies.

3.1.3 Small microcolonies are more frequently founded by non new-born cells

Less than 10% of small microcolonies formation can be explain due to the anisotropic proliferation of its cells **(Table 1)**. However, more than 90% of the

cases have still no clear explanation. What makes a cell, and more importantly, all its progeny, proliferate slower than the rest of the culture cells?

Proliferative heterogeneity in clonal population has already been widely described but has been frustratingly difficult to study, until very recently, thanks to single cell techniques. Encapsulation of clonal cells is one of those techniques and it allows the study of the possible causes of lower proliferation rates in clonal cells. Using microencapsulation and the replicative age determination method previously described, we decided to study the implications of replicative age of the founder cell in the formation of small microcolonies.

First, we established a formula that could precisely estimate the replicative age of the founder cell before founding the small microcolony: $number\ of\ bud\ scars - number\ of\ cells + 1 = founder\ cell\ age$.

To calculate the replicative age of the founder cell we could just count the total number of cells and the total number of bud scars. In the example shown in **Figure 10 (A.1),** we observe a small microcolony that, after 3 generations, has 8 cells in total. If we count the total number of bud scars present on every cell in this example, we obtain that this number is 10. Applying the formula: 10 bud scars – 8 cells +1= 3. This is the replicative age of the founder cell prior to the formation of the small microcolony (which corresponds to the replicative age that had the founder cell before the first generation). In the example from **Figure 10 (A.2)**, we count the same number of cells, 8, and we count 7 bud scars in total, we obtain 0. This means that the small microcolony was founded by a new-born cell.

With this estimation, we analysed the 96 small microcolonies previously studied and determined the replicative age of their founders. We also took a sample of the same culture before encapsulation to obtain the distribution of the replicative age of a normal exponential culture. If the replicative age of the founder was not implicated in the slower proliferation rates of small microcolonies, the proportion of the different replicative ages found in the exponential culture prior to the encapsulation, should be still maintained in the population of small microcolony founders. However, when we compared those data, shown in **Figure 10.B**, we found that the founders of small microcolonies where, with more frequency, not new-born cells. Instead, they were more frequently founded by cells that had already undergone a few numbers of divisions, between 2 and 4 divisions, that we will designate early-aged cells from now on. To our surprise, the replicative age of the founder cells was not specially high, nor they were old enough for them to undergo longer cell cycles as described in very old cells that could explain why these cells have lower proliferation rates and how do the daughter cells inherit this lower proliferation capacity.

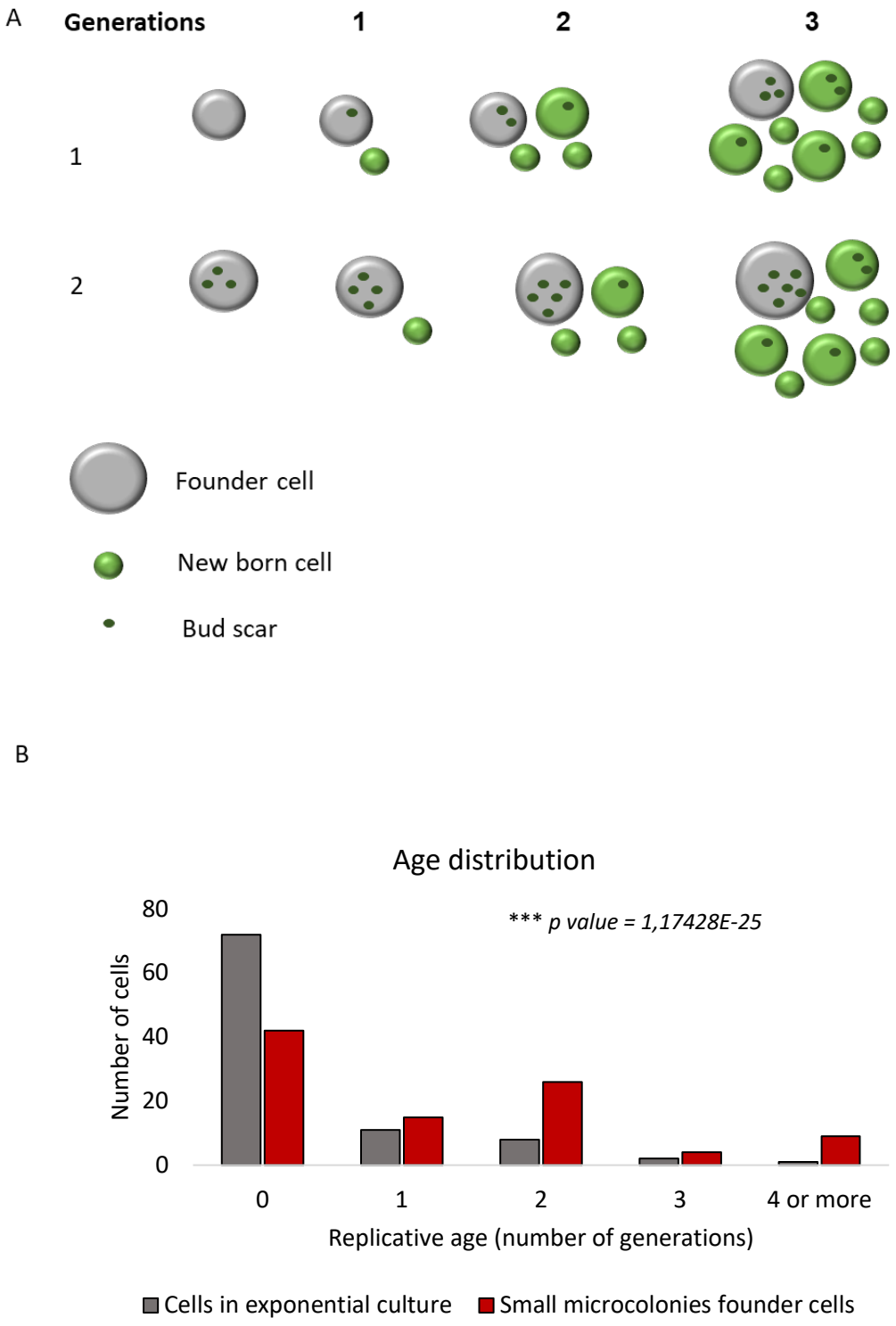

Figure 10. **Small microcolonies are frequently founded by cells with a replicative age greater than 0.** (A) Scheme of how a small microcolony might have been formed according to the replicative age of the founder cell. (A.1) A small microcolony founded by a new-born cell (it has no bud scars so the number of divisions that this cell has undergone is 0 at the time of its encapsulation as a single cell) during 3 generations. If we subtract the number of cells to the number of bud scars we obtain -1. We add 1 because the small microcolony starts by having 1 cell already at generation 0. We then obtain the replicative age of the founder cell, which is 0. (A.2) A small microcolony founded by a cell with 3 divisions. By applying the same formula, we obtain that the founder replicative age before founding the small microcolony was 3. (B) Distribution of small microcolonies founder cells (red) according to their replicative age before founding the microcolony (n=96) compared to that of the initial exponential culture before encapsulating (grey) (n=96). Small microcolonies are more frequently founded by cells with a replicative age greater than 0. The statistical test realized was a chi square test with a result of a p value equal to 1,17428E-25.

With the results obtained, we can conclude that the replicative age of the founder cell is important, or at least contribute, to the formation of the small microcolonies obtained from the clonal culture after encapsulation since mother cells perform the very first divisions.
Moreover, we studied more deeply the connection between the founder cell replicative age and the proliferative capacity in small microcolonies. The number of cells that form a small microcolony ranges from 4 to 64 cells, so we decided to analyse the replicative age of the founder cell and then correlate this to the number of cells in the small microcolony. What we observed was represented in **Figure 11**, and it shows that it was more probable that a founder with higher replicative age, founded a small microcolony with less cells. This means that, the "older" the founder cell is, the smaller is the small microcolony that it forms.

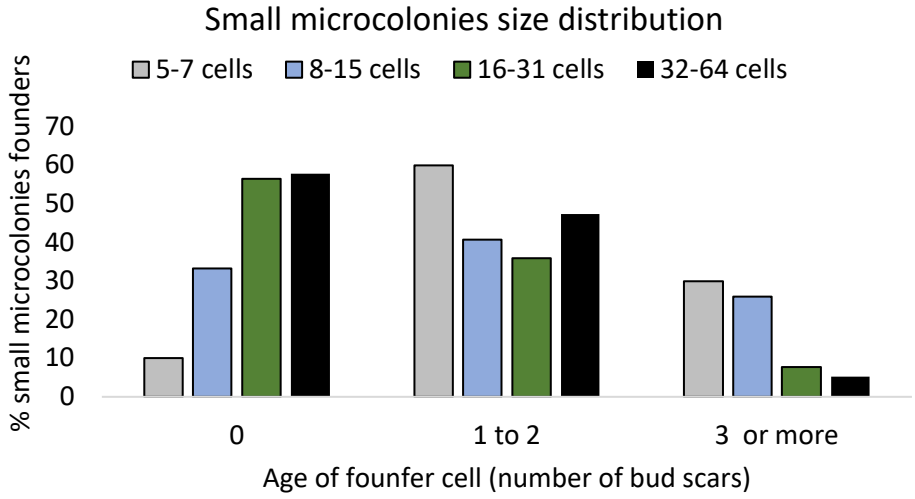

Figure 11. Frequency of founder cells according to their replicative age that founded small microcolonies of different sizes. From bigger to smaller small microcolonies, we decided to group them into 4 categories: 32-64 cells, 16-31 cells, 8-15 cells and 5-7 cells. A progressively increase in the number of founder cell bud scars can be observed in smaller categories.

3.1.4 An increase in the replicative age of wildtype cultures enhances the frequency of low proliferating small microcolonies formation.

To reinforce the contribution of the early replicative age in the formation of small microcolonies, we decided to study what happens if a culture enriched in cells with similar replicative ages as the founders of the small microcolonies is encapsulated.
In order to do this, we first used a well described strain to enrich in mother cells: MEP system strain (DNY51)(Lindstrom & Gottschling, 2009). This strain has integrated in its genome a gene that codifies for a Cre recombinase under the control of a specific daughter cell promoter. Thus, Cre recombinase can only be active in daughter cells in the presence of Estradiol, which allows the

translocation of the Cre recombinase from the cytoplasm towards the cell nucleus. Once in the nucleus, the enzyme recognises the lox P sites that are flanking two essential genes for the cell (CDC20 and UBC9), recombines them and exscinds these essential genes which imply cells not able to divide **(Figure 35).**
The experimental procedure performed consists of treating a culture of this strain with Estradiol for approximately 3 hours. During this time, the Estradiol will enter every cell in the culture but the Cre recombinase is only present in daughter cells as is expressed under the control of a specific daughter cell promoter, as mentioned above, resulting in the elimination of the just daughter cells in the cultures treated with Estradiol. In this way, we enrich for several generations in mother cells. In the not treated cultures, the Cre recombinase is also present in daughter cells, however, without the presence of Estradiol, this enzyme is not active, so mother and daughter cells are able to divide normally.
We tested several treatment times by counting the replicative age distribution of this cultures and established that at 3 hours of treatment, we were able to reproduce the replicative age distribution of the small microcolonies founder cells population (between 2 and 4 bud scars), as revealed in **Figure 12.B** where we observe that treated cells are enriched in cells with 1-3 bud scars, similarly to the small microcolonies founder cell population.

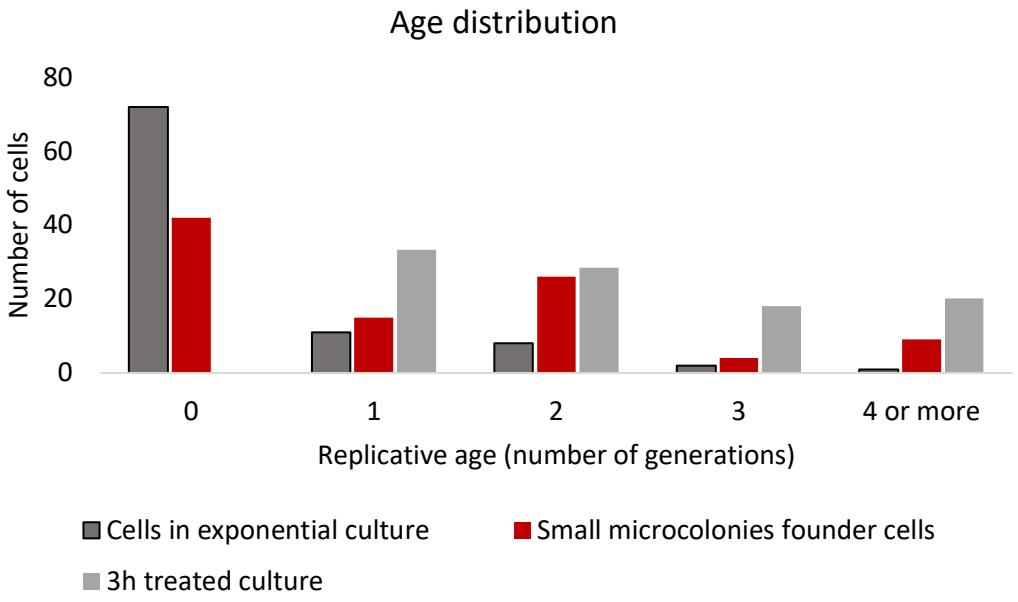

Figure 12. Mother cell enrichment of a WT culture with the MEP system. Replicative age distribution in an exponential culture (dark grey), in the small microcolonies founder population (red) and in a MEP strain treated 3 hours with estradiol (light grey).

After that, both 3h Estradiol treated culture (enriched in mother cells with 2-4 divisions performed) and the negative control (not enriched in mother cells), were encapsulated and the proportion of different microcolonies were estimated. What we observed was that after single cell encapsulation of cultures enriched in mother cells, a higher proportion of small microcolonies was clearly

generated (**Figure 13**, in red) in comparison with cultures that were not enriched in mother cells (and that had a replicative age distribution similar to the exponential culture of a wildtype prior to the encapsulation). These results suggest that early replicative age contributes to the low-proliferating rate observed in small microcolonies.

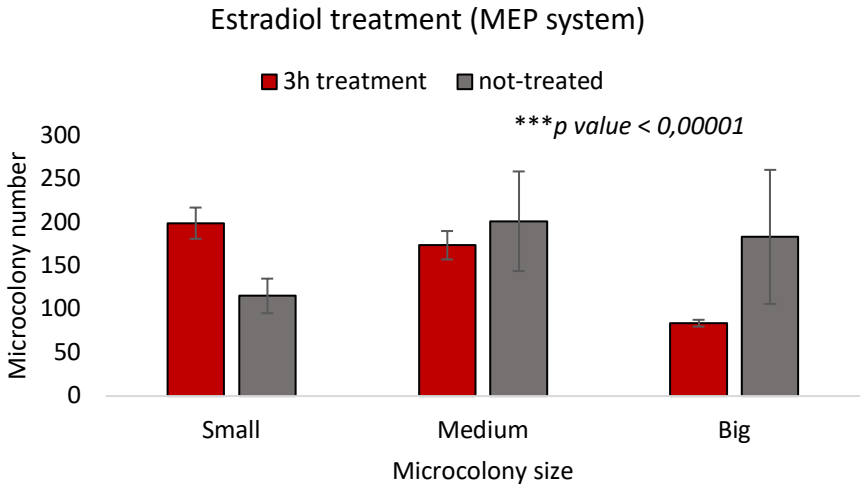

Figure 13. Distribution of microcolonies according to their size (small, medium or big) in a wildtype non aged culture (no estradiol) (gray) and in a wildtype aged culture (3 hours Estradiol treatment). Aged culture produced more small microcolonies than a not aged culture. It is remarkable that more than 75% of the cells in this aged culture had a replicative age between 1 and 5, which means they were not extremely old cells. A chi square test was realized and a p value inferior to 0,00001 was obtained.

MEP system uses a Cre recombinase to "kill" daughter cells. To discard that the results that we are observing were affected, by a hypothetical replication stress produced by unspecific cuts in the DNA during recombination, we decided to enrich in mother cells a wildtype BY4741 culture using a recombination independent process. To do so, we took advantage of the described biotin-streptavidin affinity purification protocol for isolating aged yeast cells[122]. Thus, a wildtype exponential culture was treated with biotin, that links to yeast cell wall. All cells present in the culture will be "marked" with this biotin. Then we let cells divide for several hours, allowing them to reach the desired replicative age. At this point, mother cells are purified from the rest of new born cells by streptavidin extraction. Streptavidin has specific affinity for biotin, and has also magnetic beads attached that allows the pull down of cells marked with biotin with the help of a magnet. This way, we obtain a culture enriched in cells with higher replicative age with little presence of new-born cells.

In this case, we also tested several hours of incubation to determine conditions to enrich in early-aged cells to reproduce better the early replicative age observed in small microcolonies founders. We established that at 6 hours these cultures were more similar to this population of founders. The negative control was treated with biotin for just half an hour and then subjected to the same treatment as the tested culture. After 6 hours of biotin incubation and streptavidin extraction, the enrichment in early-aged cells were verify and then

encapsulated and incubated as usual. What we observed after the incubation was that, similarly to what happens in the MEP system, when we enrich in mother cells with higher, but early, replicative age (2-5 bud scars), we obtain higher proportions of small microcolonies, compared with the control (**Figure 14**).

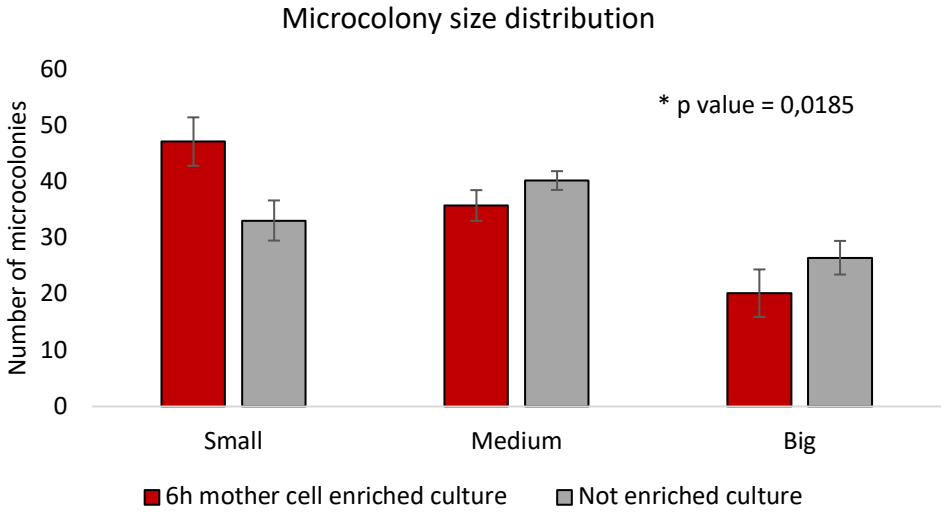

Figure 14. Microcolonies distribution profile according to their size in a not enriched culture (grey) and in a mother cell enriched culture (replicative age between 2 and 5) (red). These cultures were marked with biotin and mother cells were extracted after 6 hours of incubation with streptavidin. We observe an increase in small microcolonies in the enriched culture compared to the negative control. To determine the statistical significance of this differences, a chi square test was performed (p value obtained=0.0185).

This result confirms that the replicative age, moreover, the early replicative age, of the founder cell is important for the formation of an important portion of the small microcolonies present in the encapsulated culture. As small microcolonies are generated by a low-proliferating rate, it is clear that a correlation between the early replicative age and the proliferation rate exist: from the very first divisions a mother cell has higher probability to present lower proliferation rate.

3.1.5 Analysis of cell cycle progression of single cells by live-imaging

Since the results presented up to now demonstrate a correlation between the replicative age and the proliferation rate, we wonder how the length of cell cycle is affected in early-aged cells. Two scenarios can be considered: i) the length of the cycle increases because the length of each phase does, or ii) the cell cycle length increases at the expense of specific phases elongation. To get insight into this aspect and due to the limitations of the experiments performed to determine the real length of cell cycle phases in wildtype cultures according to their replicative age, we decided to perform a live-imaging analysis of single cells using specially designed devices to trap them and track their cell cycle progression by fluorescence microscopy.

This experiment was developed during a short stay in Gothemburg, under the supervision of Drs. Marija Cvijovic and Niel Welkenhyusen from system Biology research group (Department of Mathematical Sciences from Chalmers). Their special device for cell tracking consisted on a flexible plastic chip with laser-engraved wells connected through tunnels that allowed media flux (**Figure 15**). These wells were narrow enough to trap single cells within them and, also, to allow the division of the cells trapped there in a monolayer. This allowed a better visualization of the progeny by microscopy.

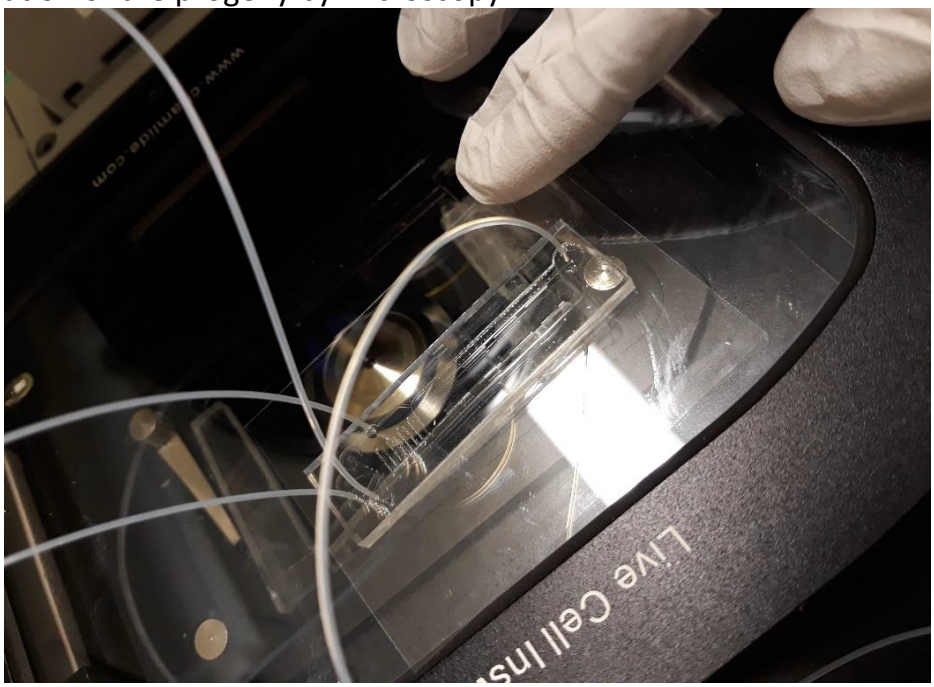

Figure 15. Microchip used for single cell live-imaging attached to a flourescence microscope. The tubes attached are 1) vacuum syringe 2) YNB media influx syringe 3) calcofluor syringe and 4) waste exit tube (See matherials and methods).

The strain used in this experiment was a Whi5-GFP tagged strain that enabled the identification of cell cycle phases: Whi5 is clearly visible in the nucleus in G1, and exits to cytoplasm when G1 is over (G2/M phase). Our first approach was to follow cell proliferation and cell cycle progression using this device and try to find a correlation between small microcolonies formation, replicative age and cell cycle lengths of the cells forming them.

Cells trapped in these wells were recorded for 13 hours by capturing images in brightfield and GFP channel every 5 minutes. After this, we tried to analyse these images by developing relatively simple Matlab (MathWorks®) script to track and quantify the time spent for each cell in every cell cycle phase. However, tracking of cells was not possible with this method. Then, they were analysed manually visualizing them and quantifying the time spent on each cell cycle phase for every cell.

As the number of experiments performed during the short stay was very low due to technical problems and the difficulty of translating these experiments to our

current laboratory, the results obtained are very preliminary and no clear conclusions can be extracted from them.

An example of the preliminary images of what we could obtain from these experiments are shown in **Figure 16**. In **Figure 16.A**, one of the wells filled with cells after 13 hours of growth (brightfield channel). In **Figure 16.B**, GFP channel of the same well, where we can visualize Whi5 (marked with a GFP tag). Cells with an accumulation of GFP signal in the nucleus are in G1, while cells with cytoplasmic signal of Whi5-GFP are in G2/M. In **Figure 16.C**, cells are stained with calcofluor after the recording of the colony proliferation (during 13 hour), enabling the visualization of bud scars.

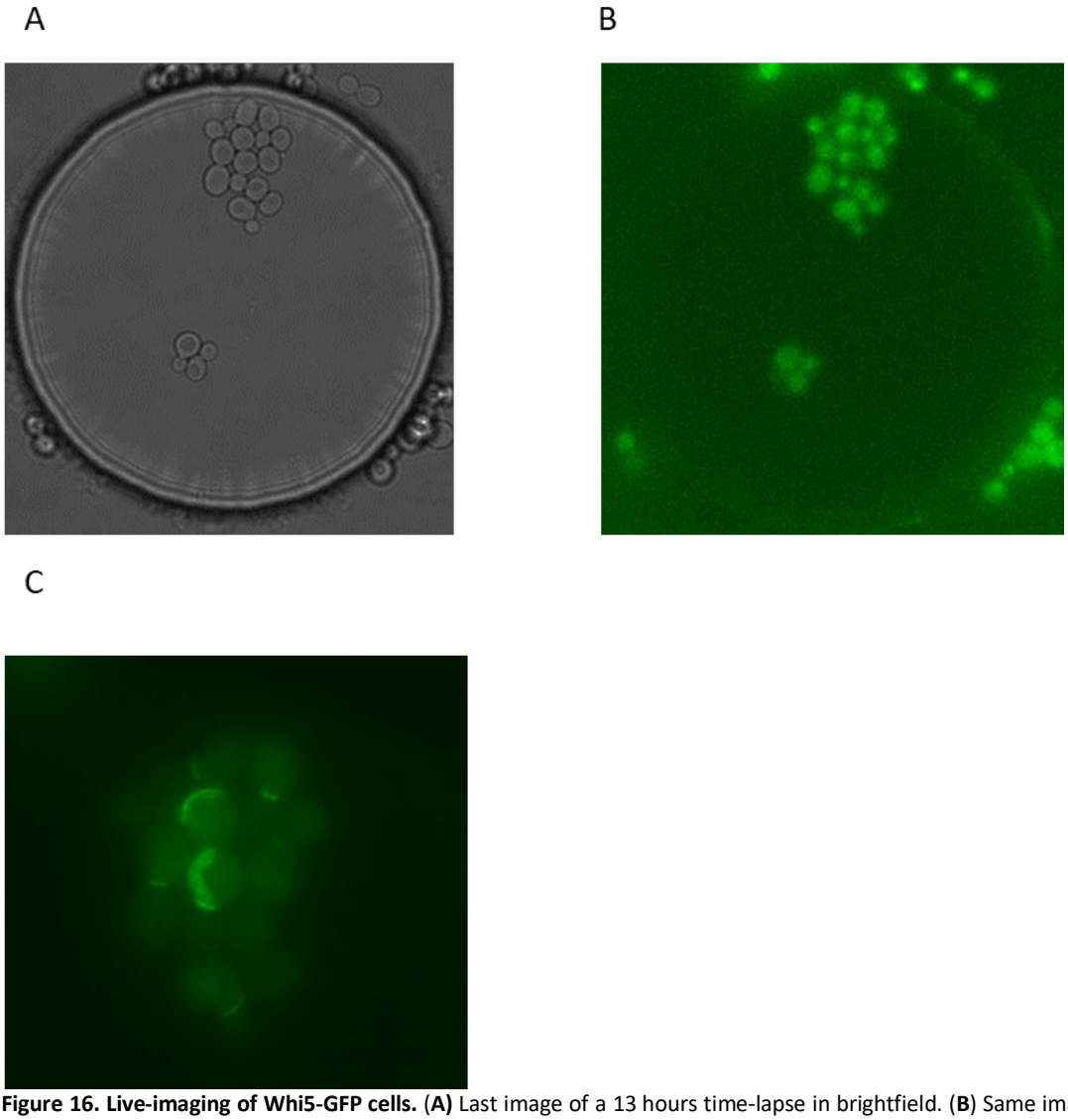

Figure 16. Live-imaging of Whi5-GFP cells. (**A)** Last image of a 13 hours time-lapse in brightfield. (**B**) Same image in GFP channel. Knowing the localization of Whi5, thanks to a GFP tag, allows us to know the cell cycle phase of each cell: G1 if the signal is nuclear, G2 if the signal is cytoplasmic. Whi5 protein is tagged with GFP, which is useful to know the cell cycle phase of each cell using its localization. (**C**) Last image of the same time-lapse after being stained with calcofluor to visualize bud scars.

3.2 Chapter 2: Contribution of cell cycle progression to low-proliferating small microcolonies formation: a role for WHI5

Previous RNA-seq results from our group, comparing small and big microcolonies, showed that small microcolonies have enriched expression of cell cycle regulation genes. In fact, *WHI5* was one of the most upregulated genes in the slow proliferating population of small microcolonies[52 37].
Whi5 is a G1/S transition repressor that acts through the inhibition of MBF and SBF transcription factors, preventing them from transcribing G1 cyclins, among other elements, necessary for the G1/S transition. It was an interesting candidate to investigate due to its important implication in cell cycle regulation as well as in the regulation of threshold size which a new born cell must reach before dividing. As transcriptomic results described above indicate that high Whi5 levels correlates with small slow-proliferating microcolonies, we decided first to investigate the effect of different Whi5 levels on small microcolonies formation.

3.2.1 Increasing levels of Whi5 positively correlates with a lower proliferation rate

In order to clarify whether Whi5 plays or not a role in the proliferative capacity of cells, we decided to, firstly, check if small microcolonies express more Whi5 at protein level. Once this is ascertained, we considered quite interesting to investigate what happens when cultures overexpress Whi5, and how this alters microcolonies formation.

3.2.1.1 Whi5-GFP encapsulation reveals higher Whi5 expression in small microcolonies

To unravel the role of Whi5 in small microcolonies low proliferative capacity, we first decided to analyse whether small microcolonies have more Whi5 expression at protein level compared to the big ones.
For this, we used a strain with a GFP tagged Whi5 located in the endogenous locus. We encapsulated this strain following the same encapsulation method already described and, after the 13 hours incubation, microcolonies were washed and resuspended in Synthetic complete media to avoid the autofluorescence of the YPAD media. They were then analysed using a Large Particle Cytometer Biosorter®. We encapsulated six independent Whi5-GFP cultures in order to achieve the optimal amount of microcolonies for its analysis under this cytometer. Microcolonies were segregated according to their “time of flight” or TOF, which correlates with their size, in three different groups: small microcolonies, medium microcolonies and big microcolonies.

These measures were tested by sorting some microcolonies for every group and, under the microscope, we ascertained that their size corresponded to the group in which they were segregated. These sizes or TOF vary among measure times so we decided to analyse the six independent encapsulations of Whi5-GFP together at once. As a negative control we used a Rpl38-GFP tagged strain.
We normalised the green signal perceived by the cytometer to the TOF of the microcolony and calculated the average green signal on each group. We obtained that small microcolonies have more Whi5 GFP signal than medium and big microcolonies and, when compared to the negative control, we observe a difference in expression patterns (**Figure 17**).

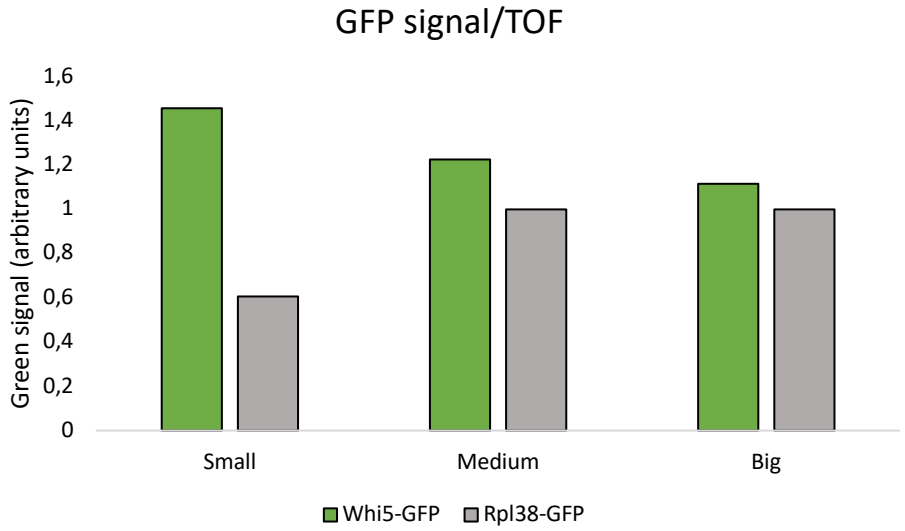

Figure 17. Whi5-GFP signal according to microcolony size. In green, we observe the signal of Whi5-GFP, which is noticeably higher in small microcolonies. In grey, as negative control, a Rpl38-GFP tagged culture analysed similarly is displayed. Rpl38 is a ribosomal protein that was not detected into the differential expressed genes category in small microcolonies.

Rpl38 shows lower GFP signal in small microcolonies, although in medium and big microcolonies the signal obtained was almost the same. RPL38 was used as a negative control because it was not among the differential expressed genes in small microcolonies compared to the big ones. However, the slow proliferation rates may explain these differences of expression among the microcolonies. All other negative controls tested showed similar results. We decided to keep Rpl38 as the negative control due to the lower differences in GFP signals displayed according to their size.

3.2.1.2 Higher Whi5 levels correlates with an increase in small microcolonies production

In light of the previous result, we wanted to elucidate the role of Whi5 levels in the proliferation rates of cultures, as we observed an increase of this protein in small microcolonies that present low proliferating rates. In order to do so, we

decided to study the overexpression of Whi5 in clonal cultures using the inducible Whi5 strain KSY098[123] which has Whi5 in its original ORF but under the control of an Estradiol dose-dependent promoter. This implies that the higher the concentration of Estradiol added to the culture, the higher the expression and, consequently, the concentration of Whi5 in those cells.
The experimental procedure consisted of growing this inducible Whi5 strain culture until exponential phase. As detailed in **Figure 18**, after this, the culture was encapsulated as usual and then, similar amounts of microcapsules were distributed into several flask with fresh YPAD media with increasing concentration of Estradiol. They were equally incubated for 13 hours at 30ºC and collected after the incubation. They were then analysed by counting the number of microcolonies according to their size for each concentration of Estradiol used. These concentrations were 0nM for the negative control, 2nM, 4nM, 6nM, 8nM and 10nM.

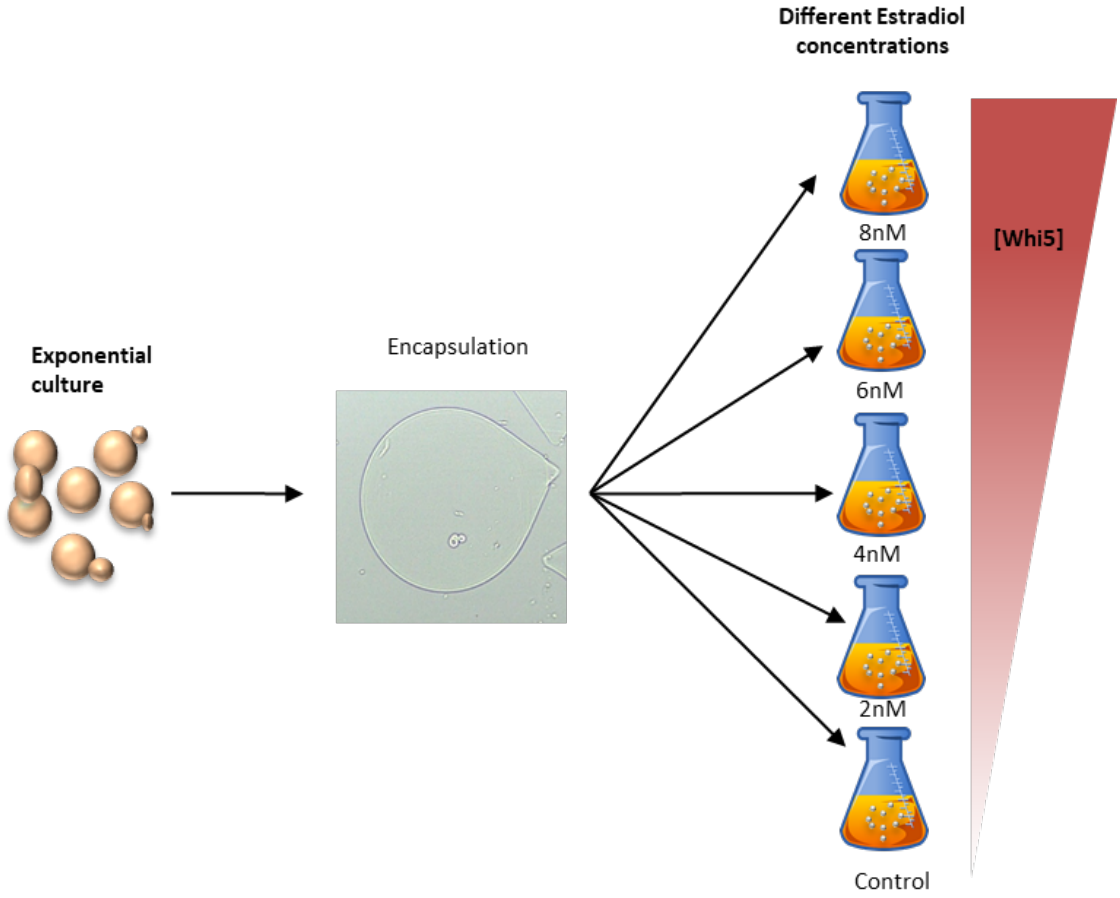

Figure 18. Experimental procedure to obtain capsule cultures with increasing Whi5 concentration using KSY098 strain and Estradiol. In this strain *WHI5* transcription is under the control of an Estradiol-dependent promoter. The increase in the concentration of Whi5 in the cells is Estradiol dose-dependent. First, an exponential KSY098 culture is encapsulated without Estradiol, then, capsules from the same encapsulation experiment are inoculated in flask with YPD with a certain concentration of Estradiol (2nM, 4nM, 6nM, 8nM or 10nM) or in YPD without Estradiol as a negative control.

To ensure that Whi5 levels were, in fact, increasing with higher Estradiol concentrations, we performed a WB of Whi5, that is tagged with m-cherry in this

strain, in the different Estradiol concentrations tested. As we can observe in **Figure 19.A**, Whi5 does increase with Estradiol concentration. In the absence of no or 2nM Estradiol, Whi5 protein is undetectable, indicating no or very low levels.

Interestingly, the firs observation when we compared the negative control (that has no, or little expression of Whi5) to the isogenic wildtype, was, in this case, that Whi5 absence does alter the proportion of small microcolonies in the culture. Noticeably, a clear decrease in the proportion of small microcolonies can be observed in the negative control compared to the wildtype (**Figure 19.B**).

After encapsulation and incubation of the cultures treated with Estradiol, analyses revealed a clear and significant correlation between the concentration of Estradiol and, consequently, Whi5 levels, and higher proportion of small microcolonies. In the **Figure 19.C**, we see an increase in small microcolonies population, proportionally to the concentration Whi5 of the culture.

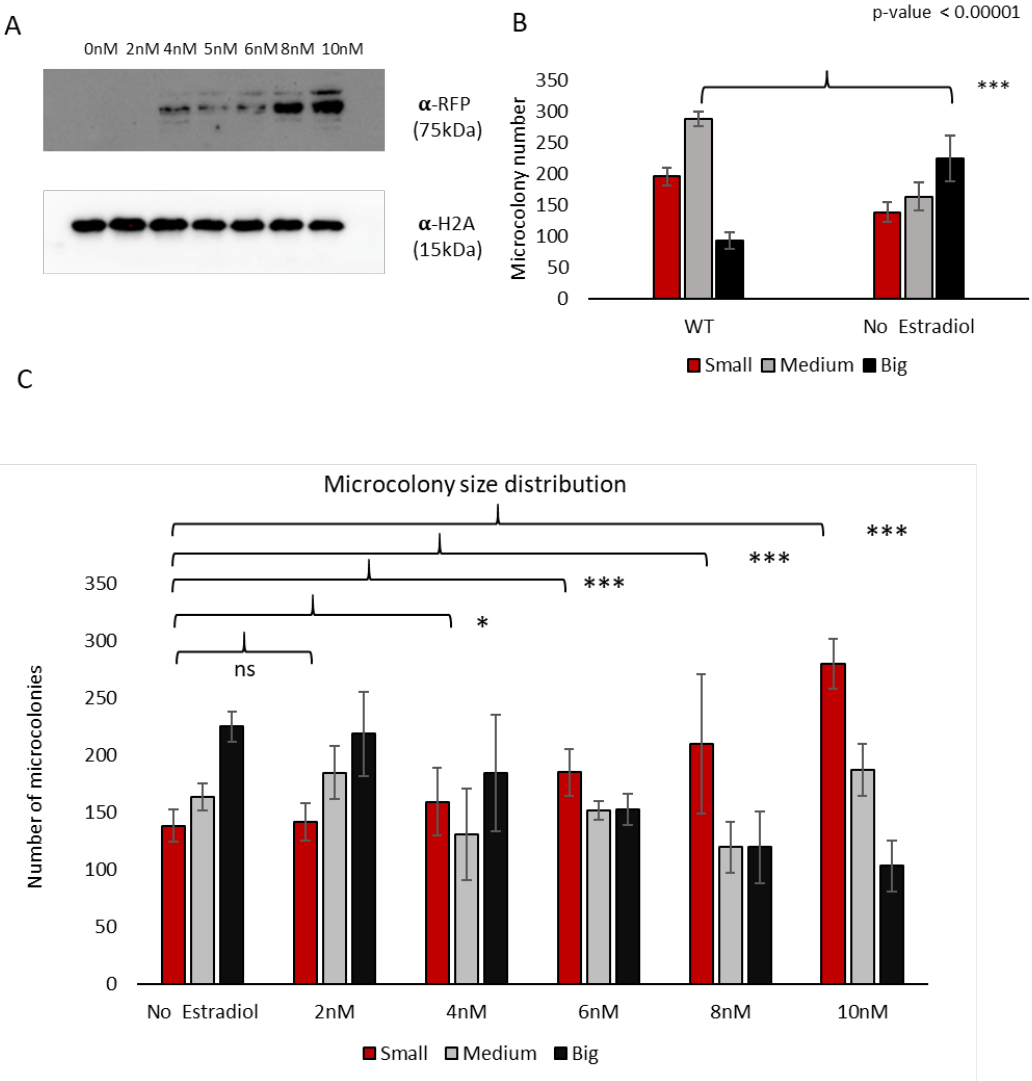

Figure 19. Size microcolonis distribution under Increasing Whi5 concentration in an inducible Whi5 strain. (A) Western Blot of inducible Whi5 strain at different Estradiol concentration. This confirms the Whi5 accumulation according to the increasing concentration of Estradiol in the media. (B) Microcolony size distribution analysis of a WT strain and the KSY098 control without Estradiol. Compared to the wildtype profile, the conditional deletion of Whi5 when there is no Estradiol in the media produces an increase in big microcolonies (black) and a decrease in small microcolonies (red). (C) Microcolonies size distribution profile of KSY098 strain cultured without Estradiol (control),

or with 2, 4, 6, 8 or 10nM, respectively. As Estradiol concentration increases, expression levels of whi5 get proportionally higher, which produces a progressive raise in the proportion of small microcolonies (red bars). To determine the statistical significance of this differences, a chi square test was performed.

This suggests, that increased Whi5 levels enhances the formation of low proliferating small microcolonies and, therefore, contributes to the proliferative heterogeneity in clonal yeast cells.

3.2.2 The concentration of Whi5 increases with the replicative age of the cells

Finally, we tried to unravel the role of Whi5 in proliferation rates and its relationship with the replicative age of the founder cell. Small microcolonies display slow proliferative rates and higher Whi5 expression. Moreover, a large number of them are founded by not new born cells that have undergone several divisions prior to the formation of the small microcolony. If this is somehow correlated to Whi5, we could test it by investigating the differential Whi5 expression among cells with different replicative ages.
In pursuance of this, we developed the following experimental procedure **(Figure 20)** in which an exponential culture of a Whi5 GFP tagged strain is sorted by its expression of Whi5. In this strain, *WHI5-GFP* is expressed under the control of its endogenous promoter. As shown in **Figure 20**, cells sorted where separately stained with calcofluor and analysed under the fluorescent microscope to count their replicative age (number of bud scars). First, we selected cells of the same size and sorted them by their Whi5-GFP expression: approximately 20% of cells with lowest GFP signal and 20% of the cells with highest signal (**Figure 21.A**). As a control of the whole population, we also obtained a sample of the bulk not sorted population.

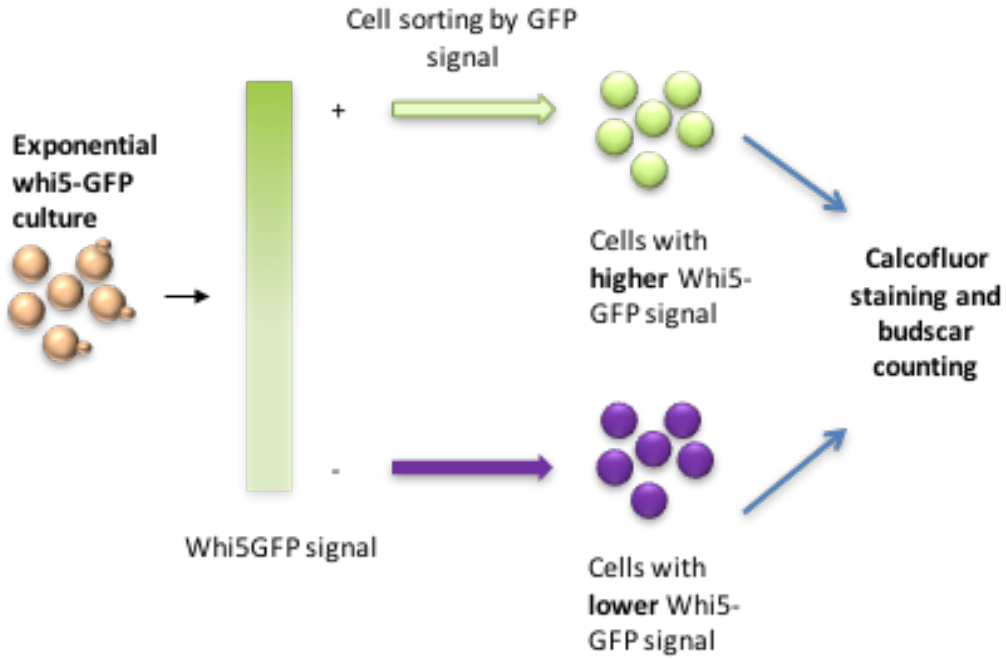

Figure 20. Cell sorting of a Whi5-GFP strain according to GFP intensity signal. First, an exponential Whi5-GFP cultured in YPD was collected and sorted according to their GFP signal. Three different samples were collected: cells with higher Whi5GFP expression, cells with the lowest Whi5 GFP expression and a sample of the whole population as a control of the culture. After that, each sample was stained with calcofluor and analysed separately.

What we observe in **Figure 21.B** is that the replicative age of cells with higher Whi5 expression is slightly higher than the population with less Whi5 expression. The low-Whi5 population displayed almost twice the amount of new born cells compared to the high-Whi5 expression population. Finally, if we calculate the percentage of cells with higher Whi5 expression versus total cells according to their replicative age, we obtain the graph shown in **Figure 21.C**. With this, we can easily see that Whi5 levels increase with the replicative age of the cell.
Considering all these results, we can confirm that Whi5 is associated with the replicative age, since the very first divisions, of the cells and assume that Whi5 plays some sort of role in the correlation between low proliferation rates of small microcolonies and the replicative age of their founder.

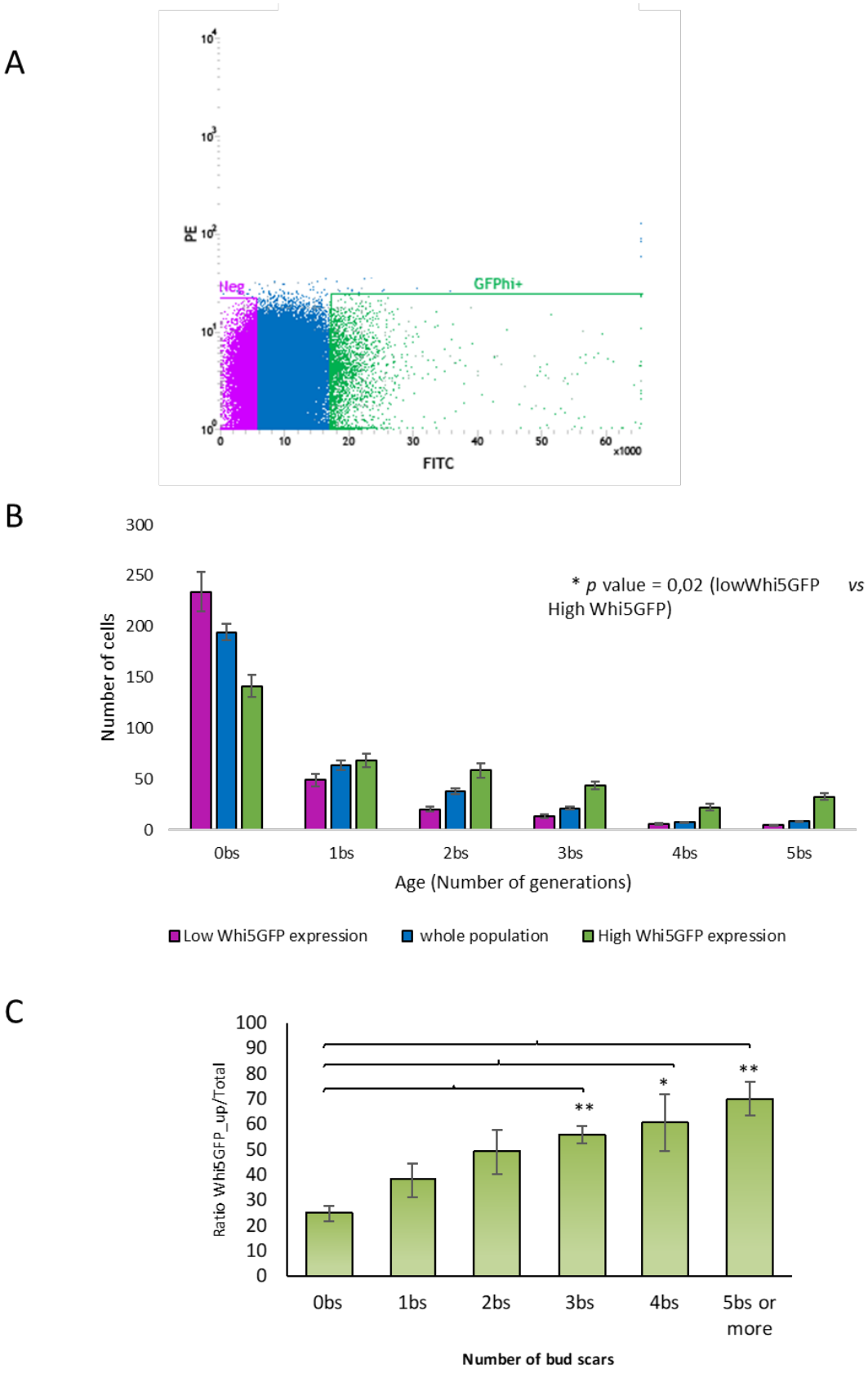

Figure 21. Whi5 expression in cells according to their replicative age. (A) Cell sorting according to Whi5-GFP signal. In purple, cells sorted as the "low Whi5 expression" group, in green, cells sorted as the "high Whi5 expression" group. (B) Replicative age distribution, represented as the number of bud scars, for low Whi5 expression sample(purple), whole population (blue) and high Whi5 expression (green). The proportion of cells with higher Whi5 expression changes with the replicative age of the cell: cells with higher number of bud scars frequently have higher Whi5

expression. To determine the statistical significance of this differences, a chi square test was performed (p value obtained=0.02). (C) Proportion of cells with higher Whi5 expression found for each replicative age group (represented as the number of bud scars). It is remarkable that cells that have undergone more divisions, also have higher Whi5 expression levels, compare to virgin cells (0 bud scars). To determine the statistical significance of this differences, the statistical analysis used was a t test, comparing every group to the 0 bud scars group.

3.3 Chapter 3: Interplay between cell cycle, early replicative aging and proliferation capacity

3.3.1 Replicative age and cell cycle

Considering the results exposed in chapters I and II, we suggest that cell cycle and replicative aging, surprisingly, since very early stages, are both playing a role in the proliferative capacity of cells and therefore contributing to the proliferative heterogeneity.
To investigate whether these roles are connected, we decided to study how cell cycle phases change during the replicative aging of the cells.

3.3.1.1 Cell cycle phases relative lengths vary according to replicative age in a wildtype strain

We first chose to determine in a wildtype strain if cells presented any difference in cell cycle phases G1 and G2/M among the different replicative ages. For that, we stained a wildtype exponential culture with calcofluor and then, cell where visualized in a direct fluorescence microscope for bud scar counting and cell cycle phase identification. In brightfield, cells display well differentiable morphologies according to their cell cycle phase. In G1 they are almost perfectly round and in G2/M phase cell present a bud that varies in size according to the stage of division in which they are. With DAPI filter, we are able to identify the bud scars present on each cell. In this manner, we can count the number of bud scars in each cell and correlate it to the cell cycle phase that cell is currently in.
After the quantifications, data was displayed in the graph of **Figure 22**. As it has been previously described[98] , it was noticeable that new born cells are enriched in G1 phase and can be explained by the time that new born cells need to reach the size threshold necessary for cell cycle progression. Interestingly, we can observe that after that, G1 phase seems to shorten its length during the first 3-4 divisions to finally catch up to G2 length in cells with 4 or more bud scars.

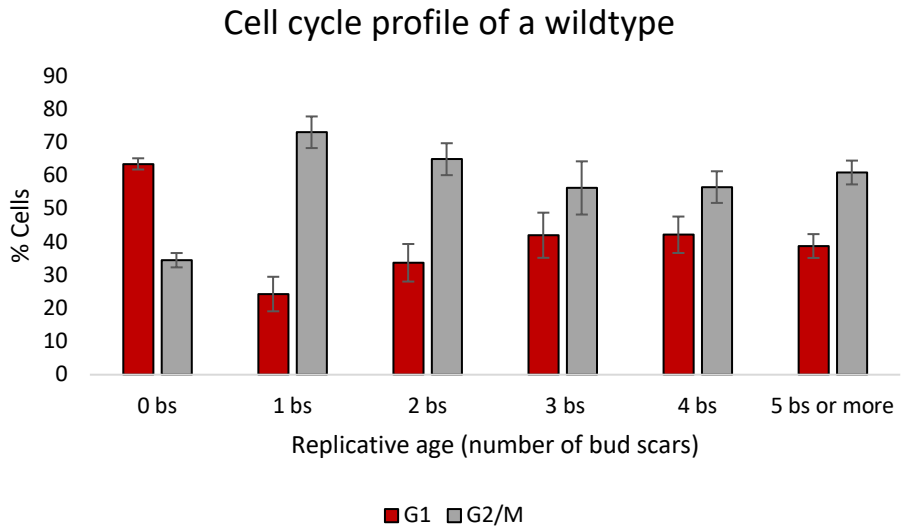

Figure 22. Cell cycle profile of a wildtype according to the replicative age of the cell. Cells were stained with calcofluor to quantify their bud scars. After that, they were categorized by the cell cycle phase in which they were by analysing the morphology of the cell: G1 if they had no buds, or G2/M if a bud, small or large, was present in the cell. We observe that G1 is relatively shorter during the first 2-3 divisions and, after that, G1 and G2/M phases are similar in proportion.

Although we do not know yet the explanation for this cell cycle profile according to age, as different factors can contribute, we suggest that cell cycle phases length is tightly regulated during every step of the replicative lifespan of a cell.

3.3.1.2 Whi5 deletion does not alter the cell cycle phase replicative age-dependent variance

To further analyse this, we wondered whether Whi5 could be implied in this cell cycle regulation during aging. For this, we analysed a *whi5Δ* mutant in the same manner as the wildtype.

It was no surprise to see a suppression of the enrichment in G1 present in new born cells (**Figure 23**), as it has been previously demonstrated that Whi5 regulates size and cell cycle entry in new born cells. Without Whi5, cells pass through G1 restriction point or START before they reach the optimal size for division. In consequence, *whi5Δ* cells are smaller than wildtype cells.

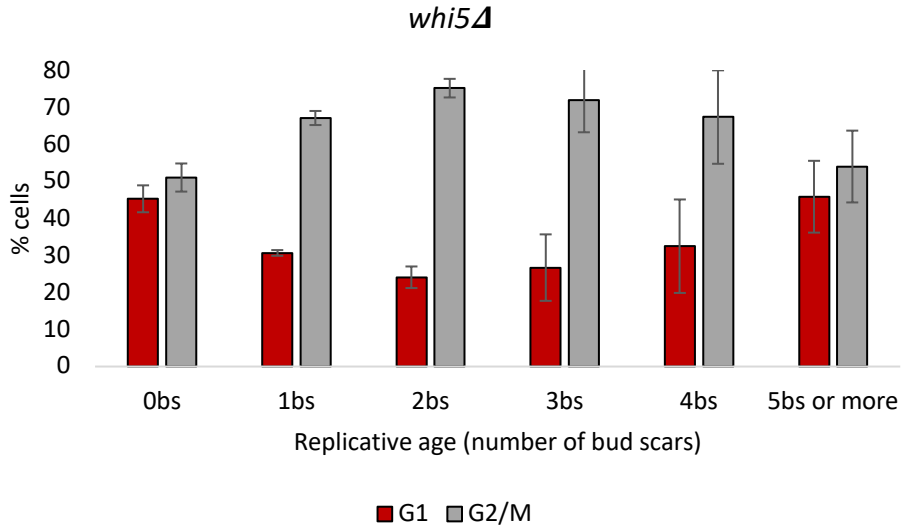

Figure 23. Cell cycle profile of a *whi5Δ* mutant according to the replicative age of the cell. Similarly to the wildtype, cells were stained with calcofluor to quantify their bud scars and, after that, categorized cell cycle phase. We observe that new born cells show a shorter G1 compared to the wildtype. This is due to the fact that Whi5 is implied in the size control of daughter cells in order to divide. After this, we observed shorter G1 in every other age category, which can be explained by the lack of an important cell cycle repressor in G1 checkpoint. However, after some divisions, as happened in the wildtype, G1 and G2/M phases reach similar in proportion.

On another hand, we can see no other differences in cell cycle progression during the different replicative ages analysed compared to the wildtype, except for an increased difference between G2/M and G1 proportions. Deletion mutants of Whi5 spend less time on G1 due to the lack of one of the G1/S transition repressors, however, after few divisions, cells lacking Whi5 are also able to recover the G2/G1 equilibrium as in the wildtype. This possibly means that, Whi5 is not implicated in this regulation of cell cycle during cell aging.

3.3.1.3 Cells lacking Sic1 have similar cell cycle profile as a whi5Δ mutant during replicative aging

Sic1 is a cyclin-dependent kinase inhibitor that controls the G1/S transitions by inhibiting the complex Cdc28/Clb5(6)[124] , the specific cyclin-dependent kinase complex responsible for the G1/S transition in *S.cerevisiae.* To shed some light into the G1/G2 proportion changes during the first steps of replicative aging, we decided to test whether a lack of this G1/S transition control could have any effect on this regulation of cell cycle.

Just as in the *whi5Δ* mutant (**figure 23**), *sic1Δ* cells present relative shorter G1 in new born cells (**Figure 24 and 25**). This means that Sic1 is also important for cell cycle regulation in daughter cells but, also as in the *whi5Δ* mutant, shows no other impact on cell cycle profile during replicative aging.

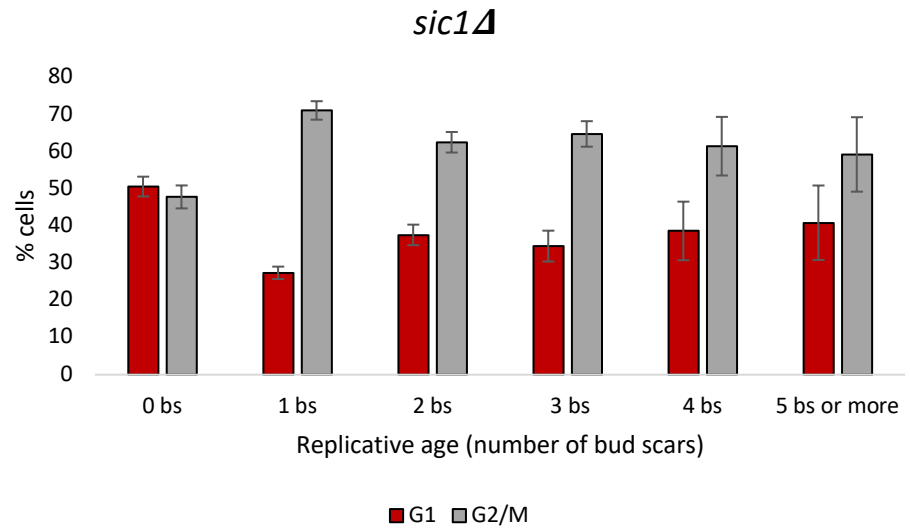

Figure 24. Cell cycle profile of a *sic1Δ* mutant according to the replicative age of the cell. As happened with the *whi5Δ* mutant, new born cells show a shorter G1 compared to the wildtype. This suggest that sic 1 is also important for the size control of daughter cells before their first division. However, for the rest of the replicative age categories, the profiles of G1 and G2/M phases are similar to the wildtype.

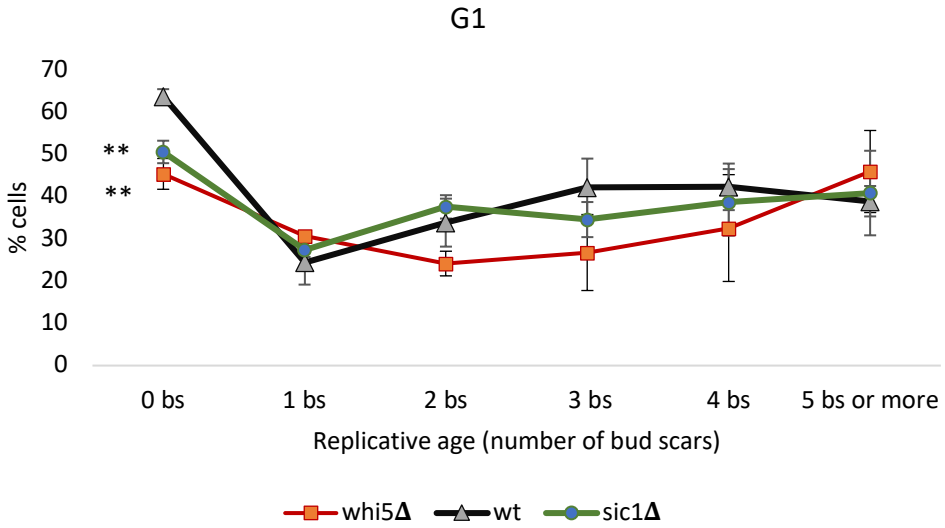

Figure 25. G1 proportions during replicative aging of cells from a wildtype culture, a *whi5Δ* mutant and a *sic1Δ*. The only statistical difference among these cultures is at 0 divisions, where both deletion mutants display a decreased percentage of cells in G1. The statistical test performed was a t test, that gave a p value of 0,006 for *sic1Δ* and 0,004 for *whi5Δ.*

3.3.1.4 Analysis of G2/M checkpoint mutants reveals no apparent role of replicative stress in G2 phase elongation on the first stages of cell replicative aging except for RAD53

Whit the aim of clarifying which other factors may be implied in the distribution of cycle phases *versus* replicative age we decided to stake on G2/M checkpoint factors.

G2/M checkpoint controls, among other things, the replicative stress response. As cells with low replicative age show relative larger G2 phases, we wondered if the cause was that replicative stress is usually present since early stages of aging. In order to analyse this, we studied several factors implicated in this checkpoint: Rad9, Chk1, Mec1 and Rad53. Rad9, Chk1 and Rad53 are factors of the DNA damage response (DDR). Rad9 activates Chk1 and Rad53 when DNA damage or replicative stress is present. It also intervenes in post replication repair pathway (PRR) and they are all necessary for cell arrest in G2/M phase.

Mec1 (mitosis entry checkpoint) participates is the genome integrity checkpoint signal and plays also a role in replicative stress and DNA replication stress signalling and cell arrest in G2/M phase.

If low replicative aged cells have longer G2/M phases due to replicative stress, we expect that any of these genes deletion mutants displayed a different cell cycle profile from what we observe in the wildtype.

In **Figure 26.A and B**, we can respectively observe the cell cycle profile of *rad9Δ* and *chk1Δ*. Rad9 activates Chk1 during DNA damage response and enable cell cycle arrest in replicative stress conditions. The lack of Rad9 and Chk1, respectively, does not have a great impact on cell cycle progression during the first steps of replicative aging, at least, in terms of proportions between G1 and G2/M phases.

Cell cycle analysis of mec1 and rad53 are shown on **Figure 26.C and D**. They both are combined with the deletion of Sml1 because the lack of these genes is lethal for cells, but in combination with the deletion of Sml1, these cultures are viable. Sml1 is a ribonucleotide reductase inhibitor that regulates dNTP pools in cells. The null mutation present higher pools of dNTPs which seem to repress *mec1Δ* and *rad53Δ* lethality. The single *sml1Δ* mutant, as a control, is also shown in Figure R E.

In the case of *mec1Δ* mutant, these cells have little differences with the wildtype profile. However, the lack of Rad53 seems to supress G1/G2 differences during the first divisions of the replicative aging of cells. In light of these results, we decided to test a viable point mutant of Rad53 that has no capacity of activating the DDR. This mutant, *rad53k227*, shows a similar profile to the null mutant (**Figure 26.F**). However, these differences with the wildtype profile are not statistically significant.

A


rad9Δ
% cells
90
80
70
60
50
40
30
20
10
0
0
1
2
3
4
5 or more
Replicative age (number of bud scars)
G1
G2/M

B

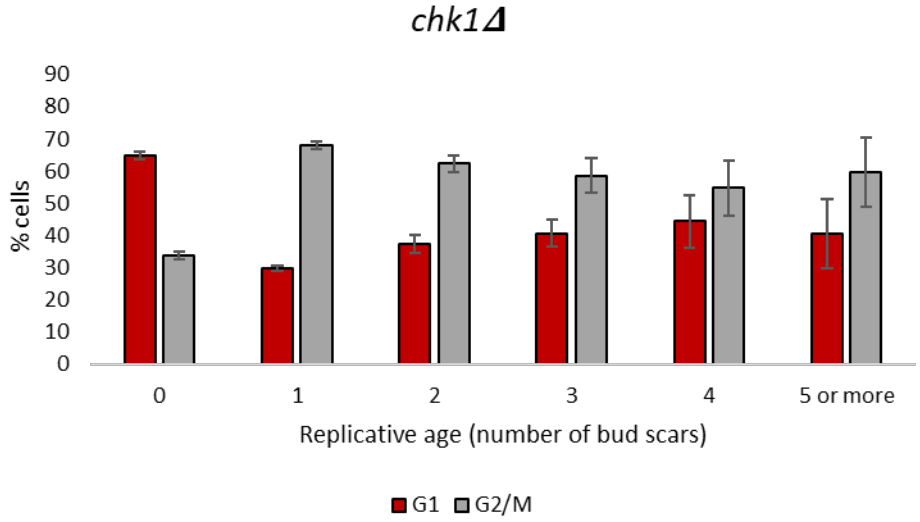
chk1Δ
% cells
90
80
70
60
50
40
30
20
10
0
0
1
2
3
4
5 or more
Replicative age (number of bud scars)
G1
G2/M

C

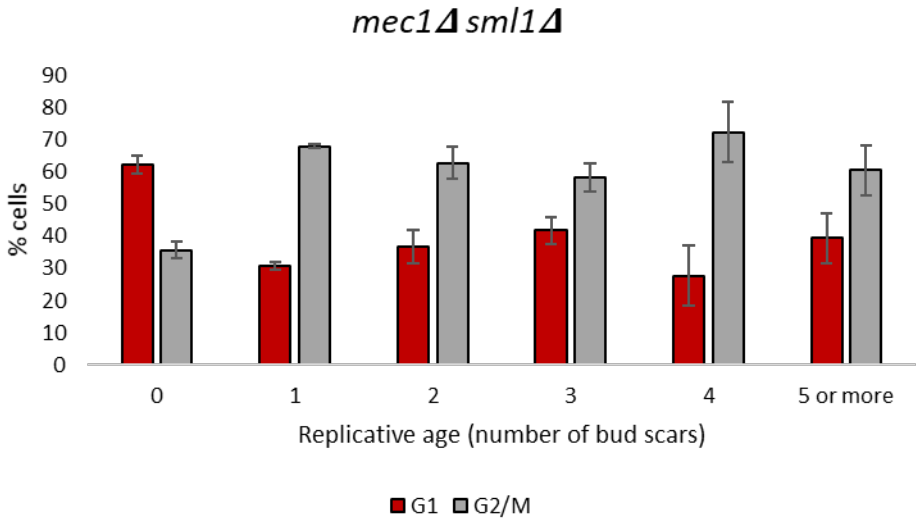
mec1Δ sml1Δ
% cells
90
80
70
60
50
40
30
20
10
0
0
1
2
3
4
5 or more
Replicative age (number of bud scars)
G1
G2/M

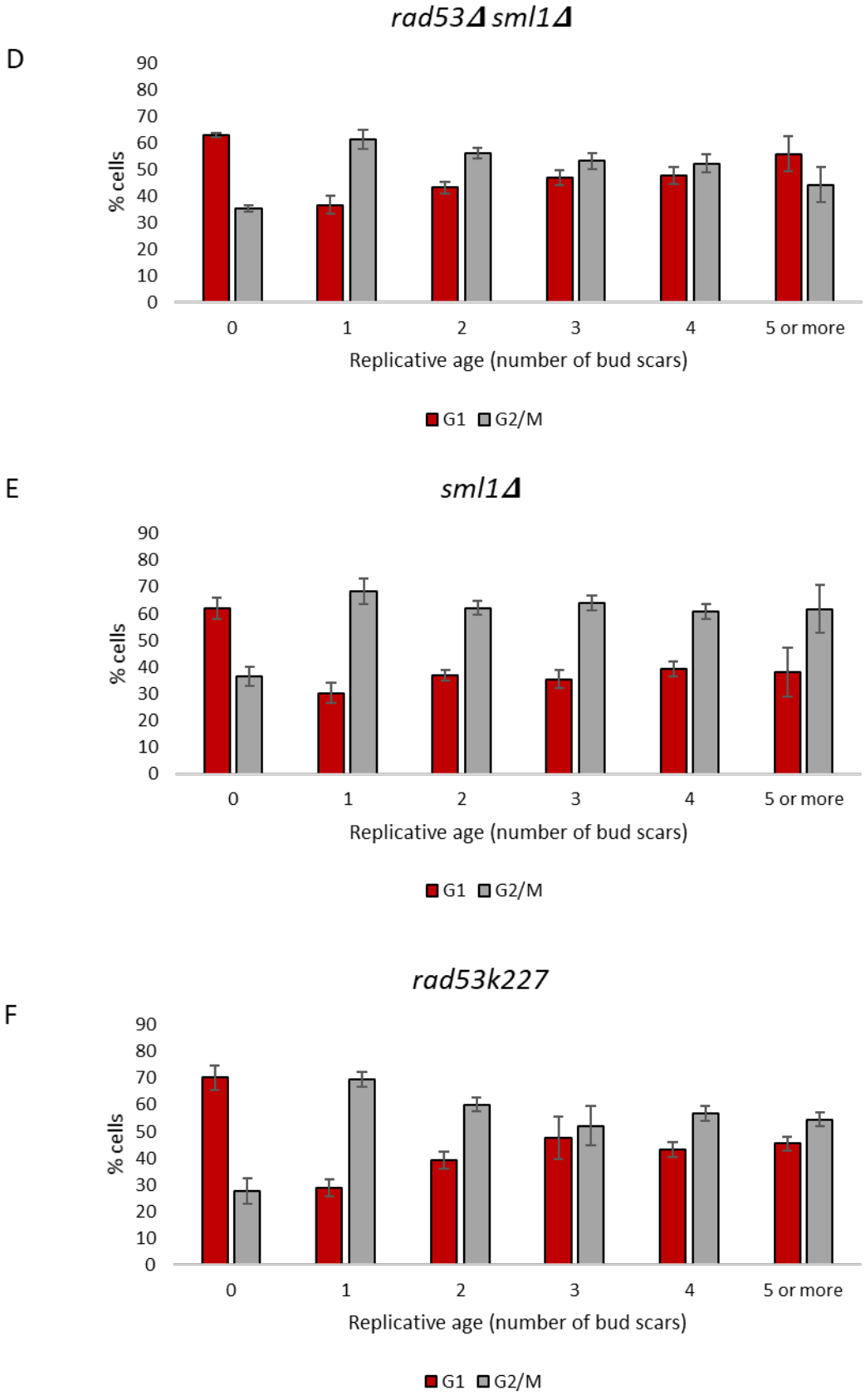

Figure 26. Cell cycle profile of different checkpoint mutants according to replicative age. (A) *rad9Δ* mutant. (B) *chk1Δ* mutant. (C) *mec1Δsml1Δ* mutant. (D)) *rad531Δsml1Δ* mutant. (E) *sml1Δ* mutant. (F) *rad53K227* mutant.

In **Figure 27** we can observe G2 relative quantification in the different mutants compared to the wildtype. The greatest differences are between mec1 and rad53 mutants, however, these differences in G2 proportion were not found statistically significant to reach any conclusions. Perhaps, the difficulty in finding a high number of cells with a number of divisions greater than 5 may be hindering the clear observation of a possible effect.

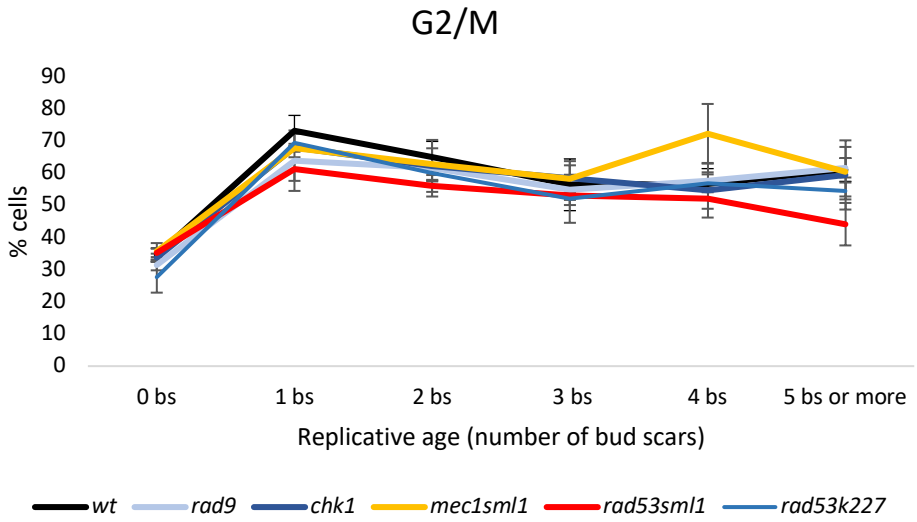

Figure 27. Proportion of cells in G2/M phase according to their replicative age. We observe a slight increase in G2/M phase cells in *mec1Δsml1Δ* mutant and a slight decrease in *rad53Δsml1Δ*

3.3.2 Analysis of synchronized cultures reveals relative shorter G1 and longer G2 phase in cells with low replicative age compared to cultures enriched in new born cells

From the experiments previously developed, we can only observe the relative number of cells in G1 or G2/M phase according to their replicative age. In order to study cell cycle progression in new born cell enriched cultures compared to mother (non-new born) cell enriched cultures, we decided to perform a G1 synchronization assay in these populations.

The first step was to enrich a wildtype culture in low replicative aged cells. To do this, we performed the biotin-streptavidin purification assay already described (see Materials and Methods) and enriched in mother cells for 6 hours (half an hour for the negative control). Differences in cell populations according to their replicative age among the different times of enrichment are displayed in **Figure 28**. We can see that with the 6 hours treatment, we enrich the culture in cells with between 3 and 5 bud scars, meaning a replicative age of 3-5 divisions. With 9 hours treatment, this number increases to 5-8 bud scars.

These results demonstrate that this technique allow us to enrich the culture in cells with the desired early replicative age, which is an essential tool in our purpose to focus on the early stages of replicative aging, less known, but with an impact on proliferation rate as this work reveals.

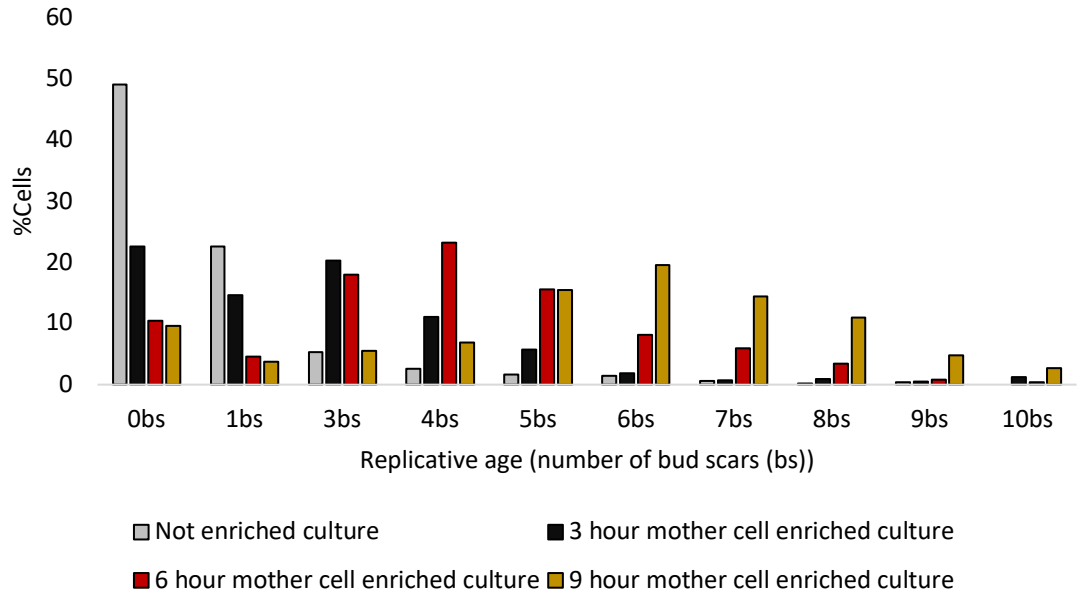

Figure 28. Proportion of cells according to their replicative age in different mother enriched cultures. In grey, replicative age distribution in a negative control (not enriches in mother cells). The vast majority of these cells are new born cells. In black, a 3-hour incubation enriched culture. We observe an increase in the replicative age of the culture. Most of these cells have between 0 and 3 bud scars. In red, a 6-hour enriched culture. The replicative age of these cells varies between 3 and 5. In yellow, a 9-hour enriched culture. The majority of the cells in this culture present a replicative age between 5 and 8. The replicative age of these cultures was estimated by calcofluor staining and bud scar counting.

These cultures were then synchronized in G1 using alfa factor treatment for 2 hours. After that, cells were washed and incubated in YAPD with pronase to degrade the alfa factor allowing the progression of the cell cycle. Samples were collected every 5 minutes for 90 minutes and, then, fixated, stained with propidium iodide and analysed by cytometry.

As we can observe in **Figure 29**, mother between 3 and 5 performed divisions before synchronization enriched cultures, display shorter G1 phase compared to the new born enriched culture: while the mother cells enriched culture clearly come out of G1 al 15-20 minutes, the exponential culture, enriched in new born cells spend, at least, 25 min to start entering S phase. This delay is statistically significant. Interestingly, despite the earlier entry into S phase of non-virgin cells, both cultures exit G2/M phase at the same time, indicating that G2/M phase is slightly longer in cells with low replicative age compared to the new born cells.

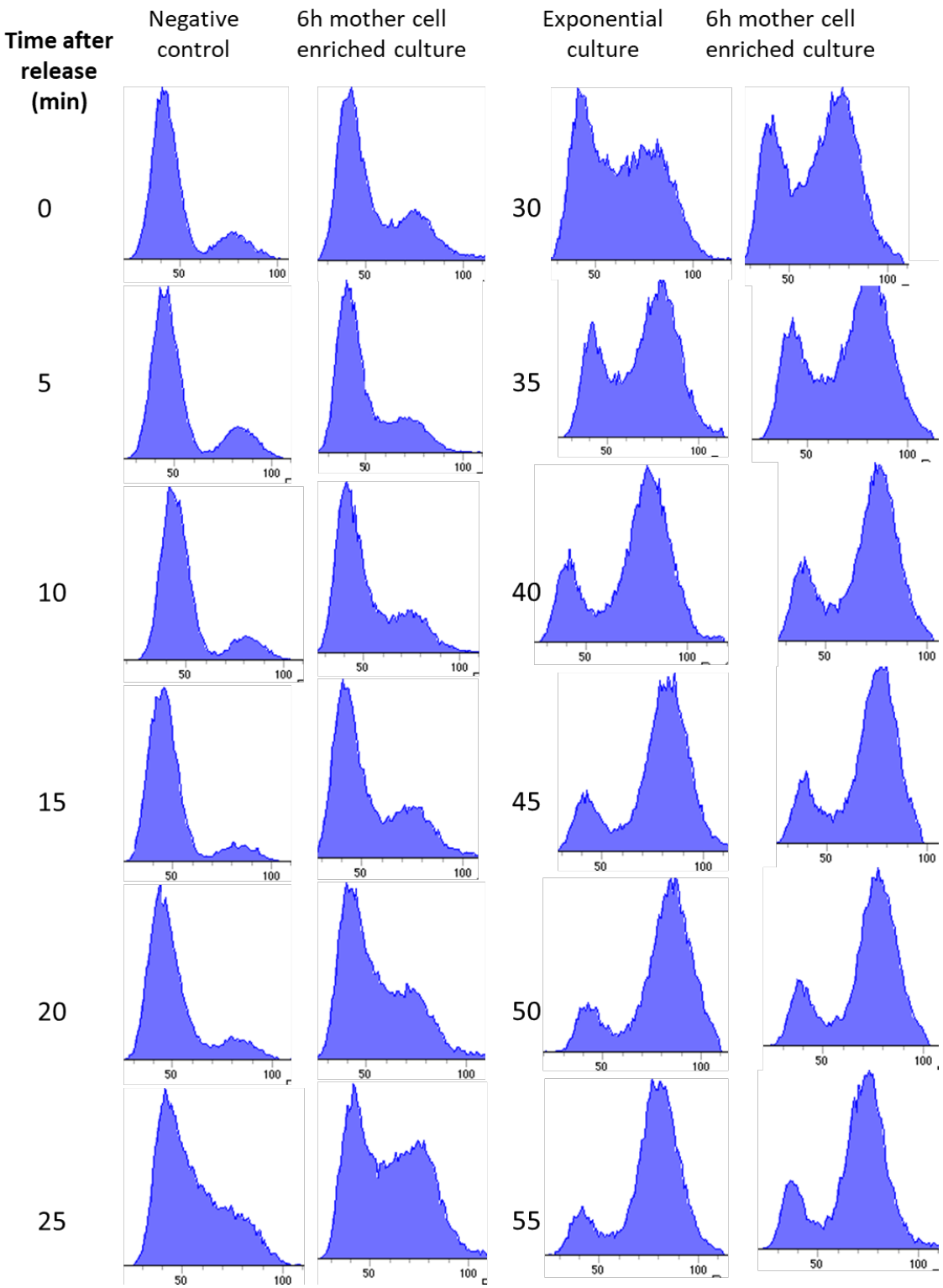
Time after release (min)
Negative control
6h mother cell enriched culture
Exponential culture
6h mother cell enriched culture
0
5
10
15
20
25
30
35
40
45
50
55
50
100

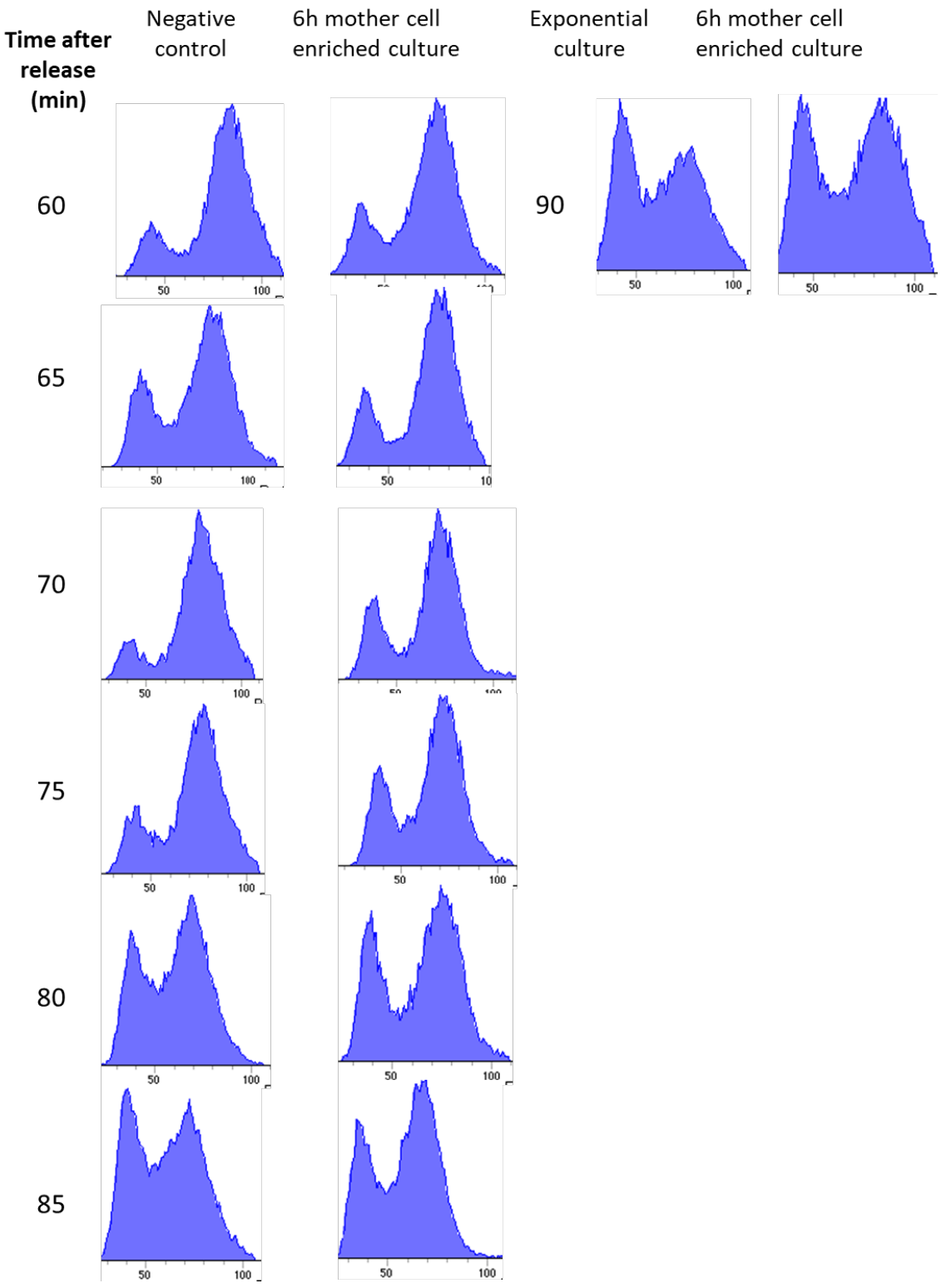

Figure 29. Comparison of cytometry profiles after alfa factor release between a 6h enriched culture and its negative control (not enriched culture). Cultures were treated with alfa factor for 2 hours and, then, released in pronase presence. Samples were taken every 5 minutes and stained with propidium iodide to analyse by flow cytometry. The first peak corresponds to cells in G1 phase, the second peak to cells in G2/M phase. We can observe that cells are in G1 right after the release until 15 minutes for the mother enriched culture and 25 minutes for the negative control, were we can observe the appearance of a peak that corresponds to S phase. Finally, the last timepoints corresponds to a re-establishment of the asynchronous culture.

With the intention of inquire whether G2 phase length is continuously elongated with replicative age, we performed the same experiment at 9 hours of mother enrichment. These cultures are enriched in cells with between 6 and 8 bud scars (see **figure 28**)

After analysing the 9 hour treated cultures, we obtained that these cultures show no differences with the cultures enriched for 6 hours in terms of cell cycle progression (**Figure 30**). Cultures enriched in cell with 5-8 bud scars go through G1/S transition 5-10 minutes before than the not enriched ones.

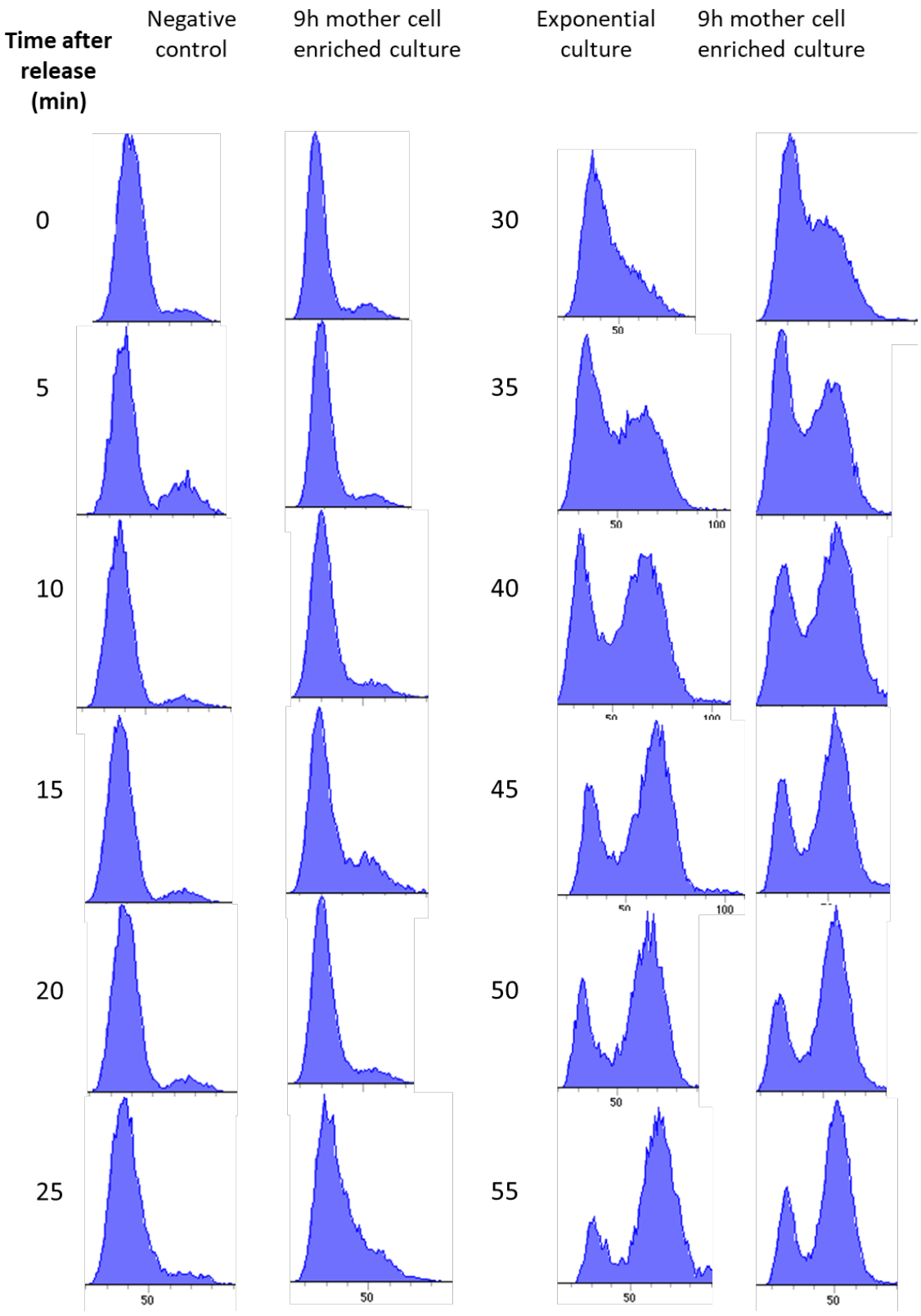
Time after release (min)
Negative control
9h mother cell enriched culture
Exponential culture
9h mother cell enriched culture
0
5
10
15
20
25
30
35
40
45
50
55
50
100

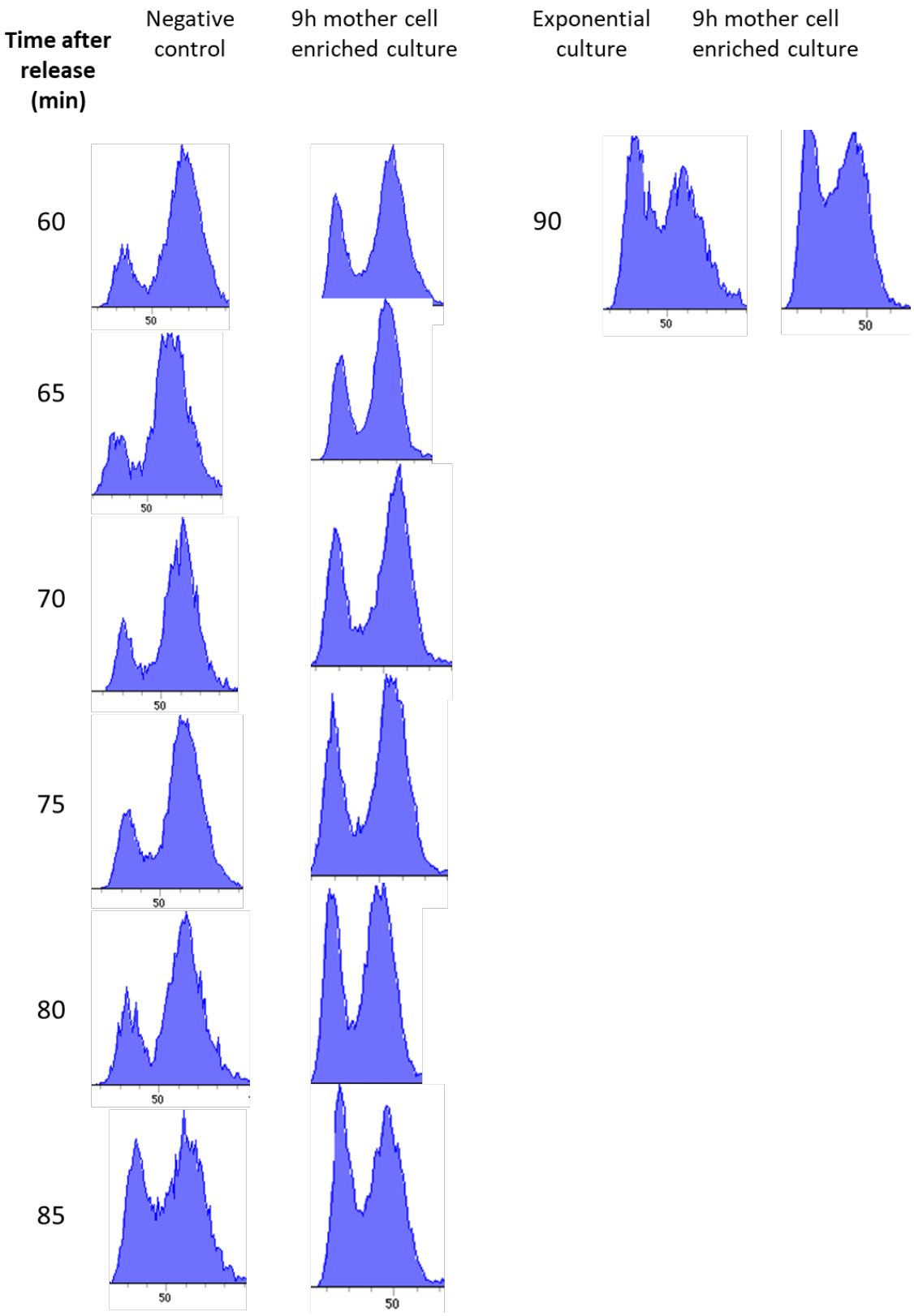

Figure 30. Comparison of cytometry profiles after alfa factor release between a 9h enriched culture and its negative control (not enriched culture). Cultures were treated with alfa factor for 2 hours and, then, released in pronase presence. Samples were taken every 5 minutes and stained with propidium iodide to analyse by flow cytometry. The first peak corresponds to cells in G1 phase, the second peak to cells in G2/M phase. We can observe that cells are in G1 right after the release until 30 minutes for the mother enriched culture and 35 minutes for the negative control, were we can observe the appearance of a peak that corresponds to S phase. Finally, the last timepoints corresponds to a re-establishment of the asynchronous culture.

We have to keep in mind that with flow cytometry, what we observe is relative percentages of cells in one phase or another, but are not able to quantify the time that cells spend on each cell cycle. This means that, if we see no big differences in cell cycle phases proportions, maybe there are differences in cell cycle lengths. For example, if G1 and G2 are both longer in aged cells, but the proportion of G2/G1 cells is maintained, we would not be able to detect changes by flow cytometry. Although this methodology has its limitations, what we are able to observe is that both cultures take similar times to complete a cell cycle, however, younger cultures spend more time in G1 than older ones, and less time in G2/M phase.

3.3.2.1 Young mother cells overexpress Whi5 in telophase compared to a new born cell enriched culture

Small microcolonies are formed by low proliferative cells. This means that all cells forming this microcolony are dividing slower. We found a correlation between small microcolonies formation and the replicative age of the founder cell. However, how the information of "lower proliferative capacity" is inherited by the daughter cells, that are new born cells, is still unknown.
We also found that replicative aged cells express more Whi5 than new-born cells in bulk populations so, we wondered if, then, cell cycle could be regulated through replicative aging by Whi5 concentration in mother cells and how this concentration is subsequently inherited by the new born daughter cell.
Whi5 expression peak is found on G2/M phase[94,125] . We can hypothesize that a relative longer G2/M phase in some cells of the population at early stages of aging, maybe due to stochastic changes, can lead to a higher Whi5 concentration by elongating the time at which Whi5 is being expressed. This could, subsequently, elongate G1 phase in these cells for the next division but, also, for their daughter cell due to the higher inheritance of Whi5 protein. As G2/M phase gets longer with the replicative age of the cell, this can be extended through a positive feedback loop during replication that finally concludes in the formation of a small microcolony.
In order to analyse this, we decided to carry out a q-PCR to study Whi5 RNAm concentrations during the different cell cycle phases of a mother enriched culture. This data was compared to a negative control enriched in new born cells. To do this, we performed the same biotin-streptavidin purification and alfa factor synchronization as described in the previous section. This time, samples were collected at the time-points that were enriched in the different cell cycle phases according to the previous studies of the cell cycle progression of a wildtype (enriched in mother cells and in the negative control). To determine these time-points, samples from the previous experiment were also analysed under the fluorescence microscope to determine, by cell morphology and nuclei

visualization, the cell cycle phase of these cells with more detail. A scheme of how cells were distributed according to their cell morphology into cell phases categories is shown on **Figure 31.A**

We then chose the time-points with more enrichment in every cell cycle phase category from four different replicas. After this, we analysed the time-points collected for the qPCR experiment and counted cells in the different cycle phases categories. The result of this analysis is shown in **Figure 31.B**

A

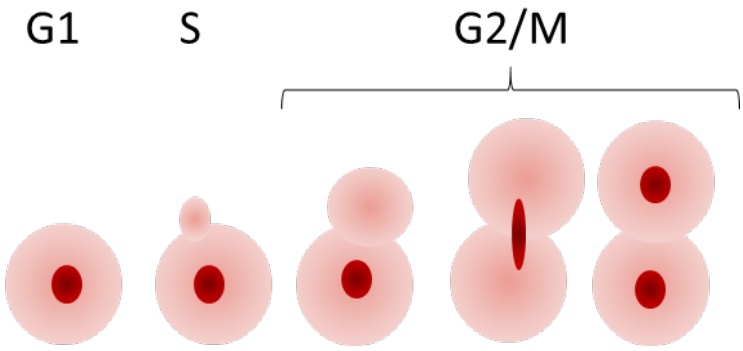

B

	Control culture						6h mother cell enriched					
START	R1	70	29	1	0	0	R1	78	12	10	0	0
	R2	83	14	3	0	0	R2	83	4	13	0	0
	R3	90	15	0	0	0	R3	83	9	8	0	0
S	R1	47	44	9	0	0	R1	34	43	23	0	0
	R2	55	40	5	0	0	R2	33	55	12	0	0
	R3	48	51	1	0	0	R3	43	42	15	0	0
G2/M	R1	25	7	60	6	2	R1	18	5	50	11	16
	R2	20	11	58	11	0	R2	17	6	59	9	9
	R3	26	5	60	9	0	R3	27	6	55	7	5
Telophase	R1	10	6	22	14	48	R1	17	3	25	5	50
	R2	11	1	18	13	57	R2	21	1	22	8	48
	R3	20	1	30	11	38	R3	28	1	30	5	36

Figure 31. (A) Scheme of how cells are categorized in the different cell cycle phases according to their morphology and the shape and number of nuclei. (B) Quantification of cells in each cell cycle phase counted under the fluorescent microscope. For every time-point used in the q-PCR, a control of the percentage of each cell cycle phase category was performed. Cells were stained with propidium iodide and manually counted under the microscope. R1-3 corresponds to each biological replica analysed by q-PCR. In red, the category of cells more represented on each culture.

After this, we performed an RNA extraction of all the samples, a retrotranscription of those RNAs and, finally, a q-PCR analysis with a Whi5 primer.

In **figure 32**, we can observe the *WHI5* expression pattern in a wildtype according to the cell cycle phase in a mother enriched culture (in red) and in a new-born enriched culture (in grey). According to what has been already described, *WHI5* expression increases in G2/M phase compared to G1 phase in both cultures. However, with high statistical significance, *WHI5* expression is higher in samples enriched with cells in telophase in the mother enriched culture.

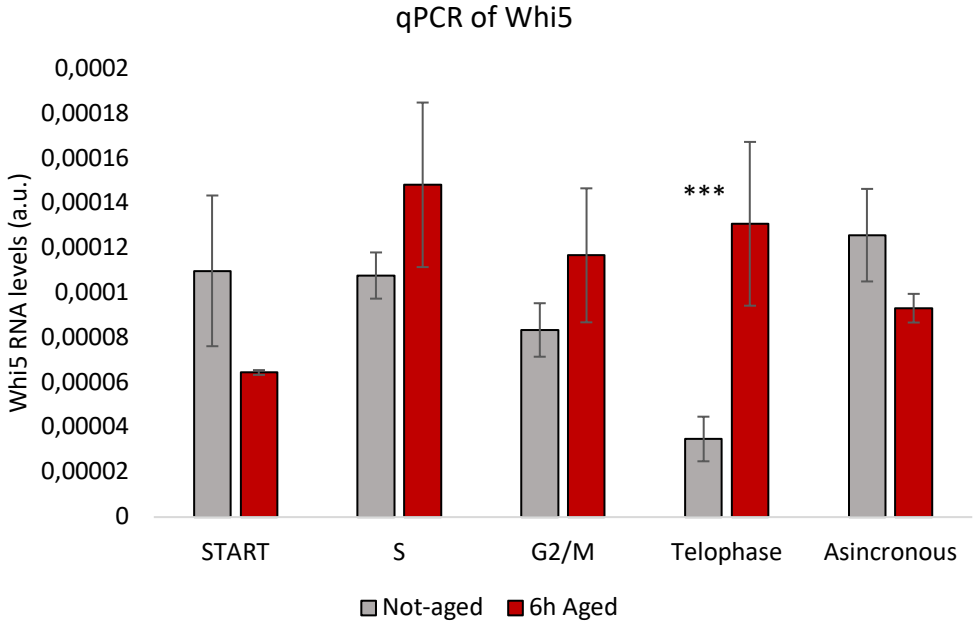

Figure 32. Quantitative PCR of Whi5 during cell cycle progression comparing a 6-hour mother cell enriched culture and a not enriched one. Samples were taken after alfa factor release at different timepoints that corresponded to a clear enrichment in each cell cycle phase mentioned. In the negative control, we observe no changes in Whi5 expression during the cell cycle, except in telophase, where it drops slightly. In the mother enriched culture, Whi5 is more expressed during telophase compared to its negative control.

This could suggest that young mother cells are more prone to accumulate Whi5 in G2/M phase and, then, this facilitates a higher inheritance of Whi5 concentration by the daughter cells. This may explain why daughter cells within a small microcolony inherit the low proliferative capacity of its mother.

4. Discussion

4.1. Combination of single-cell microencapsulation and confocal microscopy allows the study of proliferation heterogeneity in microcolonies

In contrast to other single-cell approaches that only focuses on mother cells [62,126–128], the techniques used in this work, combining microencapsulation of single yeast cells, microcolony generation and confocal microscopy, allowed us the study proliferation of a microcolony as a whole, from its founder and through all its progeny. This is a powerful tool to investigate heterogeneity of cell proliferation as a non-genetically hereditable trait, on which we are focused. There are other known methods to analyse single cell proliferation that consist on live imaging of yeast cells and their progeny for several cell cycles. However, any sort of analysis of these cells after their recording is not possible. Microencapsulation enables us to perform a wide variety of analysis of the microcolonies after their growth, such as comparative transcriptomic analysis[37].
Moreover, thanks to confocal microscopy and bud scar staining with calcofluor, we were able to recapitulate the formation of small microcolonies, which present the slow proliferation rate what we are interested in understanding. Confocal microscopy allows the disaggregation of a 3D microcolony in several 2D images of it, allowing the visualization of every cell within the microcolony. Quantifying the number of bud scars in every cell gives us the information of their replicative age, and an approach to their familiar relationship with the rest of cells within the microcolony.
Thanks to our method, we found first that there are two types of genealogies, or growth patterns, driving to small microcolonies, that is to microcolonies with a reduced proliferation rate. One of them, the one that we have called “isotropic growth” is clearly the largest group of small microcolonies (84 out of 96 analysed) and is characterised by the fact that all cells within the microcolony contribute to its formation. Under the confocal microscope, what we observe is that all cells (except for the newly born before the fixation of the microcolony) have bud scars on their cell wall, which means that they have divided at least once and the number of cells and bud scars per cell, are in concordance with a homogenous pattern of cell division. The other type of small microcolony formation is the one that presents what we have named “anisotropic growth”. It is the less represented type (12 out of 96 small microcolonies analysed) and is distinguished by the fact that the mother cell (or it and one of its daughters) is the only one dividing during the microcolony formation. In the confocal images of these small microcolonies we observe one cell with almost all the bud scars needed to explain the number of cells present in the small microcolony, surrounded by cells that have not divided yet (with no bud scars on their cell walls). In this case, the lack of proliferative capacity of the vast majority of its components, explains why these small microcolonies are, in fact, small. Their replicative capacity has been reduced to one of its members. The reason why these cells are not able to divide

is not clear. We still have no data or evidences on this matter, but in the literature, we can find several possible scenarios that might explain this phenomenon. It is known that spontaneous events of chromosomes missegregation occur and generate aneuploidies, which can contribute to anisotropic growth[129,130]. However, as our definition of "small" microcolony extends to almost 20% of colony forming cells in an exponential culture, and anisotropic growth is responsible to at least one tenth of small microcolonies, aneuploidy can hardly explain why 2% of cells produce such unexpected lineage.

This mother-restricted proliferation patterns have been described under metal-stress conditions[42]. Since our encapsulation protocol involves a transient treatment with EDTA, this subpopulation of small microcolonies might be related to this treatment.

Another possible scenario is that these founders are unable to properly retain aging factors in their cytoplasm during the asymmetric division, with the subsequent loss of proliferative capacity of its daughters[75,131–135]. Decline in mitochondrial membrane potential is also an age-dependent hereditable process that impairs daughter cell rejuvenation by asymmetric cell division[62]. However, most of those small microcolonies were founded by young mother cells with replicative age under 7, which is too low to lose its capacity for properly segregating aging factors or mitochondrial membrane potential, since these phenomena has been liked to old mother cells[62,131].

In any case, the presence of anisotropic growers only explain a minimal fraction of small microcolonies formation, which in most cases showed an isotropic growth pattern. In this case we observe a founder cell surrounded by its daughters, all of them with the expected number of bud scars. This points out the fact that the mother (founder) and all its progeny show the same slow proliferating phenotype. This necessarily implies the presence of a mechanism by which the mother cell and its progeny maintain a low proliferation rate.

Although we were able to classify small microcolonies in these two types of growth patterns, is likely that in longer genealogies the two patterns might have appeared in combination, and that they both contribute significantly to proliferation heterogeneity in budding yeast populations.

We can conclude that microencapsulation of single yeast cells and confocal microscopy, combined with calcofluor staining, are good tools for proliferation studies at single cell level, particularly if we are interested in how heterogeneous proliferative capacities are maintained through the lineages

4.2. Young mother cells already show reduced proliferation capacity, which can be transmitted to their progenies

More than 50% of small microcolonies that showed the isotropic type of growth, and the vast majority of those showing the anisotropic pattern, were founded by non-new born cells (**Figure 10**). Interestingly, in exponential *S. cerevisiae* cultures,

only less than 30% are non-new born cells, which is consistent with the loss of proliferative potential of aged cells after a high number of divisions[74,119,136].
When we analysed the replicative age of the founders, we observe that most of them had undergone only 2-4 divisions before founding the small microcolony, which is a very early stage of their replicative lifespan. From our findings, we deduced that replicative age is affecting the proliferative capacity of these young mother cells from very early stages. In this work, we have made an effort to understand the mechanisms promoting that such early replicative age could affect the replicative capacity of, not only the founders, but also their daughters. It can be considered that the replicative age of the founder cell is enough to slow the proliferative rates of it and its progeny due to lack of correct aging factors segregation, however, as previously mentioned, this loss of proliferative capacity has been described for very aged cells [137–139]. In fact, the replicative lifespan of the BY background (S288C) is around 25 divisions, and almost all studies about the implications of replicative age in proliferation have been made on bulk populations of around 18-25 divisions [78,118,139]. In contrast, our findings suggest that early replicative age already play a role in the proliferative fate of some cells. This conclusion is also strongly supported by the fact that we only need to age cultures for a small number of generations (the mean replicative age of these cultures is among 2 and 5 divisions) to see a significant increase in the formation of small microcolonies. Furthermore, the replicative age of the founder cell clearly correlates to the number of cells that form the microcolony (**Figure 11**). We observed that small microcolonies with a very low number of cells were usually founded by more aged founder cells (although but not older than below 7 divisions). At this point, it is important to emphasize that the proportion of cells with more than 7 divisions, in the exponential culture that is used to encapsulate, is enormously low as previously described[140,141] . The fact that the older the founder cell, the lower the number of cells that form the microcolony, highlights the importance of the founder cell replicative age for the proliferative rate of the microcolony.
From all these results, we shall hypothesize that replicative age is an important element contributing to proliferation heterogeneity since early stages, and that it may be linked to some kind of epigenetic mechanism that allows the slow proliferation phenotype to reach the following generations.

4.3. Whi5 participates in coupling early replicative age and proliferative capacity.

In previous transcriptomic studies comparing small and big microcolonies performed in our laboratory [37], *WHI5* appeared as the most significantly overexpress mRNA in small microcolonies. As Whi5 is a G1/S transition repressor, it was consistent with the low proliferative rate of small microcolonies, as it could be enlarging the cell cycle enough to increase the generation time. To analyse if

Whi5 high levels were causing slow proliferation in small microcolonies, we first tested if Whi5 protein was also overexpressed in small microcolonies. We used the Biosorter to separate small and big microcolonies formed by a Whi5-GFP tagged strain. Consistently with the RNA-seq results, we observed that cells in small microcolonies had clearly higher Whi5 protein levels than big ones (**Figure 17**). With this result, we could conclude that slow proliferating cells are accumulating more Whi5 protein than the ones with higher proliferative activity. To study if this Whi5 accumulation causes the slow proliferative phenotype of small microcolonies, we decided to test a Whi5-inducible strain. Interestingly, higher expression of Whi5 increased the proportion of small microcolonies formed in the culture. It is important to clarify that under our experimental conditions these cells did not show a significant change in generation time in liquid culture, so the higher formation of small microcolonies was not due to a general G1 arrest. Thus, we concluded that Whi5 levels contributes to proliferation heterogeneity.

After the results presented so far revealing the importance of Whi5 levels, we decided to go deeper into the effect of Whi5 accumulation. Our results confirmed that small microcolonies that show higher Whi5 expression are more frequently founded by young mother cells than by new born cells. Moreover, both increasing the replicative age of the culture and increasing their Whi5 expression provoke higher proportion of slow-proliferating microcolonies. We propose that, given these evidences, Whi5 could be mediating the impact that replicative age has on proliferative capacity since early stages of lifespan. In line with this, we found that Whi5 concentration increases with replicative age. We propose a model in which the probability of accumulating Whi5 increases with replicative age and that, in some cells, this accumulation reaches a threshold that slows down their proliferative rate in a way that can be transmitted to its progeny.

However, Is there any potential evidence for this role of Whi5 in the literature?

Whi5 concentration and dilution has been described as a determinant element in cell size control[142–144]. In these works, Whi5 dilution with cell size due to the combination of its constant synthesis rate and the increased cell volume, is the key that controls the moment of the cell division: once a certain Whi5 concentration threshold has been achieved, the inhibitors of Whi5 and the activators of the cell cycle are able to start a positive feedback loop that inevitably leads to cell cycle entry and progression. However, there have been recent publications that disagree with this conclusions and points towards the activators[116,117,145] (mainly Cln3) [115]and inhibitors differential scaling with cell size event as the main responsible for this decision [113,146,147]. Whether Whi5 determines cell volume at G1/S transition or not, our own microscopy observations of the Whi5 inducible strain treated cultures suggest that an accumulation of Whi5 does increase the cell volume and decreases the proliferative capacity of the cell. Increased cell volume may also lead to transcriptional alterations and cytoplasm dilution that ends with cell senescence, as a consequence the dilution of transcription machinery[78].

Whi5 has been proposed to regulate the mother-restricted proliferation pattern of stressed cells by transmitting from mother to daughter cells and blocking G1[42,106,148].

On another hand, in a cell replicative lifespan context, G1 arrest or delay [119] and Whi5 accumulation has been described as one of the causes of mortality in old yeast cells[78,118]. The accumulation of this cell cycle repressor in the mother cell during replicative aging due to asymmetric cell division, produces a G1 delay in these cells that, combined with other Whi5-independent mechanisms, are responsible for cell cycle defects and deregulation of G1 cyclins expression, leading to cell death. Although the mentioned works have focused on aged cells after performing a high number of divisions, consistently with them, our findings demonstrate that Whi5 expression increases with cells replicative age since the very first divisions.

From these results, we propose that Whi5 accumulation in early replicative aged cells increases their probability of reducing proliferative capacity due to a Whi5-dependent increased cell volume and cytoplasm dilution. In a clonal yeast culture, the probability of accumulating Whi5 increases with cell replicative age. The daughter cells of these mothers will have higher probability to inherit higher doses of Whi5 and, for this reason, to reach the threshold of Whi5 concentration needed for G1 delay and volume increase, leading to small microcolonies formation.

4.4. Cell cycle is tightly regulated during the replicative aging process

Our data suggests that small microcolonies are more frequently founded by non-new born cells and that these founders have more probability to accumulate Whi5 with every division, which could lead to a reduced proliferative capacity. In fact, increasing the Whi5 concentration in cultures, increases the proportion of small microcolonies that they form. Taking all this into account, we wondered what is the mechanism by which Whi5 accumulation is affecting proliferative capacity. Does Whi5 alter the cell cycle profile of these replicating cells?

With the aim of clarifying this, we studied the cell cycle profile of an exponential wildtype culture, relating it to their replicative age. What we observed was that new born cells spend proportionally more time on G1, as expected, as new born cells need more time to reach the correct size threshold to divide[98,149] . However, for the following replicative ages, we observed that cells spend proportionally more time in G2/M phase than in G1 until division 4 or 5, in which cells spend more or less the same amount of time in both phases. It has been described that some old yeast cells spend increasingly higher amounts of time in G2/M until they reach senescence and die[39,141]. Some other studies reveal that some other cells choose another aging pathway and spend increasingly time length in G1, until they reach a size that is not compatible with functional transcription and

translation, which lead them to death[139]. In any case, deregulated cell cycle, whether it is spending more time than needed in G2/M or G1, triggers transcriptional defects that end with cell death. However, this is described for very old cells (from 20-25 divisions) and what we are observing are newly born cells with 1 to 5 divisions.
The fact that we observed this phenomenon in several different backgrounds points towards sophisticated changes in the regulation of cell cycle across the early lifespan of young mother cells.
Then, why do young mother cells undergo longer G2/M phase? We tested several G2/M checkpoint mutants to test whether longer G2/M was a consequence of DNA damage caused by replicative stress even in early stages of their replicative lifespan. Some studies reveal that aged cells are more prone to have replicative stress and DNA damage [70], nonetheless, this can also be found in young cells. What we observed from these experiments was that no tested checkpoint mutant showed significant differences with the wildtype cell cycle profile in the replicative age range that we analysed. For this, we conclude that the longer G2/M phase that we observe in young mother cells is probably not due to any DNA damage or replicative stress response activation.
However, this method has a clear limitation, as we are not able to quantify the actual time length that each cell spends on each cell cycle phase. We are just observing the relative proportions of cells in one phase or another. This implies that we do not know whether longer G2/M involves longer cell cycle duration or whether longer G2/M is compensated by shorter G1 producing no change in global cell cycle length. We hope to solve this question by single cell live imaging in the next future.

As an alternative analysis to this differential cell cycle profile between new born and young mother cells, we synchronized an exponential culture, rich in new born cells, and a 6-hour aged culture using the biotin-streptavidin extraction method. After this, we released them and collected samples every 5 minutes to study how each culture progress through a complete cell cycle. We observed that early replicative aged cells spend 5 minutes less in G1 compared to the one rich in new born cells. This difference might be related to the fact that, as mention before, new born cells need more time in G1 to reach the correct cell size before cell division[98,101,110] . In any case, young mothers seemed to show longer G2/M than new born cells, suggesting than the high G2/M:G1 proportion detected in young mother cells is, at least partially, due to longer G2/M.
Whi5 transcription is regulated through the cell cycle, with maximum expression in S and G2/M phases[150]. Accordingly, longer G2/M in young mother cells might explain why we detected higher Whi5 levels in this type of cells. Our results confirmed in fact that cultures enriched in young mother cells expressed significant higher levels of Whi5 in telophase (**Figure 32**).

Considering all our experimental evidence and the ideas taken from the literature, we propose a model for Whi5-regulated proliferation heterogeneity that would involve the following elements:

- Whi5 expression has a certain probability to increase every division cycle, since the earliest stages of lifespan.
- High Whi5 levels contribute to reduce proliferation rates by extending the cell cycle.
- Long cell cycle favours keeping high Whi5 expression levels.
- High Whi5 concentration would be transmitted from mother to daughter cell during budding

Taken altogether, these elements would explain the activation of the slow proliferation pattern at any moment of a mother cell lifespan, and its epigenetic (non-genetic) transmission throughout generations by a robust self-maintaining loop.

The fact that our model is derived from studying young mother cells, which are abundant in exponential cultures, makes our conclusion linking age to proliferation particularly more relevant than those concluded from very old cells, which are always an absolute minority in growing populations.

This model is a tool to approach proliferation heterogeneity but does not intent to be a total explanation of such phenomenon. In fact, deleting Whi5 in a replicative aged culture (using the mother enrichment programme) did not alter the increase in small microcolonies that we detected in the wildtype aged culture. This reveals that, even though Whi5 is one of the drivers of proliferation heterogeneity, it is not the only actor in the interplay between replicative age and proliferation that we observe in yeast populations.

The combination of our results is compatible with a model in which a newborn cell with optimal proliferation capacity can undergo an increase in Whi5 expression at any division cycle, since the very first. This increased in Whi5 levels would negatively condition the proliferation rate of its progeny, favoring extensive growth heterogeneity of the whole population. Increase of Whi5 might be due to stochastic noise in its expression, but might also be linked to its time of expression during the cell cycle, which seems to be maximal in G2/M. Any delay in G2/M, due for instance to activation of checkpoint mechanisms, might provoke increased Whi5 levels, which in turn would induce subsequent cell-cycle alterations, enabling a self-regulatory loop that propagates throughout the cell linage. Such activation of checkpoints has been described to play a role in mitotic catastrophe during late aging [70]. The findings made in this thesis work suggest that it may be a more common phenomenon than expected, potentially being triggered in any stage of replicative life span, and explaining the high proliferative heterogeneity of cell populations.

5. Conclusions

1. Combination of cell microencapsulation and confocal microscopy is a reliable method to analyze cell lineages.

2. Replicative age substantially contributes to proliferative heterogeneity in clonal populations.

3. Decrease in proliferative capacity of young mother cells arises after the first mitotic division.

4. The progeny of a young mother cell can non-genetically inherit its decreased proliferative capacity.

5. The cell cycle regulator Whi5 participates in one of the mechanisms that links replicative age and cell proliferative capacity.

6. Materials and methods

6.1 Strains and growth conditions

All strains were cultured at 30ºC in constant agitation at 180 rpm in the indicated media for every experiment.

The wildtype BY4741 strain was obtained from the EUROSCARF yeast collection. Whi5 tagged with GFP was obtained from Thermo Fisher Scientific GFP yeast clone collection. See **table 2** for a list of all strains used in this work.

Name	Genotype	Source
BY4741	*MATa; his3D1; leu2D0; met15D0; ura3D0*	Euroscarf
DNY51	*Mat a can1::PSTE2-Sp_his5 leu2Dyp1D met15D hoD::PSCWII-cre-EBD78-NATMX loxP-ubc9-LOXp-Leu2 loxP-CDC20-Intron-loxP-HPHMX*	Kindly provided by
DNY51-*whi5Δ*	*Mat a whi5::kanMX6 can1::PSTE2-Sp_his5 leu2Dyp1D met15D hoD::PSCWII-cre-EBD78-NATMX loxP-ubc9-LOXp-Leu2 loxP-CDC20-Intron-loxP-HPHMX*	This work
KSY098-1	*Mat a; his3::LexA-ER-AD-TF-HIS3 whi5::kanMX6-LexApr-Whi5-mCherry-Adh1term-Leu2*	Kindly provided by
W303	*Mat a leu2D3 112 trp1-1 can1-100 ura3D1 ade2D1 his3D11 15*	Kindly provided by Dr. Francesc Posas
Whi5GFP	*Mat a his3Δ1 leu2Δ0 met15Δ0 ura3Δ0 Whi5-GFP::HIS3*	Thermo Fisher Scientific GFP yeast clone collection
whi5Δ	*MATα; whi5::kanMX6 his3D1; leu2D0; met15D0; ura3D0*	Euroscarf
whi7Δ	*MATα; whi7::kanMX6 his3D1; leu2D0; met15D0; ura3D0*	Euroscarf
whi5Δ whi7Δ	*MATα; whi5::kanMX6 whi7::kanMX6 his3D1; leu2D0; met15D0; ura3D0*	This work
msa1Δ	*W303 MATa msa1::LEU2* (**YAG1**)	Kindly provided by Dr. Francesc Posas

msa2Δ	*W303 MATa msa2::HPH* (**YAG5**)	Kindly provided by Dr. Francesc Posas
msa1Δ msa2Δ whi5Δ	*W303 MATa whi5::URA3 msa1::LEU2 msa2::hph* (**YAG13**)	Kindly provided by Dr. Francesc Posas
***whi5Δ* (w303 background)**	*W303 MATa whi5::LEU2* (**YPC455**)	Kindly provided by Dr. Francesc Posas

Tale 2. Strains used in this work

6.2 Media

- **YPAD rich medium:** 1% yeast extract, 2% bacterial peptone, 0,2% adenine, 2% glucose (added after autoclaving)
- **SC-URA, Synthetic minimal medium without uracile**: 0,17% yeast nitrogen bases without amino acids, 0,5% ammonium sulphate, 2% glucose (added after autoclaving). This media is supplemented with the essential amino acids lysine, adenine, methionine, tryptophan, leucine and histidine.

For agar plates of the same media, 2% agar was added before autoclaving.

6.3 Probes used in this work

Name	**Sequence**
Chk1 Down	CAATTAGGCCAAGCCCACACAG
Chk1 up	TCACTGTAATGATCAAGTTA
cln3up	TGTACGACGGCACCGCCTC
rad53 down	CGTATCAAAACGTCACTCTATATG
rad53 down 2	GCAACGGGAGTGACGCGTAA
rad53 up	CCTTGGCGTTTCTCATCTCACC
Rad9 Down	GGA GAG AAT GTT TCG AGA
Rad9 Up	GTCCCAAA AAGGAAATAG
sml1 down	CTT TCT TCG CAG CTA TAT AC
sml1 up	GCA ATG AAA TGT TTC GTT ATT
Whi7-down	CAATTAGGCCAAGCCCACACAG
Whi7-up	TCACTGTAATGATCAAGTTA

6.4 Drugs and reagents used in this work

- α-factor (α matig pheromone GenScript)
- 6-Azauracile (6AU) (Sigma-Aldrich)
- Biotin (EZ-Link ™ Sulfo-NHS-LC-Biotin, Thermo Scientific)
- Calcofluor (Fluorescent Brightener 28, Sigma)
- Doxycycline (DOX) (Sigma-Aldrich)
- Estradiol (Sigma-Aldrich)
- Mycophenolic Acid (MPA)(Sigma-Aldrich)
- Pronase E (Merk)
- Propidium iodide (Sigma-Aldrich)
- Streptavidin (New England Biolabs)

6.5 RNA extraction

10 ml of every culture at an $O.D_{600nm}$ of 0,5 were collected in 15 ml Falcon tubes. They were centrifuged and washed with distilled water and then frozen in liquid N_2. Samples were preserved maximum 3 days at -20ºC.
After this, samples were washed again with distilled water and then resuspended in 400µl of TES (DEPC water, 10nM Tris-HCL 7.5 pH, 10mM EDTA and 0,5% SDS). Then samples were washed twice with 400µl Acid-phenol and once with 400µl of chloroform. They were resuspended in 40 µl of sodium acetate and 1ml of ethanol 96% and incubated overnight at -20ºC. Finally, samples were washed with 70% ethanol and the dried pellet was resuspended bi-distilled water.
For qPCR experiments, samples were treated with DNAase before the RT-PCR

6.6 Protein extraction and Western-Blot

10ml of cultures at $D.O_{600nm}$ were collected and washed with distilled water. Proteins were extracted by FastPrep-24 ®5G breaking method by adding equal parts of lysis tampon and glass beads and then subjected to 3 cycles of 30 seconds breaking (5M/s). Samples were then centrifuged and supernatants were collected for boiling 3 minutes with 2X laemmli buffer.
For the western blot, samples were subjected to a 180V current in a SDS-page gel (12%) for 60 minutes. After this, proteins were transferred to a membrane using a wet transfer protocol with a current of 80V for 90 minutes.
The membrane was blocked using 5% solution of formula for 1 hour and then incubated overnight with the primary antibody (anti-RFP in this case). After 3 washes of 5 minutes with TTBS, the membrane was incubated with the secondary

antibody (anti-rat in this case) for 45 minutes. The results were revealed using a Chemidoc imaging system from BioRad®.

6.7 Microencapsulation

Microencapsulation conditions were set to obtain a single cell into every alginate microcapsule to ensure that all the cells growing inside every capsule were clonal.

First, cells were cultured to 0,5 O.D to ensure that it was at exponential growth phase. In the next step, for every 3ml of microencapsulation solution 2,7 ml of 1,66% sodium alginate was added, plus 290 µl of YAPD and 10 µl of cells. This solution was injected into a 5ml syringe and placed into the correct position (**Figure 33**) in an Ingeniatrics® Cellena microencapsulator following a well described protocol already published[37] . The solution was injected from the syringe into a microparticle nebulizator with a constant air flux, which allowed the formation of approximately 100 µm alginate microparticles that continuously fell into a solution of calcium chloride (3%) for its jellification.

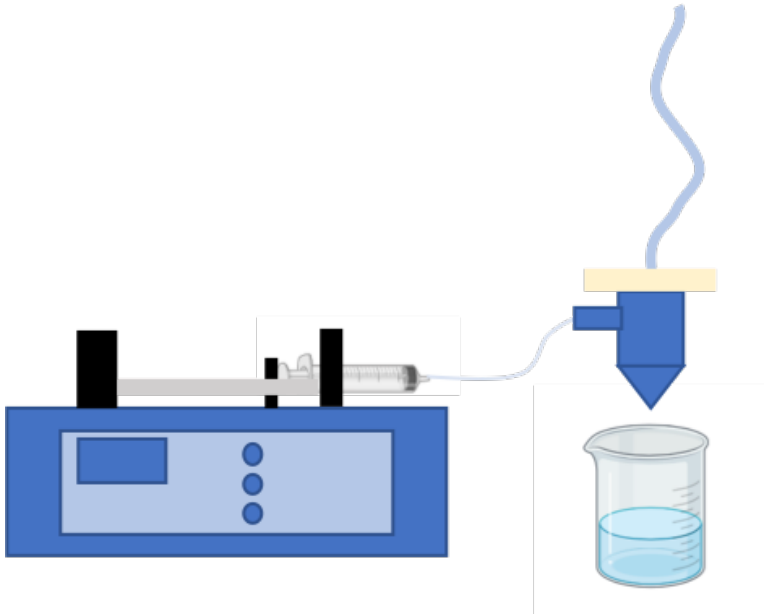

Figure 33. Cellena encapsulator scheme. The encapsulation mix is transferred from the syringe towards the nebulizator, and from this, in beads form, to a 3% calcium chloride for its jellification.

After the microencapsulation, capsules were collected using a Falcon ® cell filter 40 µm, and cultured together in 30 ml of YPAD for the indicated number of hours at 30ºC in continuous stirring. After the incubation, microcapsules were collected again and fixated in 70% ethanol and YPAD proportions 1:1.

6.8 Light microscopy and microcolony size analysis

Microcolony sizes analysis was performed using an optical microscope (Leica DM750). Microcolonies were classified according to their size in small, medium and big microcolonies. As capsule diameter is stable (approximately 100mm), big microcolonies are considered those that surpass the radio of the capsule, medium microcolonies are those whose size range between half the radio and the radio, and the ones smaller than half the radio are considered small microcolonies (**figure 34**).

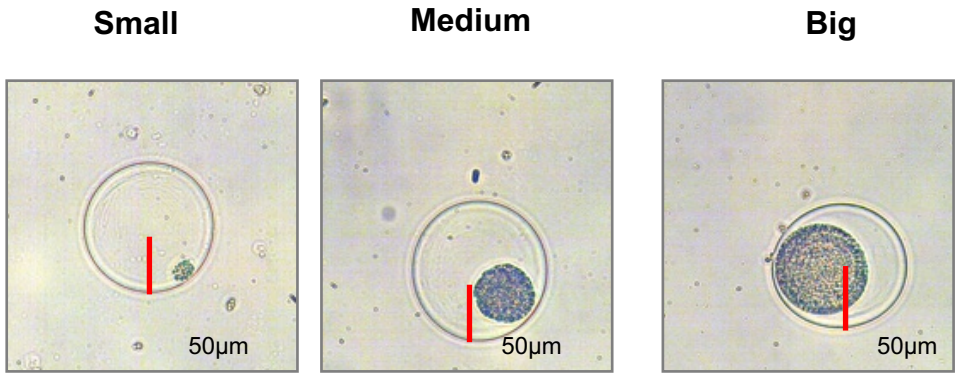

Figure 34. Guide scheme for microcolonie sizes. Small microcolonies are smaller than half the ratio of the capsule. Big microcolonies exceeds the capsule radio length. Medium microcolonies ranges between half the radio and the radio of the capsule.

6.9 Mother cell enrichment assay

- **MEP strains**: Our first approach for this consisted of using DNY51 strain (**Figure 35**). First, cells were grown at normal culture conditions to exponential phase (0,5 O.Ds approximately), they were then collected and inoculated in 10ml of YPD (previously preheated at 30ºC) and Estradiol at a final 1mM concentration. They were cultured at 30ºC for 3 hours. The Estradiol was then washed, and cells were resuspended in YPD to finally add them to the microencapsulation mixture. After the microencapsulation, capsules were collected and cultured in YPD (without Estradiol) for 13 hours at 30 ºC. Finally. Microcapsules were collected and fixated as usual.

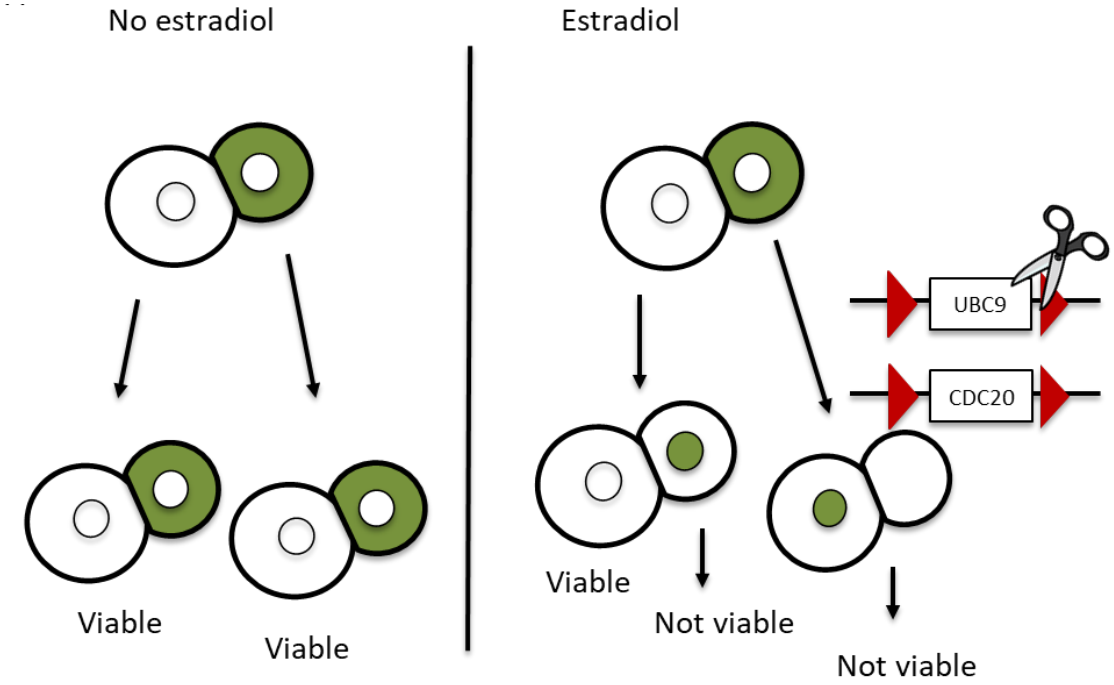

Figure 35 Scheme of the Mother Enrichment Programme mechanism. Yeast strain with Cre recombinase under the control of a specific daughter cell promoter. This Cre recombinase is activated in the presence of Estradiol, enters daughter cell nucleus and deletes two essential genes for cell cycle. This causes an irreversible arrest just in the daughter cell while mother cells keep growing unaffected.

- **Wildtype BY4741 strain:** The second approach consisted of a biotin-streptavidin purification performed in a wildtype BY4741 strain. For this experiment, 20 ml of an exponential wildtype culture (approximately at 0,4 O.D) was collected and washed with PBS twice. After this, cells were resuspended in 1ml PBS and incubated with Biotin (EZ-Link ™ Sulfo-NHS-LC-Biotin, Thermo Scientific) for 30 minutes (10mg per sample). Cells were then washed with PBS and incubated in YPAD at 30ºC in continuous agitation for 6 hours (30 minutes for the negative control). After the incubation, cells were washed again and incubated with streptavidin ((New England Biolabs) 150µl per sample) for 30 minutes at room temperature. The next step required a special Eppendorf magnet that retained the magnetic beads linked to the streptavidin, and also the cells glued to it through Biotin molecules. The supernatant was discarded and the cells linked to the magnet were washed several times. After this, cells were incubated in YPAD media for 30 minutes and then encapsulated.

Previous to the encapsulation, a sample of the treated and not treated cultures were collected and stained with calcofluor to determine the replicative age of both cultures (See Materials and Methods: *Calcofluor staining* and *Fluorescent microscopy and bud scar counting***)**

6.10 Calcofluor staining

For replicative age analysis of a wildtype exponential culture, a bud scar staining was performed. First, cells were collected at exponential growth phase, fixated with 70% Ethanol and stored at 4ºC for at least 2 hours. After that, cells were washed with PBS 1X and resuspended in a solution of PBS and calcofluor (Fluorescent Brightener 28 from Sigma Aldrich) at a final concentration of 0.1 mg/ml. They were incubated for 5 to 10 minutes in dark conditions at room temperature and then washed again with PBS. Cells were finally resuspended in 100ml of PBS.

Microcolonies were also stained with calcofluor for small microcolonies founder cell identification. First, fixated microcolonies (YPD and Ethanol 70% 1:1) were filtrated and collected. They were washed with a TrisHCl-CaCl 2:1 solution and inoculated in 0.5ml of calcofluor at 0.1 mg/ml concentration for 5 minutes at room temperature. After that, microcapsules were filtrated and washed again with TrisHCl-CaCl solution. Finally, they were collected and preserved in 0.5ml of the same solution.

6.11 Fluorescent microscopy and bud scar counting

Replicative age of not microencapsulated cultures was calculated by manually counting the number of cells bud scars using a direct fluorescent microscope Olympus BX-61. Bud scars were detectable using the DAPI filter. Cells were classified according to the number of bud scars, which is a direct method to know their replicative age.
Using Bright Field filter, cell could be also classified by their cell cycle phase into three categories: G1 (not budded, round cells), S (small bud) or G2/M (large bud).

6.12 Confocal microscopy and founder cells age analysis

Microcolonies stained with calcofluor were visualized in a A1R Confocal Nikon Microscope using the 60X oil objective and DAPI filter. Images of small microcolonies (n=187) were taken every 0.5 mM in Z-axis.
Number of cells and number of bud scars were counted going through all Z axis images. Using the formula $number\ of\ cells - number\ of\ bud\ scars + 1 = founder\ cell\ age$ the replicative age of the small microcolonies founder cells at initial time (right before founding the small microcolony) was estimated. The resulting number was corrected when incoherent: very high numbers usually meant that the small microcolony was founded by two aged cells. These cases were taken out of the analysis. On the other hand, negative numbers probably meant that the number of bud scars was underestimated. Going through the

genealogy of the small microcolony, taken into consideration the number of buds observed on each cell, these numbers were corrected according to the most probable scenario (being usually the case of a new-born cell founder). In total, 93 small microcolonies were classified as “valid” for the analysis.

6.13 Modulation of Whi5 expression

KSY098-1 strain was first growth to exponential phase (D.O.=0.5) and then microencapsulated following the usual protocol of microencapsulation. After that, microcapsules, which have one single cell trapped each, were collected and then inoculated in flasks with YPD and Estradiol at different concentrations: one flask with no Estradiol for the control, the others with 2nM, 4nM, 5nM, 6nM, 8nM and 10nM respectively.
The wildtype W303 control was separately encapsulated the same day in the presence of the highest estradiol concentration tested (10nM). Finally, these and the W303 wildtype strain were cultured for 10 hours at 30 degrees.

6.14 Whi5-GFP Cell sorting

Whi5-GFP strain was cultured to exponential growth phase in minimum media complemented with all the essential amino acids except Histidine. Then, cells were collected at DO_{600nm} 0.5 and sorted in a BD FACSJazz™ cell sorter according to the GFP intensity detected. Cells with low Whi5 expression sorting criteria was stablished according to a negative (not fluorescent) control BY4741. Cells with higher Whi5 expression were selected drawing the sorting gate for the 5% of cells with highest Whi5 GFP expression. After sorting, each sample was stained with calcofluor and analyzed.

6.15 Determination of Whi5 expression in microcolonies

To measure the Whi5 expression according to the microcolony size, a Whi5-GFP tagged strain was microencapsulated in the normal conditions specified in Materials and Methods. After 13 hours of incubation in YPAD, the microcapsules were collected in SC media and then directly analyzed using a Large Particle Cytometer Biosorter® (Union Biometrica, Inc.). Six independent microencapsulations of Whi5-GFP were used in order to get enough microcolonies for the analysis. Two different measures were performed and were classified in small, medium or big microcolonies according to their “Time of flight” (TOF). The time of flight in this cytometer is indicative of the size of the particle and does not consider the alginate particle. Microcolonies were estimated to be in the range 60-250 of time of flight and they were divided in 3 categories: big (250-185), medium (184-120) and small (119-60). The size of the sample was

101163 valid events. These events were classified into big, medium or small microcolonies according to the previously described criteria and then, their green signal (GFP signal) was relativized to their size (TOF).

6.16 Alfa-factor synchronization of aged cultures

To properly analyze relatively aged cells cell cycle, a wild type culture was enriched in mother cells, synchronized in G1 phase and analyzed by flow cytometry for the following cell cycle. With this purpose, the approach was as follows: cultures were collected at, at least, 0,4 O.Ds (a volume of 25ml o proportional part depending on the O.D). They were then centrifuged at 4.000 rpm for 4 minutes, washed with 1ml of PBS twice (2 minutes at 6000rpm) and incubated with 10 mg of Biotine for 30 minutes. Half of the culture was collected as control cells (not enriched in mother cells) and was incubated in YPAD for 30 minutes in agitation at 30ºC. The rest of the culture was incubated for 6 hours in the same conditions. After each incubation, cells were treated with 1µg/ml of alfa-factor for 2 hours (or until the shmoo structure is visible under the microscope). After this, the streptavidin extraction was performed following the same protocol already described with the additional step of inoculating more alfa factor to the streptavidin solution. After this step, cells were washed and inoculated into fresh YPAD media (previously heated at 30ºC) with pronase at 50µg/ml. Samples were collected every 5 minutes for the following 90 minutes and fixated in 500 µl of70% Ethanol.

6.17 Propidium iodide staining and flow cytometry

Fixated cells were washed twice with 1ml of sodium citrate 50mM and then treated with 500µl of sodium citrate with RNAase overnight. After this, 500µl of a solution of propidium iodide (PI)(4µg/ml) and sodium citrate 50nM was added to every sample. Cells were incubated for 30 minutes at room temperature and dark conditions.
For flow cytometry, samples were sonicated using a Bioruptor®(Diagenode). Sonications were done for 3 cycles of 1 minute (30 seconds of sonication for every cycle). After this, cell cycle analysis was performed using a BD FACSCanto™ Clinical Flow Cytometry System. Cells were classified according to their PI content, which correlates with DNA content. This allows sorting cells into G1 cells (1 content of DNA) and G2/M (2 contents of DNA).

6.18 Determination of Whi5 mRNA in synchronized aged cells

In order to determine Whi5 mRNA levels for every cell cycle phase, samples of an aged alfa-factor synchronized wildtype culture were collected and then analysed by qPCR.

First, cultures were collected at exponential growth and enriched in mother cells using the same protocol already described. After alfa factor treatment, cells were enriched in mother cells (early aged cells) through streptavidin extraction and then inoculated into YPAD and pronase. 15 ml samples were collected at the indicated times for every experiment and then washed and frozen in N_2.
RNA of each sample was extracted and then analysed using a Roche LightCycler 480 with a Whi5 probe. SCR1 probe was used as a normalising control.

6.19 Live-imaging experiments

Whi5-GFP culture was growth overnight in 5ml YPAD media and then diluted in YNB media previously filtered. Once cultures reached 0,3 $O.D_{600nm}$ they were collected and inoculated into a specially designed chamber (Figure 15) to capture single cells into wells and allowing them to grow in a monolayer. To ensure that most wells were filled with just one single cell, conditions were optimized to 1 drop of 3 µl of the culture at 0,3 O.D in each chamber. This was then disposed over a special cover (Cover glass D 263®) and then in this order:

1. Tubes of approximately 30cm are introduced in every position marked in the figure X.
2. The chamber disposed in the cover is placed into the microscope, using a specially adapted platform.
3. The tube placed in the position 1, is connected to an empty syringe that will allow the vacuuming of the chamber. This will ensure the media flow from the beginning of the chamber towards the end.
4. The tube placed in the position 2 is connected to a syringe full of YNB media (filtered in order to facilitate the flow and impede any clogs).
5. The tube placed in position 3 is connected to a small syringe that will later allow the injection of calcofluor into the chambers (after the recording).
6. The tube placed in position 4 is the waste exit.

Chambers are connected via tubular structures that allows the flow of the media towards every well and, finally, towards the end of the chamber that is the waste exit (position 4).
After vacuuming the chamber, and placing it in the microscope, wells are visualized making a wide range scanning of the chamber. After this, positions in which we are able to localize one single cell in a well are selected (10 or 11 per recording) and marked for recording. After the recording, the calcofluor is slowly injected into the chambers. One snapshot at every selected position is taken in DAPI channel in order to visualize the bud scars.

Microscope settings:
Snapshot: every 5 minutes for 13 hours in Brightfield channel and GFP channel.
GFP laser power: 30%. 80 ms exposure time.
DAPI laser power: 30%.100 ms exposure time.

7. Bibliography

1. Ackermann, M. A functional perspective on phenotypic heterogeneity in microorganisms. *Nature Reviews Microbiology* vol. 13 497–508 Preprint at https://doi.org/10.1038/nrmicro3491 (2015).
2. Sánchez-Romero, M. A. & Casadesús, J. Contribution of phenotypic heterogeneity to adaptive antibiotic resistance. *Proc Natl Acad Sci U S A* **111**, 355–360 (2014).
3. Ryall, B., Eydallin, G. & Ferenci, T. Culture History and Population Heterogeneity as Determinants of Bacterial Adaptation: the Adaptomics of a Single Environmental Transition. *Microbiology and Molecular Biology Reviews* **76**, 597–625 (2012).
4. Newman, J. R. S. *et al.* Single-cell proteomic analysis of S. cerevisiae reveals the architecture of biological noise. *Nature* **441**, 840–846 (2006).
5. Martins, B. M. C. & Locke, J. C. W. Microbial individuality: how single-cell heterogeneity enables population level strategies. *Current Opinion in Microbiology* vol. 24 104–112 Preprint at https://doi.org/10.1016/j.mib.2015.01.003 (2015).
6. Levy, S. F., Ziv, N. & Siegal, M. L. Bet hedging in yeast by heterogeneous, age-correlated expression of a stress protectant. *PLoS Biol* **10**, (2012).
7. Lee, J. A. *et al.* Microbial phenotypic heterogeneity in response to a metabolic toxin: Continuous, dynamically shifting distribution of formaldehyde tolerance in Methylobacterium extorquens populations. *PLoS Genet* **15**, (2019).
8. Li, S., Giardina, D. M. & Siegal, M. L. Control of nongenetic heterogeneity in growth rate and stress tolerance of Saccharomyces cerevisiae by cyclic AMP-regulated transcription factors. *PLoS Genet* **14**, (2018).
9. Arlia-Ciommo, A., Piano, A., Leonov, A., Svistkova, V. & Titorenko, V. I. Quasi-programmed aging of budding yeast: A trade-off between programmed processes of cell proliferation, differentiation, stress response, survival and death defines yeast lifespan. *Cell Cycle* **13**, 3336–3349 (2014).
10. van Dijk, D. *et al.* Slow-growing cells within isogenic populations have increased RNA polymerase error rates and DNA damage. *Nat Commun* **6**, (2015).
11. Lipinski, K. A. *et al.* Cancer Evolution and the Limits of Predictability in Precision Cancer Medicine. *Trends in Cancer* vol. 2 49–63 Preprint at https://doi.org/10.1016/j.trecan.2015.11.003 (2016).
12. Singh, S. P. *et al.* Different developmental histories of beta-cells generate functional and proliferative heterogeneity during islet growth. *Nat Commun* **8**, (2017).
13. Marusyk, A. & Polyak, K. Tumor heterogeneity: Causes and consequences. *Biochimica et Biophysica Acta - Reviews on Cancer* vol. 1805 105–117 Preprint at https://doi.org/10.1016/j.bbcan.2009.11.002 (2010).
14. El-Sayes, N., Vito, A. & Mossman, K. Tumor heterogeneity: A great barrier in the age of cancer immunotherapy. *Cancers* vol. 13 1–14 Preprint at https://doi.org/10.3390/cancers13040806 (2021).
15. Davis, K. M. & Isberg, R. R. Defining heterogeneity within bacterial populations via single cell approaches. *BioEssays* vol. 38 782–790 Preprint at https://doi.org/10.1002/bies.201500121 (2016).

16. Cota, I., Blanc-Potard, A. B. & Casadesús, J. STM2209-STM2208 (opvAB): A phase variation locus of salmonella enterica involved in control of O-antigen chain length. *PLoS One* **7**, (2012).
17. Sampaio, N. M. V. & Dunlop, M. J. Functional roles of microbial cell-to-cell heterogeneity and emerging technologies for analysis and control. *Current Opinion in Microbiology* vol. 57 87–94 Preprint at https://doi.org/10.1016/j.mib.2020.08.002 (2020).
18. Ghosh, D., Veeraraghavan, B., Elangovan, R. & Vivekanandan, P. Antibiotic resistance and epigenetics: More to it than meets the eye. *Antimicrob Agents Chemother* **64**, (2020).
19. Ziv, N., Siegal, M. L. & Gresham, D. Genetic and nongenetic determinants of cell growth variation assessed by high-throughput microscopy. *Mol Biol Evol* **30**, 2568–2578 (2013).
20. Olivenza, D. R. *et al.* A portable epigenetic switch for bistable gene expression in bacteria. *Sci Rep* **9**, (2019).
21. Pelechano, V., Wei, W. & Steinmetz, L. M. Extensive transcriptional heterogeneity revealed by isoform profiling. *Nature* **497**, 127–131 (2013).
22. Gasch, A. P. *et al.* Single-cell RNA sequencing reveals intrinsic and extrinsic regulatory heterogeneity in yeast responding to stress. *PLoS Biol* **15**, (2017).
23. Welkenhuysen, N. *et al.* Single-cell study links metabolism with nutrient signaling and reveals sources of variability. *BMC Syst Biol* **11**, (2017).
24. Sánchez-Romero, M. A., Mérida-Floriano, Á. & Casadesús, J. Copy Number Heterogeneity in the Virulence Plasmid of Salmonella enterica. *Front Microbiol* **11**, (2020).
25. O'Kane, C. J. & Hyland, E. M. Yeast epigenetics: The inheritance of histone modification states. *Bioscience Reports* vol. 39 Preprint at https://doi.org/10.1042/BSR20182006 (2019).
26. Casadesús, J. & Low, D. A. Programmed heterogeneity: Epigenetic mechanisms in bacteria. *Journal of Biological Chemistry* vol. 288 13929–13935 Preprint at https://doi.org/10.1074/jbc.R113.472274 (2013).
27. Sánchez-Romero, M. A., Olivenza, D. R., Gutiérrez, G. & Casadesús, J. Contribution of DNA adenine methylation to gene expression heterogeneity in Salmonella enterica. *Nucleic Acids Res* **48**, 11857–11867 (2020).
28. Acar, M., Mettetal, J. T. & van Oudenaarden, A. Stochastic switching as a survival strategy in fluctuating environments. *Nat Genet* **40**, 471–475 (2008).
29. Radzinski, M. *et al. Temporal profiling of redox-dependent heterogeneity in single cells*.
30. Acar, M., Mettetal, J. T. & van Oudenaarden, A. Stochastic switching as a survival strategy in fluctuating environments. *Nat Genet* **40**, 471–475 (2008).
31. Dubnau, D. & Losick, R. Bistability in bacteria. *Molecular Microbiology* vol. 61 564–572 Preprint at https://doi.org/10.1111/j.1365-2958.2006.05249.x (2006).
32. Veening, J. W., Smits, W. K. & Kuipers, O. P. Bistability, epigenetics, and bet-hedging in bacteria. *Annual Review of Microbiology* vol. 62 193–210 Preprint at https://doi.org/10.1146/annurev.micro.62.081307.163002 (2008).
33. Davis, K. M. & Isberg, R. R. Defining heterogeneity within bacterial populations via single cell approaches. *BioEssays* vol. 38 782–790 Preprint at https://doi.org/10.1002/bies.201500121 (2016).

34. Sánchez-Romero, M. A. & Casadesús, J. Contribution of phenotypic heterogeneity to adaptive antibiotic resistance. *Proc Natl Acad Sci U S A* **111**, 355–360 (2014).
35. Olivenza, D. R. *et al.* A portable epigenetic switch for bistable gene expression in bacteria. *Sci Rep* **9**, (2019).
36. Levy, S. F., Ziv, N. & Siegal, M. L. Bet hedging in yeast by heterogeneous, age-correlated expression of a stress protectant. *PLoS Biol* **10**, (2012).
37. García-Martínez, J. *et al.* The cellular growth rate controls overall mRNA turnover, and modulates either transcription or degradation rates of particular gene regulons. *Nucleic Acids Res* **44**, 3643–3658 (2016).
38. Li, S., Giardina, D. M. & Siegal, M. L. Control of nongenetic heterogeneity in growth rate and stress tolerance of Saccharomyces cerevisiae by cyclic AMP-regulated transcription factors. *PLoS Genet* **14**, (2018).
39. Campisi, J. & D'Adda Di Fagagna, F. Cellular senescence: When bad things happen to good cells. *Nature Reviews Molecular Cell Biology* vol. 8 729–740 Preprint at https://doi.org/10.1038/nrm2233 (2007).
40. Kundu, K., Weber, N., Griebler, C. & Elsner, M. Phenotypic heterogeneity as key factor for growth and survival under oligotrophic conditions. *Environ Microbiol* **22**, 3339–3356 (2020).
41. Arlia-Ciommo, A., Piano, A., Leonov, A., Svistkova, V. & Titorenko, V. I. Quasi-programmed aging of budding yeast: A trade-off between programmed processes of cell proliferation, differentiation, stress response, survival and death defines yeast lifespan. *Cell Cycle* **13**, 3336–3349 (2014).
42. Avraham, N., Soifer, I., Carmi, M. & Barkai, N. Increasing population growth by asymmetric segregation of a limiting resource during cell division. *Mol Syst Biol* **9**, (2013).
43. Martins, B. M. C. & Locke, J. C. W. Microbial individuality: how single-cell heterogeneity enables population level strategies. *Current Opinion in Microbiology* vol. 24 104–112 Preprint at https://doi.org/10.1016/j.mib.2015.01.003 (2015).
44. Ryall, B., Eydallin, G. & Ferenci, T. Culture History and Population Heterogeneity as Determinants of Bacterial Adaptation: the Adaptomics of a Single Environmental Transition. *Microbiology and Molecular Biology Reviews* **76**, 597–625 (2012).
45. Saint, M. *et al.* Single-cell imaging and RNA sequencing reveal patterns of gene expression heterogeneity during fission yeast growth and adaptation. *Nat Microbiol* **4**, 480–491 (2019).
46. Radzinski, M. *et al. Temporal profiling of redox-dependent heterogeneity in single cells*.
47. Lee, J. A. *et al.* Microbial phenotypic heterogeneity in response to a metabolic toxin: Continuous, dynamically shifting distribution of formaldehyde tolerance in Methylobacterium extorquens populations. *PLoS Genet* **15**, (2019).
48. Gasch, A. P. *et al.* Single-cell RNA sequencing reveals intrinsic and extrinsic regulatory heterogeneity in yeast responding to stress. *PLoS Biol* **15**, (2017).
49. van Dijk, D. *et al.* Slow-growing cells within isogenic populations have increased RNA polymerase error rates and DNA damage. *Nat Commun* **6**, (2015).

50. Martín-Banderas, L. *et al.* Flow focusing: A versatile technology to produce size-controlled and specific-morphology microparticles. *Small* **1**, 688–692 (2005).
51. José Luis Pedraz & Gorka Orive. *Therapeutic Applications of Cell Microencapsulation*. vol. 670 (Springer New York, NY, 2010).
52. Delgado-Ramos, L. Microbial analysis by microencapsulation and its application to study proliferation heterogeneity. (Universidad de Sevilla, 2016).
53. Lubeck, E. & Cai, L. Single-cell systems biology by super-resolution imaging and combinatorial labeling. *Nat Methods* **9**, 743–748 (2012).
54. Constantinou, I. *et al.* Self-learning microfluidic platform for single-cell imaging and classification in flow. *Micromachines (Basel)* **10**, (2019).
55. Durmus, N. G. *et al.* Magnetic levitation of single cells. *Proc Natl Acad Sci U S A* **112**, E3661–E3668 (2015).
56. Chen, K. L., Crane, M. M. & Kaeberlein, M. Microfluidic technologies for yeast replicative lifespan studies. *Mechanisms of Ageing and Development* vol. 161 262–269 Preprint at https://doi.org/10.1016/j.mad.2016.03.009 (2017).
57. Jo, M. C. & Qin, L. Microfluidic Platforms for Yeast-Based Aging Studies. *Small* vol. 12 5787–5801 Preprint at https://doi.org/10.1002/smll.201602006 (2016).
58. Wang, Y. *et al.* A high-throughput microfluidic diploid yeast long-term culturing (DYLC) chip capable of bud reorientation and concerted daughter dissection for replicative lifespan determination. *J Nanobiotechnology* **20**, (2022).
59. Lee, P. J., Helman, N. C., Lim, W. A. & Hung, P. J. A microfluidic system for dynamic yeast cell imaging. *Biotechniques* **44**, 91–95 (2008).
60. Welkenhuysen, N. *et al.* Single-cell study links metabolism with nutrient signaling and reveals sources of variability. *BMC Syst Biol* **11**, (2017).
61. Durán, D. C. *et al.* Slipstreaming mother machine: A microfluidic device for single-cell dynamic imaging of yeast. *Micromachines (Basel)* **12**, 1–11 (2021).
62. Fehrmann, S. *et al.* Aging yeast cells undergo a sharp entry into senescence unrelated to the loss of mitochondrial membrane potential. *Cell Rep* **5**, 1589–1599 (2013).
63. Asbury, C. L., Uy, J. L. & van den Engh, G. Polarization of scatter and fluorescence signals in flow cytometry. *Cytometry* **40**, 88–101 (2000).
64. Boyd, A. R. *et al.* A flow-cytometric method for determination of yeast viability and cell number in a brewery. *FEMS Yeast Res* **3**, 11–16 (2006).
65. Ho, H. J. *et al.* Parametric modeling of cellular state transitions as measured with flow cytometry. *BMC Bioinformatics* **13 Suppl 5**, (2012).
66. Mirisola, M. G. & Longo, V. D. Yeast Chronological Lifespan: Longevity Regulatory Genes and Mechanisms. *Cells* vol. 11 Preprint at https://doi.org/10.3390/cells11101714 (2022).
67. Michael Breitenbach, S. Michal Jazwinski & Peter Laun. *Aging Research in Yeast*. vol. 57 (Springer Dordrecht, 2012).
68. MORTIMER RK & JOHNSTON JR. Life span of individual yeast cells. *Nature* **183**, 1751–1752 (1959).
69. Yi, D. G., Hong, S. & Huh, W. K. Mitochondrial dysfunction reduces yeast replicative lifespan by elevating RAS-dependent ROS production by the ER-localized NADPH oxidase Yno1. *PLoS One* **13**, (2018).

70. Hao, N. *et al.* DNA damage checkpoint activation impairs chromatin homeostasis and promotes mitotic catastrophe during aging. (2019) doi:10.7554/eLife.50778.001.
71. Pal, S., Postnikoff, S. D., Chavez, M. & Tyler, J. K. *Impaired cohesion and homologous recombination during replicative aging in budding yeast*. (2018).
72. Lee, M. B. *et al.* Defining the impact of mutation accumulation on replicative lifespan in yeast using cancer-associated mutator phenotypes. *Proc Natl Acad Sci U S A* **116**, 3062–3071 (2019).
73. Frenk, S. & Houseley, J. Gene expression hallmarks of cellular ageing. *Biogerontology* **19**, 547–566 (2018).
74. Smith, J., Wright, J. & Schneider, B. L. A budding yeast's perspective on aging: The shape I'm in. *Exp Biol Med* **240**, 701–710 (2015).
75. Manzano-López, J., Matellán, L., Álvarez-Llamas, A., Blanco-Mira, J. C. & Monje-Casas, F. Asymmetric inheritance of spindle microtubule-organizing centres preserves replicative lifespan. *Nat Cell Biol* **21**, 952–965 (2019).
76. Manzano-López, J. & Monje-Casas, F. Asymmetric cell division and replicative aging: a new perspective from the spindle poles. *Current Genetics* vol. 66 719–727 Preprint at https://doi.org/10.1007/s00294-020-01074-y (2020).
77. Yang, J. *et al.* Systematic analysis of asymmetric partitioning of yeast proteome between mother and daughter cells reveals 'aging factors' and mechanism of lifespan asymmetry. *Proc Natl Acad Sci U S A* **112**, 11977–11982 (2015).
78. Neurohr, G. E. *et al.* Excessive Cell Growth Causes Cytoplasm Dilution And Contributes to Senescence. *Cell* **176**, 1083-1097.e18 (2019).
79. Knorre, D. A., Azbarova, A. v., Galkina, K. v., Feniouk, B. A. & Severin, F. F. Replicative aging as a source of cell heterogeneity in budding yeast. *Mechanisms of Ageing and Development* vol. 176 24–31 Preprint at https://doi.org/10.1016/j.mad.2018.09.001 (2018).
80. Xu, Z. & Teixeira, M. T. The many types of heterogeneity in replicative senescence. *Yeast* **36**, 637–648 (2019).
81. Kamei, Y., Tamada, Y., Nakayama, Y., Fukusaki, E. & Mukai, Y. Changes in transcription and metabolism during the early stage of replicative cellular senescence in budding yeast. *Journal of Biological Chemistry* **289**, 32081–32093 (2014).
82. Wang, Y., Lo, W. C. & Chou, C. S. A modeling study of budding yeast colony formation and its relationship to budding pattern and aging. *PLoS Comput Biol* **13**, (2017).
83. Vaiserman, A. M., Koliada, A. K. & Jirtle, R. L. Non-genomic transmission of longevity between generations: Potential mechanisms and evidence across species. *Epigenetics and Chromatin* vol. 10 Preprint at https://doi.org/10.1186/s13072-017-0145-1 (2017).
84. Sinclair, D. A. & Guarente, L. *Extrachromosomal rDNA Circles-A Cause of Aging in Yeast*. *Cell* vol. 91 (1997).
85. Morlot, S. *et al.* Excessive rDNA Transcription Drives the Disruption in Nuclear Homeostasis during Entry into Senescence in Budding Yeast. *Cell Rep* **28**, 408-422.e4 (2019).

86. Hull, R. M. & Houseley, J. The adaptive potential of circular DNA accumulation in ageing cells. *Current Genetics* vol. 66 889–894 Preprint at https://doi.org/10.1007/s00294-020-01069-9 (2020).
87. Smith, J. T., White, J. W., Dungrawala, H., Hua, H. & Schneider, B. L. Yeast lifespan variation correlates with cell growth and sir2 expression. *PLoS One* **13**, (2018).
88. Kyu Kang, W., Hyeock Kim, Y., Ah Kang, H., Kwon, K.-S. & Kim, J.-Y. Sir2 phosphorylation through cAMP-PKA and CK2 signaling inhibits the lifespan extension activity of Sir2 in yeast. doi:10.7554/eLife.09709.001.
89. Song, J. *et al.* Essential Genetic Interactors of SIR2 Required for Spatial Sequestration and Asymmetrical Inheritance of Protein Aggregates. *PLoS Genet* **10**, (2014).
90. Johnson, A. & Skotheim, J. M. Start and the restriction point. *Current Opinion in Cell Biology* vol. 25 717–723 Preprint at https://doi.org/10.1016/j.ceb.2013.07.010 (2013).
91. Cho, C. Y., Kelliher, C. M. & Haase, S. B. The cell-cycle transcriptional network generates and transmits a pulse of transcription once each cell cycle. *Cell Cycle* **18**, 363–378 (2019).
92. de Bruin, R. A. M., Mcdonald, W. H., Kalashnikova, T. I., Yates, J. & Wittenberg, C. *Cln3 Activates G1-Specific Transcription via Phosphorylation of the SBF Bound Repressor Whi5 fall into the G1-specific gene family (Cho et al they govern the events associated with cell cycle initiation, including DNA repli*. *Cell* vol. 117 (2004).
93. Wagner, M. v. *et al.* Whi5 regulation by site specific CDK-phosphorylation in Saccharomyces cerevisiae. *PLoS One* **4**, (2009).
94. Taberner, F. J., Quilis, I. & Igual, J. C. Spatial regulation of the start repressor Whi5. *Cell Cycle* **8**, 3013–3022 (2009).
95. Atencio, D., Barnes, C., Duncan, T. M., Willis, I. M. & Hanes, S. D. The yeast Ess1 prolyl isomerase controls swi6 and whi5 nuclear localization. *G3: Genes, Genomes, Genetics* **4**, 523–537 (2014).
96. Chandler-Brown, D., Schmoller, K. M., Winetraub, Y. & Skotheim, J. M. The Adder Phenomenon Emerges from Independent Control of Pre- and Post-Start Phases of the Budding Yeast Cell Cycle. *Current Biology* **27**, 2774-2783.e3 (2017).
97. Dirick1, L., Bohm, T. & Nasmyth2, K. *Roles and regulation of Cln-Cdc28 kinases at the start of the cell cycle of Saccharomyces cerevisiae*. *The EMBO Journal* vol. 14 (1995).
98. Cooper, K. Rb, whi it's not just for metazoans anymore. *Oncogene* vol. 25 5228–5232 Preprint at https://doi.org/10.1038/sj.onc.1209630 (2006).
99. Pramila, T., Wu, W., Miles, S., Noble, W. S. & Breeden, L. L. The forkhead transcription factor Hcm1 regulates chromosome segregation genes and fills the S-phase gap in the transcriptional circuitry of the cell cycle. *Genes Dev* **20**, 2266–2278 (2006).
100. Adames, N. R. *et al.* Experimental testing of a new integrated model of the budding yeast Start transition. *Mol Biol Cell* **26**, 3966–3984 (2015).
101. Palumbo, P. *et al.* Whi5 phosphorylation embedded in the G 1 /S network dynamically controls critical cell size and cell fate. *Nat Commun* **7**, (2016).

102. Wijnen, H., Landman, A. & Futcher, B. The G 1 Cyclin Cln3 Promotes Cell Cycle Entry via the Transcription Factor Swi6 . *Mol Cell Biol* **22**, 4402–4418 (2002).
103. Forsburg SL & Nurse P. Identification of a G1-type cyclin puc1+ in the fission yeast Schizosaccharomyces pombe. *Nature* **351**, 245–248 (1991).
104. Deprez, M. A., Eskes, E., Winderickx, J. & Wilms, T. The TORC1-Sch9 pathway as a crucial mediator of chronological lifespan in the yeast Saccharomyces cerevisiae. *FEMS Yeast Research* vol. 18 Preprint at https://doi.org/10.1093/femsyr/foy048 (2018).
105. Miles, S., Croxford, M. W., Abeysinghe, A. P. & Breeden, L. L. Msa1 and Msa2 Modulate G1-Specific Transcription to Promote G1 Arrest and the Transition to Quiescence in Budding Yeast. *PLoS Genet* **12**, (2016).
106. González-Novo, A. *et al.* Hog1 Targets Whi5 and Msa1 Transcription Factors To Downregulate Cyclin Expression upon Stress. *Mol Cell Biol* **35**, 1606–1618 (2015).
107. Thurston, A. K., Radebaugh, C. A., Almeida, A. R., Argueso, J. L. & Stargell, L. A. Genome instability is promoted by the chromatin-binding protein spn1 in saccharomyces cerevisiae. *Genetics* **210**, 1227–1237 (2018).
108. Allen/'^, J. B., Zhou/-^, Z., Siede, W., Friedberg, E. C. & Elledge^, S. J. *The SAD1/RAD53 protein kinase controls multiple checkpoints and DNA damage-induced transcription in yeast*. (1994).
109. Yao, S., Feng, Y., Zhang, Y. & Feng, J. DNA damage checkpoint and repair: From the budding yeast Saccharomyces cerevisiae to the pathogenic fungus Candida albicans. *Computational and Structural Biotechnology Journal* vol. 19 6343–6354 Preprint at https://doi.org/10.1016/j.csbj.2021.11.033 (2021).
110. Kumar, A. *et al.* Daughter-cell-specific modulation of nuclear pore complexes controls cell cycle entry during asymmetric division. *Nat Cell Biol* **20**, 432–442 (2018).
111. Schmoller, K. M., Turner, J. J., Kõivomägi, M. & Skotheim, J. M. Dilution of the cell cycle inhibitor Whi5 controls budding-yeast cell size. *Nature* **526**, 268–272 (2015).
112. Kukhtevich, I. v., Lohrberg, N., Padovani, F., Schneider, R. & Schmoller, K. M. Cell size sets the diameter of the budding yeast contractile ring. *Nat Commun* **11**, (2020).
113. Swaffer, M. P. *et al.* Transcriptional and chromatin-based partitioning mechanisms uncouple protein scaling from cell size. *Mol Cell* **81**, 4861-4875.e7 (2021).
114. Kõivomägi, M., Swaffer, M. P., Turner, J. J., Marinov, G. & Skotheim, J. M. G1 cyclin-Cdk promotes cell cycle entry through localized phosphorylation of RNA polymerase II. *Science (1979)* **374**, 347–351 (2021).
115. Litsios, A. *et al.* The timing of Start is determined primarily by increased synthesis of the Cln3 activator rather than dilution of the Whi5 inhibitor. *Mol Biol Cell* **33**, rp2 (2022).
116. Barber, F., Amir, A. & Murray, A. W. Cell-size regulation in budding yeast does not depend on linear accumulation of Whi5. *Proceedings of the National Academy of Sciences* **117**, 14243–14250 (2020).

117. Barber, F., Min, J., Murray, A. W. & Amir, A. Modeling the impact of single-cell stochasticity and size control on the population growth rate in asymmetrically dividing cells. *PLoS Comput Biol* **17**, (2021).
118. Neurohr, G. E. *et al.* Deregulation of the G1/S-phase transition is the proximal cause of mortality in old yeast mother cells. *Genes Dev* **32**, 1075–1084 (2018).
119. Moreno, D. F. *et al.* Proteostasis collapse, a hallmark of aging, hinders the chaperone-Start network and arrests cells in G1. (2019) doi:10.7554/eLife.48240.001.
120. Neurohr, G. E. *et al.* Deregulation of the G1/S-phase transition is the proximal cause of mortality in old yeast mother cells. *Genes Dev* **32**, 1075–1084 (2018).
121. Lindstrom, D. L. & Gottschling, D. E. The mother enrichment program: A genetic system for facile replicative life span analysis in Saccharomyces cerevisiae. *Genetics* **183**, 413–422 (2009).
122. Xiao, W. Isolation of Aged Yeast Cells Using Biotin-Streptavidin Affinity Purification. in *Yeast Protocols* (ed. Wei Xiao) vol. 2196 223–228 (2021).
123. Ottoz, D. S. M., Rudolf, F. & Stelling, J. Inducible, tightly regulated and growth condition-independent transcription factor in Saccharomyces cerevisiae. *Nucleic Acids Res* **42**, (2014).
124. Schwob, E., Ihm,', T. B., Mendenhall, M. D. & Nasmyth', K. *The B-Type Cyclin Kinase Inhibitor p4@'c7 Controls the Gl to S Transition in S. cerevisiae*. *Cell* vol. 79 (1994).
125. Spellman, P. T. *et al. Comprehensive Identification of Cell Cycle-regulated Genes of the Yeast Saccharomyces cerevisiae by Microarray Hybridization □ D*. *Molecular Biology of the Cell* vol. 9 http://cellcycle-www.stanford.edu (1998).
126. Chen, K. L., Crane, M. M. & Kaeberlein, M. Microfluidic technologies for yeast replicative lifespan studies. *Mechanisms of Ageing and Development* vol. 161 262–269 Preprint at https://doi.org/10.1016/j.mad.2016.03.009 (2017).
127. Jo, M. C. & Qin, L. Microfluidic Platforms for Yeast-Based Aging Studies. *Small* vol. 12 5787–5801 Preprint at https://doi.org/10.1002/smll.201602006 (2016).
128. Wang, Y. *et al.* A high-throughput microfluidic diploid yeast long-term culturing (DYLC) chip capable of bud reorientation and concerted daughter dissection for replicative lifespan determination. *J Nanobiotechnology* **20**, (2022).
129. Gilchrist, C. & Stelkens, R. Aneuploidy in yeast: Segregation error or adaptation mechanism? *Yeast* vol. 36 525–539 Preprint at https://doi.org/10.1002/yea.3427 (2019).
130. Torres, E. M. *et al.* Effects of aneuploidy on cellular physiology and cell division in haploid yeast. *Science (1979)* **317**, 916–924 (2007).
131. Klecker T & Westermann B. Asymmetric inheritance of mitochondria in yeast. *Journal of Biological Chemistry* **401**, 779–791 (2020).
132. Budovsky, A., Fraifeld, V. E. & Aronov, S. Linking cell polarity, aging and rejuvenation. *Biogerontology* vol. 12 167–175 Preprint at https://doi.org/10.1007/s10522-010-9305-4 (2011).
133. Higuchi-Sanabria, R. *et al.* Role of asymmetric cell division in lifespan control in Saccharomyces cerevisiae. *FEMS Yeast Res* **14**, 1133–1146 (2014).
134. Zhou, C. *et al.* Organelle-based aggregation and retention of damaged proteins in asymmetrically dividing cells. *Cell* **159**, 530–542 (2014).

135. Saarikangas, J. *et al.* Compartmentalization of ER-Bound Chaperone Confines Protein Deposit Formation to the Aging Yeast Cell. *Current Biology* **27**, 773–783 (2017).
136. Sheldrake, A. R. Cellular senescence, rejuvenation and potential immortality. *Proceedings of the Royal Society B: Biological Sciences* vol. 289 Preprint at https://doi.org/10.1098/rspb.2021.2434 (2022).
137. Li, Y. *et al.* Multigenerational silencing dynamics control cell aging. *Proc Natl Acad Sci U S A* **114**, 11253–11258 (2017).
138. Wierman, M. B. & Smith, J. S. Yeast sirtuins and the regulation of aging. *FEMS Yeast Res* **14**, 73–88 (2014).
139. Jin, M. *et al.* Divergent Aging of Isogenic Yeast Cells Revealed through Single-Cell Phenotypic Dynamics. *Cell Syst* **8**, 242-253.e3 (2019).
140. Zhang, Y. *et al.* Single Cell Analysis of Yeast Replicative Aging Using a New Generation of Microfluidic Device. *PLoS One* **7**, (2012).
141. S. Michal Jazwinski. Molecular mechanisms of yeast longevity. *Trends Microbiol* **7**, 247–252 (1999).
142. Schmoller, K. M., Turner, J. J., Kõivomägi, M. & Skotheim, J. M. Dilution of the cell cycle inhibitor Whi5 controls budding-yeast cell size. *Nature* **526**, 268–272 (2015).
143. Chandler-Brown, D., Schmoller, K. M., Winetraub, Y. & Skotheim, J. M. The Adder Phenomenon Emerges from Independent Control of Pre- and Post-Start Phases of the Budding Yeast Cell Cycle. *Current Biology* **27**, 2774-2783.e3 (2017).
144. Schmoller, K. M. *et al.* Whi5 is diluted and protein synthesis does not dramatically increase in pre-Start G1. *Mol Biol Cell* **33**, lt1 (2022).
145. Barber, F., Amir, A. & Murray, A. W. Cell-size regulation in budding yeast does not depend on linear accumulation of Whi5. doi:10.1073/pnas.2001255117/-/DCSupplemental.
146. Chen, Y. & Futcher, B. Scaling gene expression for cell size control and senescence in Saccharomyces cerevisiae. *Current Genetics* vol. 67 41–47 Preprint at https://doi.org/10.1007/s00294-020-01098-4 (2021).
147. Chen, Y., Zhao, G., Zahumensky, J., Honey, S. & Futcher, B. Differential Scaling of Gene Expression with Cell Size May Explain Size Control in Budding Yeast. *Mol Cell* **78**, 359-370.e6 (2020).
148. Qu, Y. *et al.* Cell Cycle Inhibitor Whi5 Records Environmental Information to Coordinate Growth and Division in Yeast. *Cell Rep* **29**, 987-994.e5 (2019).
149. Crane, M. M. *et al.* Rb analog Whi5 regulates G1 to S transition and cell size but not replicative lifespan in budding yeast. *Transl Med Aging* **3**, 104–108 (2019).
150. Cho, R. J. *et al. responsiveness to external stimuli (Zanolari and Riezman*. *Molecular Cell* vol. 2 http://genomics.stanford.edu. (1998).